

1992

# Overcoming limitations of SPICE's built-in models for high speed bipolar processes

Kenneth E. Gross  
*Lehigh University*

Follow this and additional works at: <http://preserve.lehigh.edu/etd>

---

## Recommended Citation

Gross, Kenneth E., "Overcoming limitations of SPICE's built-in models for high speed bipolar processes" (1992). *Theses and Dissertations*. Paper 72.

This Thesis is brought to you for free and open access by Lehigh Preserve. It has been accepted for inclusion in Theses and Dissertations by an authorized administrator of Lehigh Preserve. For more information, please contact [preserve@lehigh.edu](mailto:preserve@lehigh.edu).

**AUTHOR: Gross, Kenneth E.**

**TITLE:**

**Overcoming Limitations of  
Spice's Built-In Models for  
High Speed Bipolar  
Processes**

**DATE: May 31, 1992**

OVERCOMING LIMITATIONS OF SPICE'S BUILT-IN MODELS  
FOR HIGH SPEED BIPOLAR PROCESSES

by

Kenneth E. Gross

A Thesis

Presented to the Graduate Committee

of Lehigh University

in Candidacy for the Degree of

Master of Science

in

Electrical Engineering

1992

This thesis is accepted and approved in partial fulfillment of the requirements for the degree of Master of Science in Electrical Engineering.

May 14, 1992  
Date

\_\_\_\_\_  
Advisor in Charge

\_\_\_\_\_  
CSEE Department Chairperson

## ACKNOWLEDGEMENTS

The development of the enhanced Gummel-Poon model detailed in this thesis entailed the effort of many people who assisted in its preparation. Interest in the subject emerged from courses instructed by Dr. Frank H. Hielscher (Lehigh University), whose help and guidance as thesis advisor throughout the development was a valuable resource. Helpful discussions with the late Professor Thomas A. Reilly (Lafayette College) resulted in valuable feedback during early attempts developing a macro-model. Conversations with several other people at AT&T Bell Laboratories in Reading, Pennsylvania were particularly helpful in the completion of this study, including: James R. Mathews, Stanley F. Moyer, and Robert D. Plummer. Thanks also goes to Junho Baek and Norma Elias for their collection and compilation of data.

The development that is detailed in this thesis would not be possible without significant financial support from AT&T and the backing of Stephen E. Parks and Bill Ballamy, who encouraged the completion of this study. A special note of appreciation is owed to my wife, Sally, whose love, patience, and understanding encouraged the completion as well as the writing of this thesis.

## TABLE OF CONTENTS

Title Page	i
Certificate of Approval	ii
Acknowledgements	iii
Table of Contents	iv
List of Tables	v
List of Figures	vi
Abstract	1
I. Introduction	3
II. Theoretical Background	9
A. Basic Equations Used in SPICE 2G.6	9
B. Invalid Assumptions Related to "Early" Effect	17
C. Contributions to High-Level Injection	19
D. Avalanche Breakdown	30
III. AT&T's CBIC-V Technology	32
A. Device Features	32
B. Process Description	36
IV. Implementation of a Unified Model and Parameter Extraction	40
A. Unified Circuit Model Including Quasi-Saturation	40
B. Modeling of Avalanche Generation for Simulation	50
V. Results	53
VI. Conclusions	71
Appendices	74
Appendix A - Detailed Model Tabulation	75
Appendix B - Transistor Test Circuits	99
Appendix C - CBIC-V Sample/Hold Schematics	103
References	106
Vita	110

## LIST OF TABLES

Table 1	SPICE BJT Model Parameters	16
Table 2	CBIC-V NPN and PNP Transistor Specifications	33
Table 3	Comparative Analysis of Quasi-sat in PSpice	70

## LIST OF FIGURES

Figure 1.	Equivalent circuit for Ebers-Moll Injection model of an <i>npn</i> transistor	10
Figure 2.	Equivalent circuit for EM2 Transport model (nonlinear hybrid- $\pi$ ) of an <i>npn</i> transistor	11
Figure 3.	Net doping profile of a high-speed <i>n-p-v-n</i> transistor showing lightly doped epitaxial collector ( <i>v</i> -region).	21
Figure 4.	Electric field and stored charge in regions of (A) non-saturation, (B) threshold of quasi-saturation, and (C) well into quasi-saturation.	22
Figure 5.	$I_C$ versus $V_{CE}$ characteristic for typical <i>n-p-v-n</i> transistor under consideration showing ohmic and nonohmic quasi-saturation regions of operation.	25
Figure 6.	NPN Cross-sectional view	35
Figure 7.	PNP Cross-sectional view	37
Figure 8.	Equivalent circuit for model of transistor intrinsic to available SPICE programs	43
Figure 9.	Equivalent circuit for 4-Terminal Extended BJT model including quasi-saturation effects	44
Figure 10.	Small-Signal Equivalent circuit for the 4-Terminal Extended BJT model	48
Figure 11.	NV231A01 Beta vs. $I_C$ at $V_{cb} = 2, 5 \text{ \& } 8 \text{ V}$	56
Figure 12.	PV231A01 Beta vs. $I_C$ at $V_{bc} = 2, 5 \text{ \& } 8 \text{ V}$	57
Figure 13.	NV231A01 $I_C$ vs. $V_{BE}$ at $V_{cb} = 2, 5 \text{ \& } 8 \text{ V}$	58
Figure 14.	PV231A01 $I_C$ vs. $V_{BE}$ at $V_{bc} = 2, 5 \text{ \& } 8 \text{ V}$	59



Figure 15.	NV231A01 $I_C$ vs. $V_{CE}$ at $V_{be} = .8, .85, .9$ V	60
Figure 16.	PV231A01 $I_C$ vs. $V_{CE}$ at $V_{eb} = .8, .85, .9$ V	61
Figure 17.	NV231A01 $I_{SUB}$ vs. $V_{CE}$ at $V_{be} = 0.8, 0.9$ V	62
Figure 18.	PV231A01 $I_{SUB}$ vs. $V_{CE}$ at $V_{eb} = 0.8, 0.9$ V	63
Figure 19.	NV231A01 $f_T$ vs. $I_C$ at $V_{ce} = 3$ V	64
Figure 20.	PV231A01 $f_T$ vs. $I_C$ at $V_{ec} = 3$ V	65
Figure 21.	NV231A01 $I_C$ vs. $V_{CE}$ at $I_b = 20, \dots, 100$ $\mu$ A	67
Figure 22.	DC Transfer response to $\pm 4$ V input swing imposed on a CBIC-V Sample/Hold Amplifier	68
Figure A1.	CBIC-V Sample/Hold Block Diagram	103
Figure A2.	Schematic for Sample/Hold Output Buffer	104

## ABSTRACT

VHF Complementary Bipolar Integrated Circuit (CBIC-V) processes which result in both high performance vertical PNP transistors as well as NPN transistors on the same silicon substrate, can give rise to modeling inaccuracy in several regimes of operation. Simulation of integrated circuits by analysis programs such as SPICE demands the specification of the element model parameters to produce a fit of the model equations to a set of measured device characteristics. The scope of these equations is often confined by assumptions or approximations made in the derivation. This is not limited to those equations that describe the Very High Frequencies (VHF) obtainable with these technologies. Several other characteristics, in addition to unity gain frequency ( $f_T$ ), where model accuracy is suspect include saturation ( $V_{CEsat}$ ), Early voltage ( $V_A$ ), and common-emitter current gain rolloff under high collector current bias ( $\beta$  vs.  $I_C$ ).

An example of parameter extraction of the SPICE 2G.6 bipolar junction transistor (BJT) model parameters for a CBIC-V transistor shows poor model accuracy. Therefore model modifications yielding a "true" four-terminal Extended Gummel-Poon BJT model are proposed that give a better fit to

measured data. Parameter extraction techniques are qualitatively explained and the "macro-model" is evaluated using simulations employing this model in a high speed bipolar process. Agreement between simulations and electrical measurements is significantly improved.

## I. INTRODUCTION

There have been many enhancements to the simple Ebers-Moll model<sup>1</sup> since Berkeley released SPICE1<sup>2</sup> in 1972. Even SPICE2<sup>3</sup>, with the addition of basewidth modulation<sup>4</sup> (Early effect) and several other enhancements primarily addressing simulation of semiconductor circuits, has every so often been updated and improved by Berkeley to the present version 2G.6. The more recent release of Berkeley's SPICE3, although a major upgrade and rewritten in C-language code, contains no significant improvements to the BJT model. The BJT model employed in SPICE 2G.6 does include the more complex integral charge control model that was proposed by Gummel and Poon<sup>5,6</sup>. Yet several commercial releases of the ever popular SPICE program have included still further updates to include other second order effects. A compact BJT model "for all occasions" is the ultimate goal in all of these endeavors.

Many circuits designed in today's high speed bipolar processes push the technology to the limits of its capabilities. With ever increasing competition in high end markets to be faster or more accurate, there is generally very little margin for error in these designs. High-

frequency (bandwidth) transistors demand shallow junctions with very high doping levels and steep profiles. These conditions can give rise to equations that are difficult to model and almost always constrain the collector-emitter sustaining voltage,  $BV_{CEO}$ . This crucial parameter, which can be as low as 5 to 10 volts, will govern what the maximum output swing can be in such applications as high speed instrumentation amplifiers and Automatic Test Equipment (ATE) pin electronics. Today's circuit designs often take these BJTs from the brink of saturation to the limits of breakdown where second order effects must be modeled accurately to obtain meaningful results.

Junction breakdown is not even modeled in most versions of SPICE today, as many attempts to approximate avalanche breakdown phenomenon<sup>7,8</sup> in the BJT model have failed. The most common cause for the failure in these attempts has been convergence difficulties that develop as a result of the exponential rise in collector current with increasing bias. Dutton's attempt was later implemented in AT&T's ADVICE<sup>9</sup> circuit simulator and subsequently withdrawn for this very reason. If a suitable approximation cannot be achieved with reasonable convergence success, then a simple flag or alarm would be an immense help to circuit designers since operation in breakdown is generally considered a fault condition anyway. Two model parameters, BVBE and BVCE, have been added which act as alarms and print warning messages

whenever the base-emitter or collector-emitter voltages, respectively, exceed these limits. Implementation of avalanche currents through a current source,  $I_C$ , is modeled by three parameters: BV, IBV, and NBV.

High-frequency transistors are typically operated under high-injection because only at high current densities is the contribution of emitter delay time to the total delay time small. Loss of common-emitter forward current gain,  $h_{FE}$ , at high current density has been attributed to high-level injection, causing current crowding and lateral current spreading at the emitter-base junction. This effect is accentuated by debiasing of the emitter due to a lateral resistive drop in the base, causing the current density to increase more rapidly than the current<sup>10</sup> (Webster effect). The effect is theoretically modeled in SPICE quite well by the parameters NE and IKF. "Base push-out", where the effective base extends into the epitaxial collector region with its consequential increase of  $\tau_f$ <sup>11</sup> (Kirk effect), is another effect which has been proposed as limiting maximum current of a transistor. This phenomenon is the primary cause of  $h_{FE}$  falloff at high current density in the variety of epitaxial transistors investigated in this work.

The now well known base push-out effect was discovered by Messenger<sup>12</sup> and first published by Kirk on transistor structures of the metal alloy and mesa variety. Hahn<sup>13,14</sup> then studied the effects of collector resistance upon the

high current capabilities of  $n^+pn^-n^+$  epitaxial transistor structures where he showed the effect of partial saturation (later dubbed quasi-saturation) upon  $h_{FE}$  and transistor switching times. He showed that the onset of conductivity modulation of the bulk collector resistance causes an abrupt decrease in  $h_{FE}$  at high current density and consequently limits the current range in which a transistor exhibits usable gain. Saturation is modeled in SPICE with the specification of 5 terms: BR, NC, ISC, IKR and RC. All of these terms are adequate in describing the operation of a BJT while *in* saturation, with RC being the only parameter defining the boundary of saturation. What RC does not do well is describe the transition region in or near saturation for such structures commonly called power transistors. By fitting some parameters, small improvements in one region of operation are possible at the expense of poor model accuracy in other regions of operation.

The validity of the simplifying assumptions on which Gummel's integral charge-control relation is based is most questionable for VHF transistors (e.g.  $f_T > 5$  GHz) which have shallow doping profiles and narrow emitter stripes. Rein, et al<sup>15</sup> showed the integral charge-control relation to be a fairly good approximation even for VHF transistors well into the high current region (including the quasi-saturation region) as long as stored excess charge outside the internal transistor to  $Q_b$  is taken into account. This is done in the

extended Gummel-Poon BJT model with the inclusion of a full parasitic transistor modeled as a partial Gummel-Poon transistor and an additional term,  $Q_{CO}$ , which represents the zero-bias stored charge in the epitaxial collector. As a result, the important relation between  $Q_b$  and the transit time,  $\tau_f$ , remains valid.

Trends to further raise both the integration level and the switching speed of fast bipolar integrated circuits dictate an increase of current density in the transistors<sup>16,17</sup>. As such, transistor operation in the quasi-saturation region may be advantageous, in spite of transit time,  $\tau_f$ , increases with collector current. Still, implications on the analysis of transistor frequency dependence on intermodulation distortion<sup>18</sup> is determined by the degree of curvature in the loaded cutoff frequency,  $f_T(R_L)$ , versus collector current curve. Therefore, it is evident that compact transistor models are required that are exact enough for simulating the small-signal and switching behavior even in the quasi-saturation region but, at the same time, are simple enough to allow acceptable simulation times.

Finally, a study of the simplifying approximations used in SPICE for the iterative solution of  $q_b$  shows how this can give rise to optimistic simulation results for large signal distortion analyses. That portion of  $q_b$  which accounts for depletion-layer charge storage in the base,  $q_1$ , is approximated and then further simplified to avoid a singularity



when the intrinsic base-collector voltage is equal to  $V_{AF}$ , the forward Early voltage. But the simplification is based on the underlying assumption that  $V_{AF} \gg V_{bc}$  with the result that the output conductance ( $I_c$  vs.  $V_{CE}$ ) is a linear relationship and all curves (of base drive) extrapolate back to  $V_{AF}$  on the  $V_{CE}$  axis. This is not the case, however, in VHF technologies where the Early voltage can be quite low ( $V_A < 10$  volts), on the same order as the base-collector voltage. These transistors exhibit changing output conductance with applied bias and the underlying assumptions in the simplifying approximation of  $q_1$  need to be revisited.

The accuracy of the compact representation for a four-terminal high speed transistor was simulated and results are presented in section V. The compact model consists of two Gummel-Poon transistors and resistors to model the extrinsic collector and base resistances. The implementation of avalanche generation currents is realized by inclusion of a diode in the final subcircuit form of the model.

## II. THEORETICAL BACKGROUND

### A. Basic Equations Used in SPICE 2G.6

For computer simulation, a model based on fundamental physics of the device allows a more thorough understanding and fewer input parameters, but generally provides this ease of use at the expense of accuracy over certain ranges of operation. Computer programs permit the designer to use conceptually and computationally complex transistor models while being free from the tedium of the computations. Since any analysis is only as accurate as the model used, it is essential to understand the origin of the models and their degree of approximation over the range of uses. The most successful programs thus far are those based on the Ebers-Moll equations, as outlined below:

$$\begin{aligned}I_C &= \alpha_F I_F - I_R \\I_E &= -I_F + \alpha_R I_R \\I_B &= (1-\alpha_F)I_F + (1-\alpha_R)I_R\end{aligned}\tag{1}$$

where

$$\begin{aligned}I_F &= I_{ES} (e^{qV_{be}/kT} - 1) \\I_R &= I_{CS} (e^{qV_{bc}/kT} - 1)\end{aligned}\tag{2}$$

and by applying the reciprocity relationship, (1) and (2) can be further reduced to yield the "injection version" of the EM<sub>1</sub> model.

$$\alpha_F I_{ES} = \alpha_R I_{CS} \equiv I_S\tag{3}$$

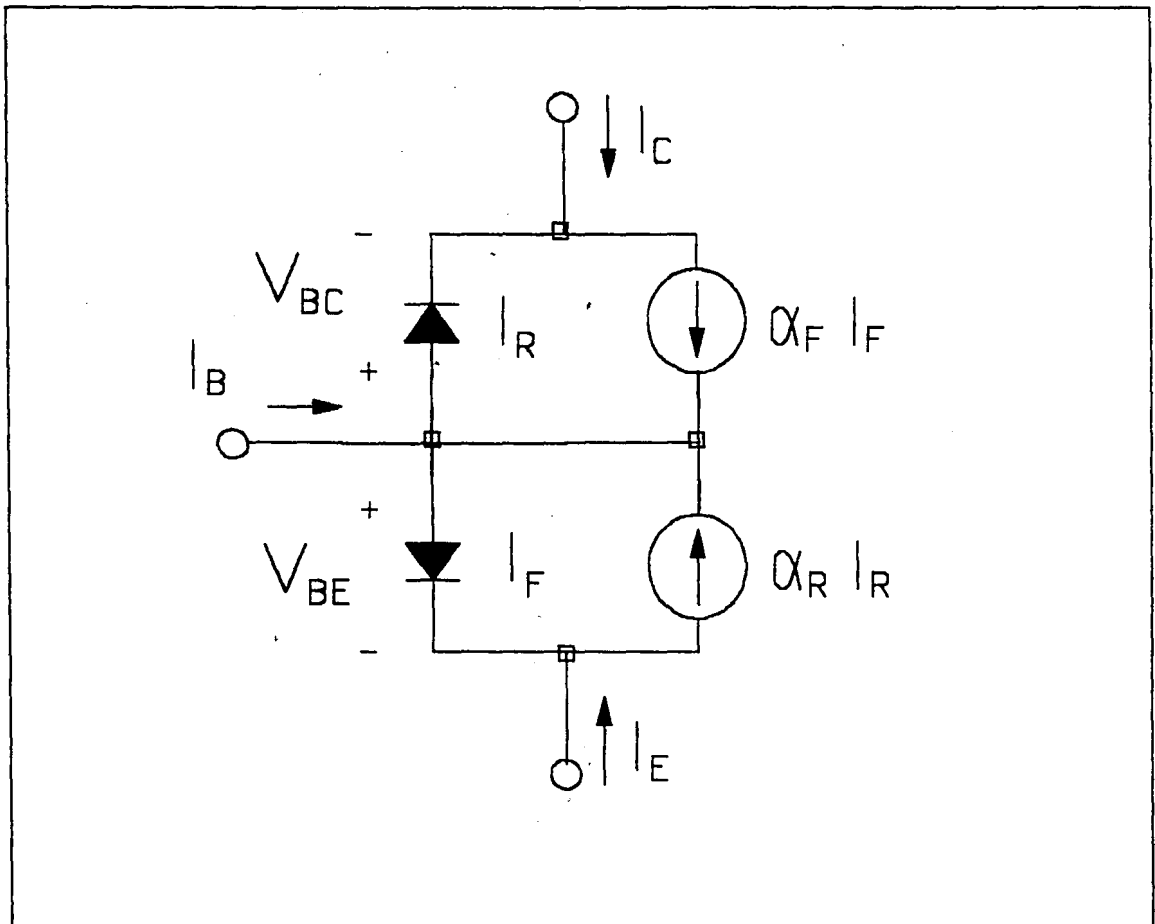


Figure 1. Equivalent circuit for Ebers-Moll Injection model of an *n*pn transistor

Using a different choice of reference currents and rearranging the fundamental Ebers-Moll equations into the "transport version"<sup>19</sup> of the model, (1) and (2) can be written in the form:

$$\begin{aligned}
 I_C &= I_{CC} - I_{EC}/\alpha_R \\
 I_E &= -I_{CC}/\alpha_F + I_{EC} \\
 I_B &= (1/\alpha_F - 1)I_{CC} + (1/\alpha_R - 1)I_{EC}
 \end{aligned}
 \tag{4}$$

where

$$\begin{aligned}
 I_{CC} &= I_S (e^{qV_{BE}/kT} - 1) \\
 I_{EC} &= I_S (e^{qV_{BC}/kT} - 1)
 \end{aligned}
 \tag{5}$$

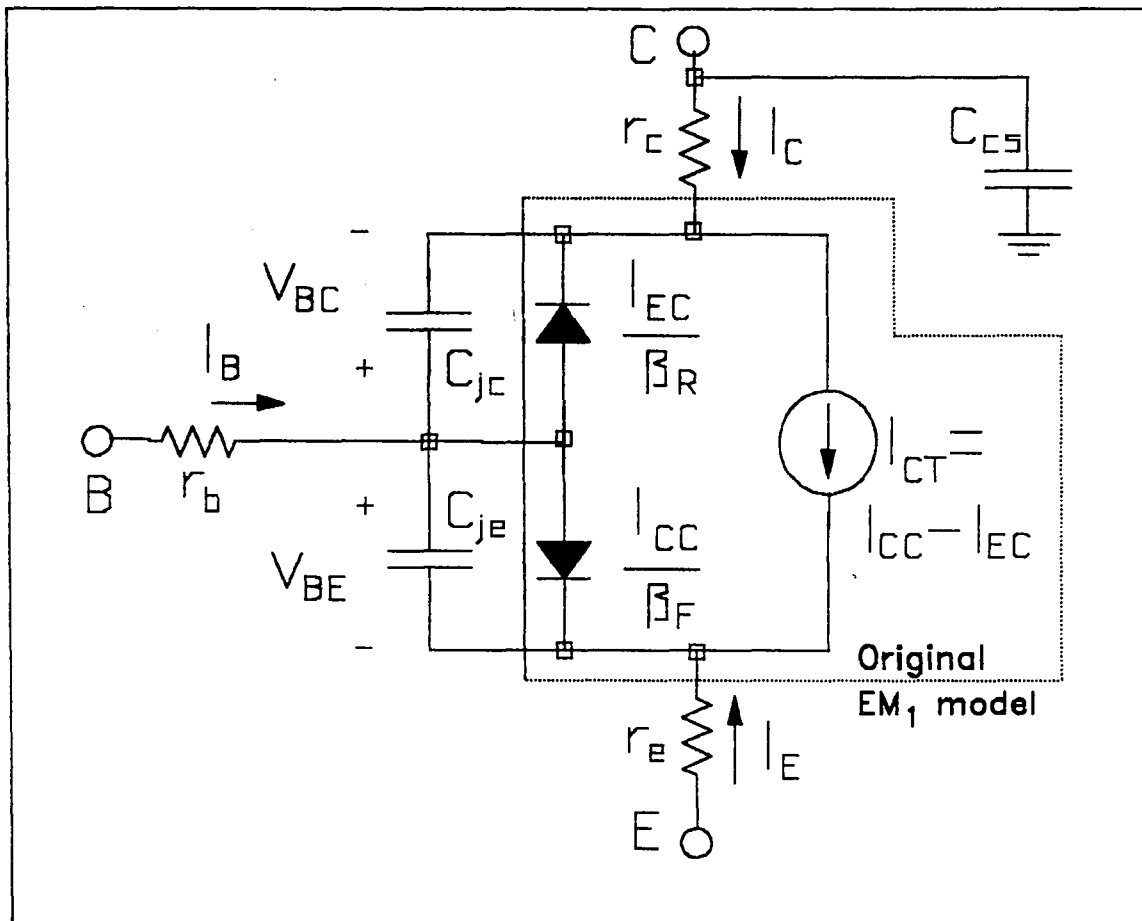


Figure 2. Equivalent circuit for EM<sub>2</sub> Transport model (nonlinear hybrid- $\pi$ ) of an *npn* transistor

and using the derived linking current

$$I_{CT} = I_S (e^{qV_{be}/kT} - e^{qV_{bc}/kT}) \quad (6)$$

and the well known expression,  $\beta = \alpha/(1-\alpha)$ , the Ebers-Moll equations (4) and (5) can be rewritten as:

$$I_C = I_{CT} - I_S/\beta_R (e^{qV_{bc}/kT} - 1) \quad (7)$$

$$I_E = -I_{CT} - I_S/\beta_F (e^{qV_{be}/kT} - 1)$$

$$I_B = I_S/\beta_F (e^{qV_{be}/kT} - 1) + I_S/\beta_R (e^{qV_{bc}/kT} - 1)$$

In this form, three parameters  $I_S$ ,  $\beta_F$ , and  $\beta_R$  characterize the basic Ebers-Moll relations. The EM<sub>2</sub> model provides modeling of charge storage effects and adds three ohmic resistors. But, additional parameters are necessary to

depict the effects of second order phenomena as described earlier.

In 1970, Gummel and Poon modified (7) to incorporate three of these second order effects: 1) space-charge layer widening (Early effect) through a modified  $I_S$  by specifying the Early voltage,  $V_A$ , and its reverse bias equivalent  $V_B$ , 2) recombination in the emitter-base space-charge region at low  $V_{BE}$  bias (Sah-Noyce-Shockley effect) through  $n_E$  and its reverse equivalent  $n_C$ , and 3) current-gain rolloff at high current levels due to conductivity modulation in the base (Webster effect) through  $I_S$  once again, by defining the "knee current",  $I_{KF}$ , and its counterpart  $I_{KR}$ .

$$I_B = I_S/\beta_F (e^{V_{be}/V_t} - 1) + I_1 (e^{V_{be}/(n_e V_t)} - 1) \quad (8)$$

$$+ I_S/\beta_R (e^{V_{bc}/V_t} - 1) + I_2 (e^{V_{bc}/(n_c V_t)} - 1)$$

where  $I_1$  and  $I_2$  are non-ideal leakage saturation currents, and  $V_t = kT/q$ , the thermal voltage.

In all, Gummel and Poon added eight new parameters to describe the large-signal (static) behavior of a BJT. Based on Beaufoy and Sparkes' article<sup>20</sup> about the basic concept of charge control theory, Gummel proposed his integral charge-control relation (*ICCR*) to model the non-idealities cited. The new charge control relation was derived from basic physical considerations and obtains the dominant current components of  $I_C$  without using piece-wise fitted models:

$$I_{CT} = I_S Q_{bo} (e^{qV_{be}/kT} - e^{qV_{bc}/kT}) / Q_b \quad (9)$$

This unified theory became the foundation for the original SPICE2 work and has remained the core of present day SPICE derived programs. The key variable that is used to modify  $I_S$  in (8) is  $Q_b$ , the total base majority-carrier charge.

Study of the device physics shows that<sup>21</sup>

$$I_S = q^2 \cdot A_E^2 \cdot n_i^2 \cdot D_n / Q_b$$

$$\text{and } Q_b = q \cdot A_E \int_0^{x_b} p(x) \cdot dx \quad (10)$$

where the static or "built-in" base charge at zero bias is

$$Q_{bo} = q \cdot A_E \int_0^{x_b} N_a(x) \cdot dx \quad (11)$$

Gummel and Poon also added four other charge storage parameters, linking  $I_S$  to emitter and collector depletion capacitances ( $Q_e$  and  $Q_c$ ) in the base and to forward and reverse transit times ( $\tau_f$  and  $\tau_r$ ). These are summed to represent:

$$\begin{aligned} Q_b &= Q_{bo} + Q_e + Q_c + \tau_f \cdot I_{CC} + \tau_r \cdot I_{EC} \\ &= Q_{bo} + C_{je} V_{be} + C_{jc} V_{bc} + Q_{bo}/Q_b \cdot \tau_f I_S (e^{V_{be}/V_t} - 1) \\ &\quad + Q_{bo}/Q_b \cdot \tau_r I_S (e^{V_{bc}/V_t} - 1). \end{aligned} \quad (12)$$

When  $Q_b$  is normalized with respect to  $Q_{bo}$  and is represented in its five components, it can be written in the form:

$$\begin{aligned} q_b &= 1 + V_{be}/V_B + V_{bc}/V_A + I_S/I_{KF} (e^{V_{be}/V_t} - 1) \\ &\quad + I_S/I_{KR} (e^{V_{bc}/V_t} - 1) \end{aligned} \quad (13)$$

where we define

$$\begin{aligned} q_b &= Q_b/Q_{bo} ; & I_{KF} &= Q_{bo}/\tau_f ; & I_{KR} &= Q_{bo}/\tau_r \\ |V_A| &= Q_{bo}/C_{jc} ; & |V_B| &= Q_{bo}/C_{je} \end{aligned} \quad (14)$$

Here we see that the two charge-control time constants  $\tau_f$  and  $\tau_r$  with  $Q_{bo}$  define the "knee currents"  $I_{KF}$  and  $I_{KR}$ . See Ref. [19] or [21] for a complete derivation of the Early voltages  $V_A$  and  $V_B$ . By grouping together the basewidth modulation effects into  $q_1$  and the high-level injection effects into  $q_2$ ,

$$q_1 = 1 + q_e + q_c = 1 + V_{be}/V_B + V_{bc}/V_A \quad (15)$$

$$q_2 = I_S/I_{KF} (e^{V_{be}/V_t} - 1) + I_S/I_{KR} (e^{V_{bc}/V_t} - 1)$$

we can put (13) into a more manageable format

$$q_b = q_1 + q_2/q_b \quad (16)$$

and solving the quadratic expression for  $q_b$ :

$$q_b = q_1/2 + [(q_1/2)^2 + q_2]^{1/2} \quad (17)$$

The overall model is thus specified by 11 parameters and temperature which is used to calculate  $V_t$ . Finally, the collected equations that define the Gummel-Poon model for an *npn* transistor consist of (8) for the base current and (15) through (17) for the dimensionless normalized base charge or Gummel number. The collector current can be derived from the *ICCR* in (9) which does not use low-injection approximations developed in (8). By substituting (9) back into the basic Ebers-Moll equations in (7) and including Sah-Noyce-Shockley recombination at low bias we obtain:

$$\begin{aligned} I_C &= (I_{CC} - I_{EC})/q_b - I_{EC}/\beta_R - I_{EC2} \\ &= I_S (e^{V_{be}/V_t} - e^{V_{bc}/V_t})/q_b - I_S/\beta_R (e^{V_{bc}/V_t} - 1) \\ &\quad - I_2 (e^{V_{bc}/(nc.V_t)} - 1). \end{aligned} \quad (18)$$

The actual SPICE2 implementation of the model embodies a complete EM<sub>2</sub> model and includes the three ohmic bulk resistors  $r_c'$ ,  $r_b'$  and  $r_e'$ , and three junction capacitances  $C_{jc}$ ,  $C_{je}$  and  $C_{cs}$  as indicated in Figure 2. All of the bulk resistors and  $C_{cs}$  are constants and the junction capacitors  $C_{jc}$  and  $C_{je}$  vary with voltage in the form:

$$C_j = C_{j0} (1 - V_j/\phi)^{-m} \quad (19)$$

where  $C_{j0}$  is the value of the junction capacitance at  $V_j=0$ ,  $\phi$  is the junction barrier potential, and  $m$  is the gradient factor. Other small signal (linearized) parameters for the familiar hybrid- $\pi$  model include  $\tau_f$  and  $\tau_r$ . Flicker noise model parameters  $k_f$  and  $a_f$  round out ac analysis capabilities of SPICE. The junction saturation currents vary with temperature according to the equation

$$I_s(T) = I_s(T_0) \cdot (T/T_0)^{\phi_T} e^{qE_g/kT(T/T_0-1)} \quad (20)$$

where the parameter  $E_g$  is the bandgap voltage and typically is 1.11 and  $\phi_T$  typically is 3. The temperature,  $T$ , and the reference temperature,  $T_0$ , are in degrees Kelvin.

Revisions leading to the present SPICE version 2G.6 added extensions taking into account the base resistance on the current due to crowding, voltage and current dependence of  $\tau_f$ , voltage dependence of collector-substrate capacitance  $C_{cs}$ , and temperature dependence of  $\beta_F$  and  $\beta_R$ . A summary of these extensions as well as the 27 original SPICE2 model parameters is provided in Table 1.



TABLE 1

SPICE BJT Model Parameters

Symbol	SPICE2	SPICE 2G	Parameter name	Default
$I_S$	IS	IS	saturation current	$10^{-16}$ A
$\beta_F$	BF	BF	ideal maximum forward current gain	100
$\beta_R$	BR	BR	ideal maximum reverse current gain	1
$n_F$	....	NF	forward current emission coefficient	1
$n_R$	....	NR	reverse current emission coefficient	1
$I_1$	C2	ISE = $C_2 I_S$	forward nonideal base current coefficient	0 A
$I_2$	C4	ISC = $C_4 I_S$	reverse nonideal base current coefficient	0 A
$n_e$	NEL	NE	nonideal b-e emission coefficient	1.5
$n_c$	NCL	NC	nonideal b-c emission coefficient	2
$I_{KF}$	IK	IKF	high current $\beta_F$ knee	$\infty$ A
$I_{KR}$	IKR	IKR	high current $\beta_R$ knee	$\infty$ A
$V_A$	VA	VAF	forward Early voltage	$\infty$ V
$V_B$	VB	VAR	reverse Early voltage	$\infty$ V
$r_c$	RC	RC	collector resistance	0 $\Omega$
$r_e$	RE	RE	emitter resistance	0 $\Omega$
$r_b$	RB	RB	zero-bias (maximum) base resistance	0 $\Omega$
$r_{bm}$	....	RBM	minimum base resistance	RB $\Omega$
$I_{rb}$	....	IRB	current where $r_b$ falls halfway to RBM	$\infty$ A
$C_{je}$	CJE	CJE	zero-bias b-e junction capacitance	0 F
$\phi_e$	PE	VJE	b-e junction potential	0.75 V
$m_e$	ME	MJE	b-e junction grading coefficient	0.33
$C_{jc}$	CJC	CJC	zero-bias b-c junction capacitance	0 F
$\phi_c$	PC	VJC	b-c junction potential	0.75 V
$m_c$	MC	MJC	b-c junction grading coefficient	0.33
$C_{cs}$	CCS	CJS	zero-bias c-substrate capacitance	0 F
$\phi_s$	....	VJS	c-s junction potential	0.75 V
$m_s$	....	MJS	substrate grading coefficient	0
$X_{cjc}$	....	XCJC	fraction of $C_{jc}$ that connects internal to $r_b$	1
$FC$	....	FC	forward bias depletion capacitor coefficient	0.5
$\tau_f$	TF	TF	forward transit time	0 s
$\tau_r$	TR	TR	reverse transit time	0 s

**TABLE 1** **SPICE BJT Model Parameters (Continued)**

Symbol	SPICE2	SPICE 2G	Parameter name	Default
$X_{\tau f}$	....	XTF	$\tau_f$ bias dependence coefficient	0
$V_{\tau f}$	....	VTF	$\tau_f$ dependency on $V_{bc}$	$\infty$ V
$I_{\tau f}$	....	ITF	$\tau_f$ dependency on $I_C$	0 A
$P_{\tau f}$	....	PTF	excess phase @ $f=1/2\pi\tau_f$	0 °
$E_g$	EG	EG	energy gap	1.11 eV
$\phi_T$	PT	XTI	saturation current temperature exponent	3
$X_{TB}$	....	XTB	$\beta_F$ and $\beta_R$ temperature coefficient	0
$k_f$	KF	KF	flicker noise coeff.	0
$a_f$	AF	AF	flicker noise exponent	1

B. Invalid Assumptions Related to "Early" Effect

The base charge  $q_b$ , as explained in the previous section, is the total base majority-carrier charge divided by the zero bias base charge as defined in (15) and (17). SPICE2 makes a modification to (17) to separate the effects described by  $q_1$  and  $q_2$ . The approximation, which pulls  $q_1$  outside of the square-root expression, causes slightly more high current roll-off of forward and reverse current gain. Equation (17) may be restated as in Nagel's thesis<sup>3</sup>

"A direct solution of (16) for  $q_b$  yields the result

$$q_b = \frac{1}{2}q_1 + \frac{1}{2}\sqrt{q_1^2 + 4'q_2} \tag{21}$$

In SPICE2, (21) is simplified further to yield the approximate expression"

$$q_b = \frac{1}{2}q_1 \cdot [1 + \sqrt{1 + 4'q_2}] \tag{22}$$

In SPICE2,  $q_1$  is approximated by the equation

$$q_1 = [1 - V_{bc}/V_A - V_{be}/V_B]^{-1} \tag{23}$$

while  $q_2$  has different expressions according to the region of operation. Both of these modifications are done in order to simplify the process of avoiding singularities in the expression under all possible operating ranges. Separation of  $q_1$  and  $q_2$  makes easier the assurance that  $q_2 \geq -\frac{1}{4}$  in order to avoid a complex result in the square-root portion of the expression. The more troublesome approximation of  $q_1$  uses the Taylor series expansion

$$[1 - X_1 - X_2 \dots]^{-1} \approx 1 + X_1 + X_2 \dots \quad (24)$$

in reverse to arrive at (23), which assumes that  $X_n \ll 1$ . Hence, the assumption that  $V_{bc} \ll V_A$  and  $V_{be} \ll V_B$  can be invalid for high frequency processes that characteristically have very low Early voltages. In the forward active region, optimistically low  $r_o$  results as  $V_{bc}$  approaches  $V_A$ .

Trying to remedy the inaccuracy in (23) by reverting to the more physical representation in (15) highlights the pretext for the approximation. As  $q_b$  is in the denominator of (9) and (18), a singularity exists at  $q_b=0$  which results in infinite collector current. This condition is met if high-level injection effects are negligible and  $V_{bc} = -|V_A|$ . One solution to the problem, as implemented in AT&T's ADVICE simulator, employs numerical integration to better estimate the depletion capacitance stored charge,  $q_1$ , as follows:

$$q_1 = 1 + \frac{1}{V_A} \int_0^{V_{bc}} [1 - V_{bc}/\phi_c]^{-mc} dV_{bc} \quad (25)$$

$$+ \frac{1}{V_B} \int_0^{V_{be}} [1 - V_{be}/\phi_e]^{-me} dV_{be}$$

Non-zero and non-negative  $q_b$  values still may need to be verified but the simulation accuracy of circuits utilizing high speed processes can be vastly improved here.

### C. Contributions to High-Level Injection

The high-level injection theory thus far has considered only the Webster effect. When the injected minority-carrier density in the base approaches the majority-carrier density, the injected carriers effectively increase the base doping, which in turn, causes the emitter efficiency to decrease. This conductivity modulation in the base is dependent on the base doping profile, as the graded base profile of implanted transistors helps by pitting the highest majority-carrier density at the emitter edge against the high density of injected minority-carriers. Other contributions to the loss of common-emitter forward current gain at high current density are current crowding and lateral current spreading that accompany this effect at the emitter-base junction. SPICE's parameter IK models these effects quite well.

High-level injection effects not taken into account in the previous considerations include Auger recombination (opposite of avalanche multiplication). Reduction of  $f_T$  by nonuniform base bandgap narrowing<sup>22</sup> due to the high doping concentration can give rise to an electric field that is comparable to and against the built-in field. Low injection assumptions also do not hold in locations where the material

is lightly doped, such as in the collector close to the base where the epitaxial material is not affected by any buried layer up-diffusions. This region is very significant since it allows a higher breakdown voltage (sustaining voltage), reduces collector capacitance, and reduces base-collector space-charge layer widening into the base (Early effect). This section presents some of the complications and undesirable consequences which arise from the low collector doping.

Base widening or "pushout" (Kirk effect), referred to as quasi-saturation in this thesis, is the primary cause of  $h_{FE}$  rolloff in  $n^+pn^-n^+$  epitaxial transistor structures.

Quasi-saturation can be defined as the condition when the internal base-collector metallurgical junction is forward biased, even though the external base-collector terminals have a reverse bias applied. At high collector currents, conductivity modulation of the collector resistance causes large internal voltage drops that lead to saturation of the intrinsic transistor. Under these operating conditions, minority-carriers are injected into the lightly doped epitaxial region, widening the electrical base of the device from  $W_B$  to  $W_{CIB}$  (current-induced base) thereby reducing  $h_{FE}$  and storing excess charge in the epitaxial region. The net effect for design considerations is a common-emitter I-V characteristic with two-region saturation<sup>23</sup> exhibiting a distinct transition region between the ohmic saturation region and the forward active region.

# Net Impurity Concentration

for an NPN Transistor

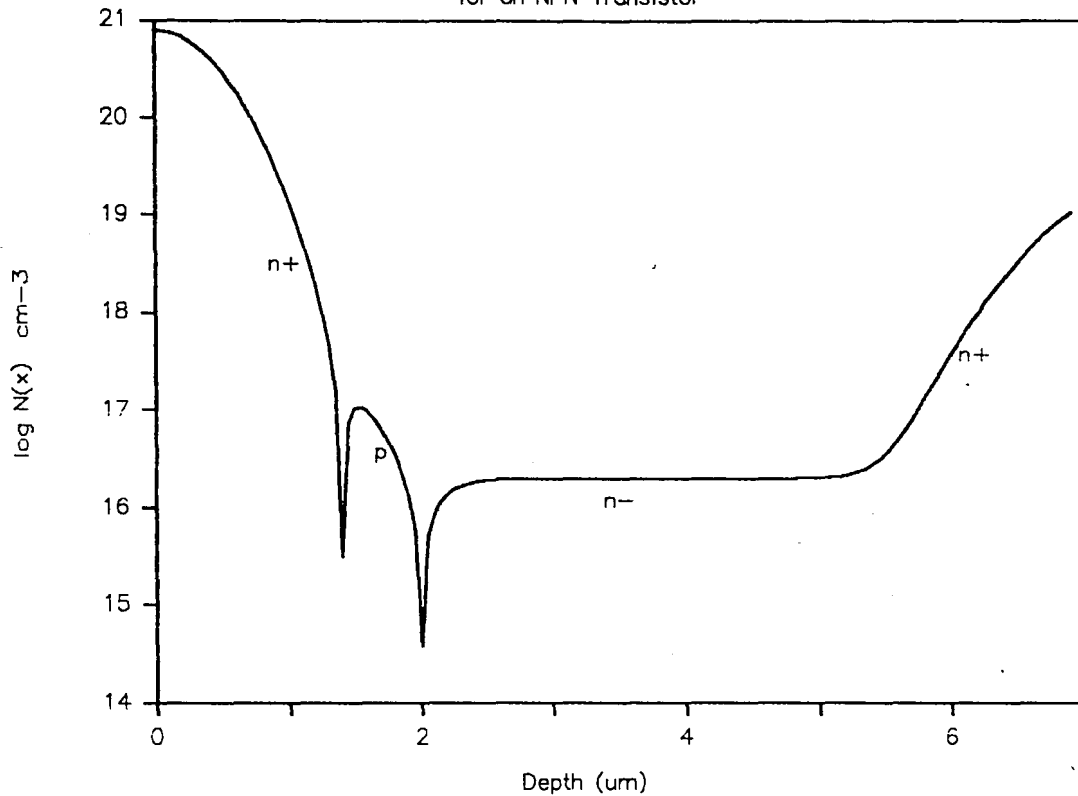


**Figure 3.** Net doping profile of a high-speed  $n-p-v-n$  transistor showing lightly doped epitaxial collector ( $v$ -region).

This section considers the one dimensional structure for a silicon epitaxial  $n-p-v-n$  transistor with a net doping profile as depicted in Figure 3 which is typical for transistors in high-speed integrated circuits ( $f_T \approx 9-10$  GHz). Here, the double-implanted transistor yields  $W_B \approx 0.5 \mu\text{m}$  and  $W_C \approx 4 \mu\text{m}$  with the arsenic doped emitter referenced at  $x_e=0$ . If we conceptualize a sketch of the typical dependence of  $\beta_F$  versus  $I_C$  (constant  $V_{CE}$ ) which can be plotted from (8) and (18), the influence of  $Q_f$  becomes noticeable at  $I_C \approx I_{KF}$ , resulting in a somewhat strong decrease of  $\beta_F$  while  $\tau_f$  remains relatively constant. Above what we will term  $I_{K2}$

base widening occurs as the *effective* base extends into the epitaxial collector region. As a consequence,  $\tau_f$  increases rapidly, which results in a stronger decrease of  $\beta_F$ . It is this current range above  $I_{K2}$  that is of particular interest for high-speed circuits that cannot be modeled accurately by present day SPICE2 based simulators.

A more detailed examination of the quasi-saturation region as discussed in Ref. [19] and Appendix A of Ref. [6] reveals a possible implementation of a *B factor*<sup>24</sup> in SPICE that is consistent with the ICCR. In low injection or when

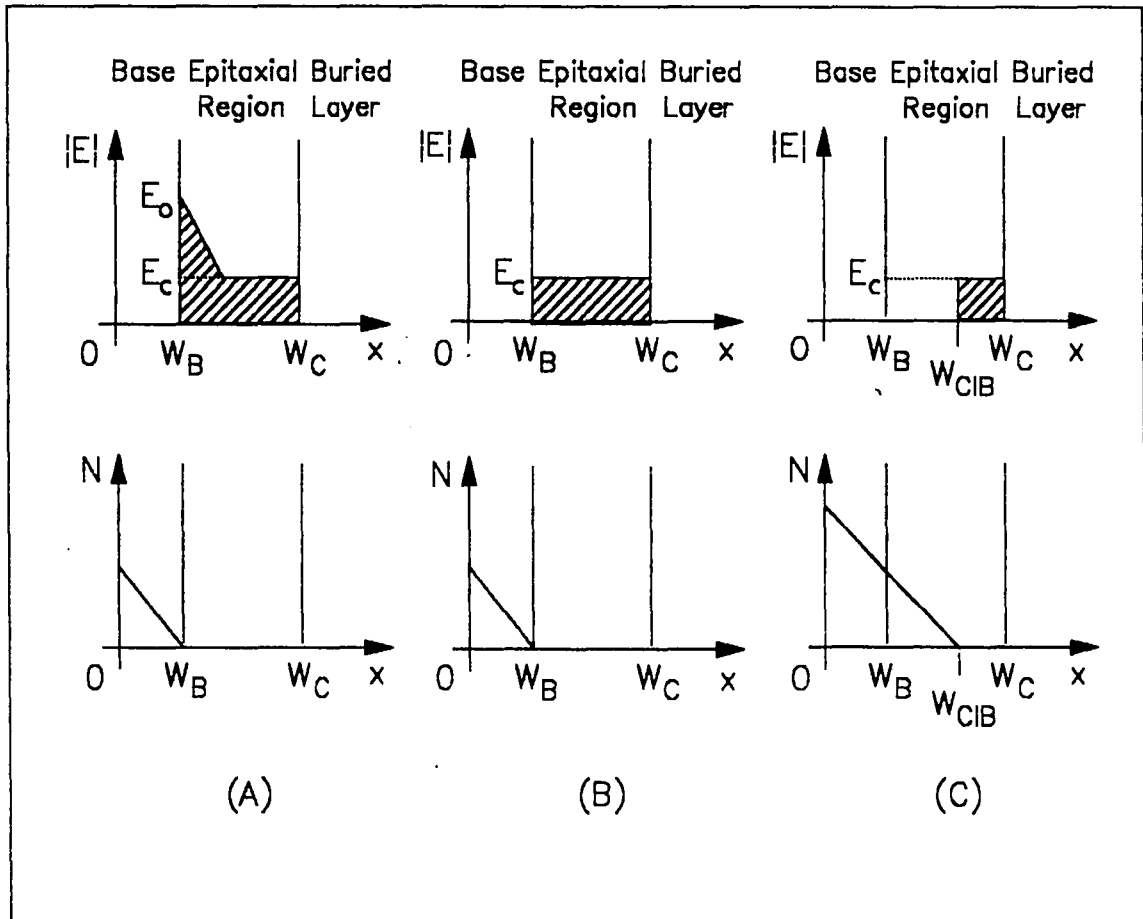


Figure 4. Electric field and stored charge in regions of (A) non-saturation, (B) threshold of quasi-saturation, and (C) well into quasi-saturation<sup>25</sup>.

$I_C < I_{K2}$ , (A) the epitaxial region is fully depleted and the transistor behaves as a base width,  $W_B$ , and the E-field region exists near the transition between base and epitaxial layer. Under high injection conditions as described above, the low-field  $E_C$ , depletion layer shrinks (B) and eventually collapses accompanied by (C) an expansion of the base width to  $W_{CIB}$ . The high-field region is finally relocated to the interface between epitaxial layer and substrate (or buried layer) and the epitaxial layer acts as an extension of the base with its attendant increase in the delay time  $\tau_f$ .

It has been argued that the ICCR still holds while in quasi-saturation as long as the basic differential equations are solved numerically with boundary conditions<sup>26</sup> applied at the electrical terminals and that the implications of using a one-dimensional model are justified. Poon, et al<sup>27</sup> addressed the problem of "high-field relocation" from the charge control point of view with detailed numerical results of the quantities electric field and carrier concentrations as discussed above. A significant finding in Poon's work was confirmation of the shape of delay time versus collector current curve. By considering the metallurgical base and the low-field region of the epitaxial region as a composite region, they surmised the high-injection delay time,  $\tau$ , through the effective base is approximately

$$\tau = w^*/4D_n \quad (26)$$



where  $w^*$  is the width of the effective base,  $W_{CIB}$ , and  $D_n$  is the diffusion constant for electrons. The additional factor of 2 in the denominator of (26), as compared to the standard expression for delay time, is due to the Webster effect assuming  $I_C > I_{K2} > I_{KF}$ .

One should note that the "knee currents"  $I_{KF}$  and  $I_{K2}$  are independent as long as  $I_{K2} > I_{KF}$ .  $I_{KF}$  is determined by the net doping profile in the base while  $I_{K2}$  is influenced by the thickness and doping concentration of the starting epitaxial collector material. Because of the modulation that occurs in the lightly doped epitaxial collector region,  $I_{K2}$  shows a much stronger dependence on  $V_{CE}$  as compared to the influence on  $I_{KF}$ . For very thick and/or lightly doped epitaxial sheets and low  $V_{CE}$ ,  $I_{K2}$  may even fall below  $I_{KF}$ .

Two distinct models have been developed to describe quasi-saturation as the current in an  $n-p-v-n$  transistor is increased. The shrinking of the depletion layer and its eventual collapse, as proposed above, drives the transistor into quasi-saturation, accompanied by expansion of the base into the collector region. The carrier drift velocity is assumed to be linearly proportional to the electric field. This scenario is most common for low voltage applications in the ohmic region of operation and is known as the constant (saturated) velocity or low-field case (*LFC*). Yet another explanation is a reduction of the space-charge density in the depletion layer, causing it to expand until it fills the

lightly doped epitaxial collector region. Further increases of collector current results in scattering-limited drift velocity (*SLDV*) in the depletion region leading to growth of the effective base width by one and two-dimensional effects. This scenario is most commonly encountered at higher supply voltages in the nonohmic region of operation and is known as the constant mobility<sup>28</sup> or high-field case (*HFC*). These two suggestions for the internal phenomena responsible are often difficult to separate in the many studies of observed transistor behavior (see dotted line, Figure 5).

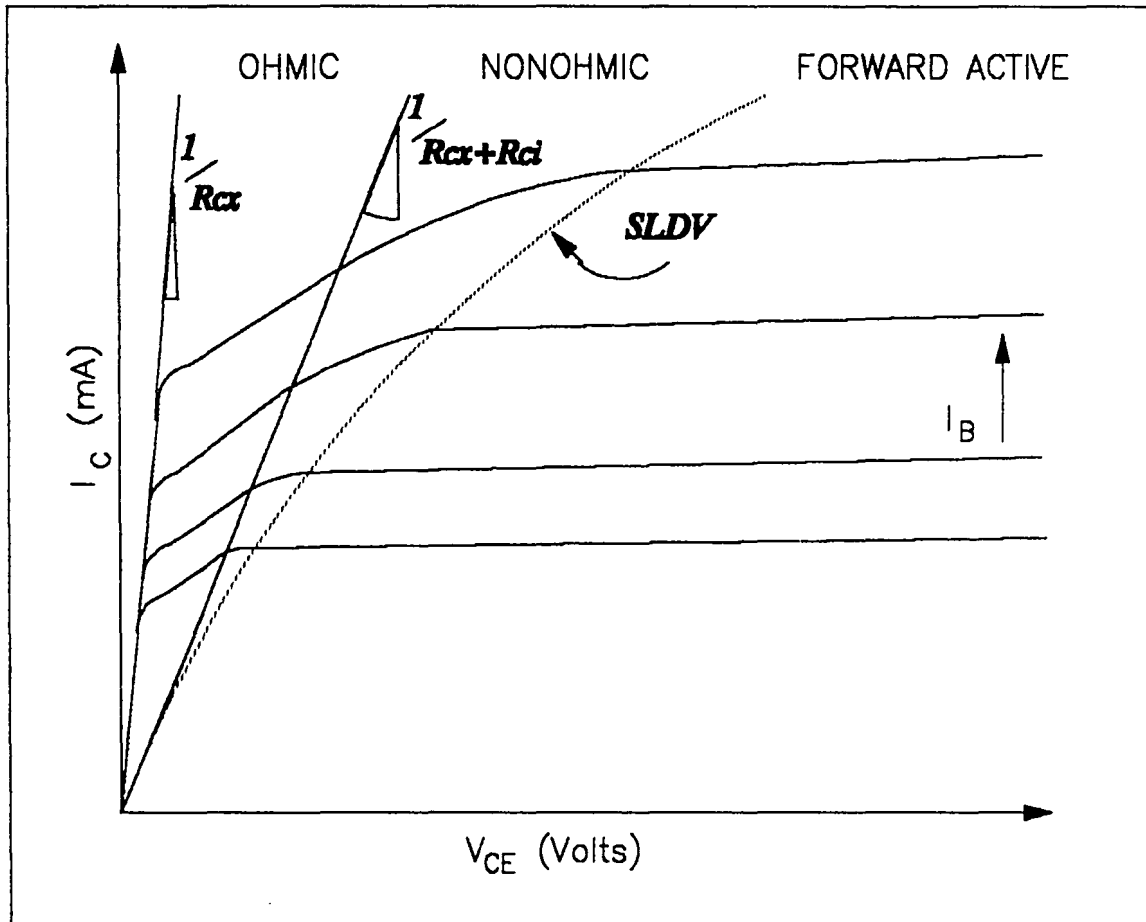


Figure 5.  $I_C$  versus  $V_{CE}$  characteristic for typical *n-p-v-n* transistor under consideration showing ohmic and nonohmic quasi-saturation regions of operation.

As it turns out, the model proposed in Refs. [6], [19], and [24] implementing a *B factor* in SPICE, affects only the constant velocity case (*LFC*).  $W_{CIB}$  takes the classical form of Kirk's results:

$$W_{CIB} = W_C (1 - I_C^*/I_C) \quad (27)$$

where  $I_C^*$  is the critical current at which the depletion layer collapses and is defined as:

$$I_C^* = (V_{bc} + \phi_c) / R_{CO} \quad (28)$$

where  $R_{CO}$  is the epitaxial region resistance to be defined later. From this, the base pushout factor, *B*, may take on many forms as explained in the references but is always used as a multiplier for  $Q_f$  in equations (12) through (15) and has a value of 1 in low level injection.

$$Q_b = 1 + V_{be}/V_B + V_{bc}/V_A + B \cdot I_S/I_{KF} (e^{V_{be}/V_t} - 1) + I_S/I_{KR} (e^{V_{bc}/V_t} - 1) \quad (29)$$

Still, there have been many studies undertaken to see which effect is dominant. When van der Ziel and Agouridis<sup>29</sup> first proposed a model based on space-charge limited current flow, extensive experimental data were taken by Beale and Slatter<sup>30</sup> and later Whittier and Tremere<sup>31</sup> in an effort to show that two-dimensional effects such as lateral injection are predominant. An important motive in Beale and Slatter's study was a small-signal equivalent circuit that included a physically based model for total minority carrier charge stored in the collector. This will be highlighted in the model development that follows. Later investigations<sup>32,33</sup>

suggest the need for a unified approach that includes both Kirk and van der Ziel and Agouridis effects. Kumar and Hunter<sup>34</sup> showed evidence that a one-dimensional model is adequate to model space-charge limited current flow as well, and used Whittier and Tremere's data to demonstrate this.

The extended model for the epitaxial collector region derived by Kull, et al<sup>35</sup> supports both constant (saturated) velocity and scattering-limited drift velocity mechanisms in the depletion region of the collector. Two other equations define the excess charge stored in the epitaxial collector represented by the term  $Q_{c0}$ . For a one-dimensional device  $\phi_p$  is the applied potential at the base side of the base-collector junction and  $\phi_n(w)$  is the potential applied at the collector terminal, neglecting any ohmic drop across the  $n^+$  buried layer. The boundary conditions used in the epitaxial region for this analysis are as follows:

$$\begin{aligned}\phi_n(0) - \phi_p &= V_{bco} \\ \phi_n(w) - \phi_p &= V_{bcw}\end{aligned}\quad (30)$$

Note that normal forward active mode is represented by the condition  $0 > V_{bco} > V_{bcw}$ , quasi-saturation by  $V_{bco} > 0$  and  $V_{bcw} < 0$  still, and full saturation or reverse mode of operation by  $0 < V_{bco} < V_{bcw}$ .

The minority current transport equation

$$\begin{aligned}J_n &= -q\mu_n n \delta\phi_n / \delta x \\ &= -q\mu_{no} / w \cdot [1 + |V_{bco} - V_{bcw}| / V_0]^{-1} \int_{\phi_{no}}^{\phi_{nw}} n d\phi_n\end{aligned}\quad (31)$$

in this form incorporates the effect of carrier velocity saturation, where  $V_0 = wv_s/\mu_{no}$  describes this effect.

Evaluating the integral portion of (31) results in

$$\int_{\phi_{no}}^{\phi_{nw}} n d\phi_n = -V_t \{ 2[p(0) - p(w)] + N \ln[p(0)/p(w)] \}$$

and assuming quasi-neutrality, can be expressed in terms of electron concentration

$$\int_{\phi_{no}}^{\phi_{nw}} n d\phi_n = -V_t \{ 2[n(0) - n(w)] + N \ln[n(0)/n(w)] + N/V_t [V_{bco} - V_{bcw}] \} \quad (32)$$

Applying quasi-neutrality and (32), (31) yields an equation for the current in the epitaxial region:

$$I_{epi} = \frac{V_t \{ K(V_{bco}) - K(V_{bcw}) - \ln[(1+K(V_{bco}))/(1+K(V_{bcw}))]] \} + V_{bco} - V_{bcw}}{R_{co} [1 + |V_{bco} - V_{bcw}|/V_0]} \quad (33)$$

where  $R_{co} = w/(q\mu_{no}NA)$ ;  $\Gamma = (2n_i/N)^2$ ;  $A$  is the device area; and  $K(V) = \sqrt{1 + \Gamma \exp(V/V_t)}$ .

This analysis can equally be applied to pnp transistors by defining a current,  $I_{epi}$ , of opposite polarity as flowing from the epitaxial region out of the collector contact.  $R_{co}$  represents a zero-bias intrinsic collector resistance of the epitaxial region under equilibrium conditions and models the conductivity modulation effect in the epitaxial collector region.  $V_0$  represents the threshold of space charge limited current flow and, as previously stated, models the effect of carrier drift velocity saturation. When the device is operating at low currents in normal forward active mode with

no quasi-saturation and the base-collector reverse biased at much less than  $V_0$ , then (33) reduces to Ohm's law

$$I_{\text{epi}} = (V_{\text{bco}} - V_{\text{bcw}})/R_{\text{CO}} \quad (34)$$

Ref. [35] goes into a detailed and lengthy derivation of a more or less exact calculation of the excess stored charge in the epitaxial region, but then goes on to say that a small signal analysis carried out shows that  $Q_{\text{epi}}$  can be modeled with a lumped representation in two parts, with

$$Q_{\text{epi}} = Q_0 + Q_W \quad (35)$$

where  $Q_0 = Q_{\text{CO}} [K(V_{\text{bco}}) - 1 - \Gamma/2]$

and  $Q_W = Q_{\text{CO}} [K(V_{\text{bcw}}) - 1 - \Gamma/2]$

Here, the apportionment of  $Q_{\text{epi}}$  results in  $Q_{\text{CO}} = qWNA/4$ .

These approximate expressions are implemented as discrete charge storage elements and this partitioning is accurate at low frequencies and under either very low or very high injection conditions. This paper investigates the use of the model as presented here, but for very high frequency (VHF) applications, other choices for distribution of the modeling term  $Q_{\text{CO}}$  are being investigated.

For completeness, well known models for bandgap and carrier drift velocity can be used to implement temperature dependence of  $R_{\text{CO}}$ ,  $V_0$ , and  $\Gamma$  as follows:

$$\begin{aligned} R_{\text{CO}}(T) &= R_{\text{CO}}(T_0) \cdot (T/T_0)^{\text{TRCO}} \\ V_0(T) &= V_0(T_0) \cdot (T/T_0)^{\text{TVCO}} \\ \Gamma(T) &= \Gamma(T_0) \cdot (T/T_0)^3 e^{qEg/kT(T/T_0-1)} \end{aligned} \quad (36)$$

In summary, with the introduction of three circuit elements  $I_{epi}$ ,  $Q_0$ , and  $Q_w$  described by four model parameters  $R_{CO}$ ,  $V_0$ ,  $\Gamma$  and  $Q_{CO}$  we are able to predict reasonably well the characteristics of a device exhibiting base push-out in various modes and degrees of quasi-saturation. The temperature dependence of these parameters is well defined by silicon material properties. This is by no means the only model suggested to predict the behavior of transistors exhibiting base push-out, as other viable choices have been suggested<sup>6,36</sup>, but its capability to model ohmic as well as space-charge limited current flow makes it particularly suitable for modeling transistors in quasi-saturation.

#### D. Avalanche Breakdown

Avalanche current multiplication and breakdown at the junction is a well understood physical phenomenon in semiconductor devices, yet its significance for proper circuit operation is often overlooked by many designers. Study is limited to the collector-base junction because consequences of  $BV_{CEO}$  breakdown in circuits are more critical, although the theory can be applied to the base-emitter junction.

The theory as outlined in several basic texts<sup>37,38</sup> is illustrated with a junction under reverse bias. Thermally generated electrons gain kinetic energy from the electric field. When the field is above some critical field,  $E_c$ , the electrons gain enough energy that collision with lattice

atoms can break the bonds producing an electron-hole pair. These new electron-hole pairs gain kinetic energy from the field and produce additional electron-hole pairs, hence the process is called *avalanche multiplication*. The rate of ionization will be studied to determine a breakdown voltage.

To derive the breakdown condition, the classical multiplication factor is defined as

$$M \equiv I_n(W)/I_{no} = (1 - |v_R|/BV)^{-m} \quad (37)$$

where the avalanche breakdown voltage is defined as the voltage where  $M$  approaches infinity. With the critical field determined, we calculate the breakdown voltage using

$$BV = E_c W/2 = \epsilon_s E_c^2 / 2q (N_B)^{-1} \quad (38)$$

where  $N_B$  is the background doping of the lightly doped side of the junction and,  $\epsilon_s$  is the permittivity of the material. It should be noted that tunneling, a characteristic of zener breakdown, occurs only in semiconductors having high doping concentrations. Hence, most breakdown scenarios would be properly modeled by an avalanche mechanism. Even most zener diodes are truly dominated by avalanche mechanisms.

Another mechanism interacts with the current gain characteristic of the transistor, which results in the breakdowns seen in typical common-emitter configurations,  $BV_{CEO}$  breakdown. Some empirical models fit this relation to the well known expression

$$BV_{CEO} = BV_{CBO} / \sqrt[n]{\beta} \quad (39)$$

where  $n$  is typically between 2 and 3.



### III. AT&T'S CBIC-V TECHNOLOGY

#### A. Device Features

CBIC-V is a complementary bipolar integrated circuit technology consisting of vertical NPN and PNP transistors, programmable MNOS capacitors, implanted boron resistors, and optional thin-film ( $Ta_2N$ ) resistors. The CBIC-V process offers the advantages of similar performance characteristics on the NPN and PNP transistors for very high frequency (VHF) applications. Peak  $f_T$  values of 10.2 GHz for the NPN and 4.3 GHz for the PNP transistors and high-current drive capability (5 mA for the 1X structures) are unique for this junction isolated technology. Interconnect is accomplished through two levels of metallization with both top-metal and bottom-metal having the same low 0.04  $\Omega$ /sq. sheet resistance and a 2 mA/ $\mu$ m of metal width current carrying capability providing a proven electromigration-resistant contact scheme. Transistor specifications can be found in Table 2.

Miniaturization has long been a trend in the modern semiconductor industry. The products of this effort are high speed and obviously high packing density. Dielectric isolation by local oxidation of silicon (LOCOS) is of some limited use but suffers due to lateral oxidation under the nitride masking process. The larger area typically needed for an individual transistor of this type leads to increased device tub parasitic capacitance. Increased parasitic

**TABLE 2 CBIC-V NPN and PNP Transistor Specifications**

Parameter	NV231A01			PV231A01			Units
	Min	Typical	Max	Min	Typical	Max	
$\beta$ (@1mA)	50	118		25	45		
$f_T$ ( $V_{CE}=3v$ )	8.0	10.2		3.0	4.3		GHz
$V_A$ (@1mA)	12	27		6.0	11		V
$V_{CE}(sat)$		86	180		188	360	mV
$V_{BE}$ (@1mA) 740	780	810	750	792	830		mV
$BV_{CEX}$ (100uA)	6.0	11.5		6.0	15		V
$BV_{CBO}$ (@1uA)	6.0	19		8.0	22		V
$BV_{EBO}$ (@10uA)	2.0			3.5			V
$BV_{EBS}$ (@1uA)	0.2			0.1			V
$C_{JE}$ (@0v)		120			120		fF
$C_{JC}$ (@0v)		80			130		fF
$C_{JS}$ (@0v)		100			510		fF
footprint		32.5 x 47.5			32.5 x 47.5		$\mu m^2$

capacitance necessitates additional current to drive the parasitics. With the increased power consumption, even medium scale integration (MSI or LSI) of high speed bipolar IC's may consume more power than is practical. A more compact, essentially planar, isolation technique such as Selective Epitaxial Growth<sup>39</sup> (SEG) allows CBIC-V to achieve high speed and a respectable level of integration (note transistor footprint in Table 2).

This novel complementary bipolar process permits fabrication of IC's with circuit speed improvements calculated to a factor of 2 to 3 over conventional pn junction isolated transistors. The increase in high speed circuit performance does not necessarily come from the individual transistors  $f_T$  but comes from the reduced collector-substrate (or epi-sub)

capacitance. This capacitance measured on SEG transistors is about half of that measured on pn junction isolated transistors. Packing density can be improved by a factor of 2 to 5 and the reduced power dissipation make the SEG process a viable candidate for future bipolar VLSI.

SEG isolation was applied to CBIC-V to achieve compact, planar oxide isolation between components. N and P-type selective epitaxial films are grown on heavily doped arsenic and boron buried layers. High speed requirements still demand that a shallow junction technology based on reduced processing temperatures be used. Therefore, low energy ion implantation, rapid thermal anneal (RTA) and low temperature dielectrics are employed extensively instead of the more conventional processes. Photolithography is done with a minimum feature size of 1 $\mu$ m and a number of self aligning mask steps are used to improve layer registration accuracy.

Device design uses a more conventional structure which reflects the need for a robust, high yield, high performance device which is compatible with the process above and equipment capabilities. The NPN transistor in Figure 6 has all of the necessary features for premium performance IC's, such as buried layer, deep collector plug, and striped bases and emitters. The NPN also has a channel-stop layer to prevent surface inversion of the lightly doped p-type substrate.

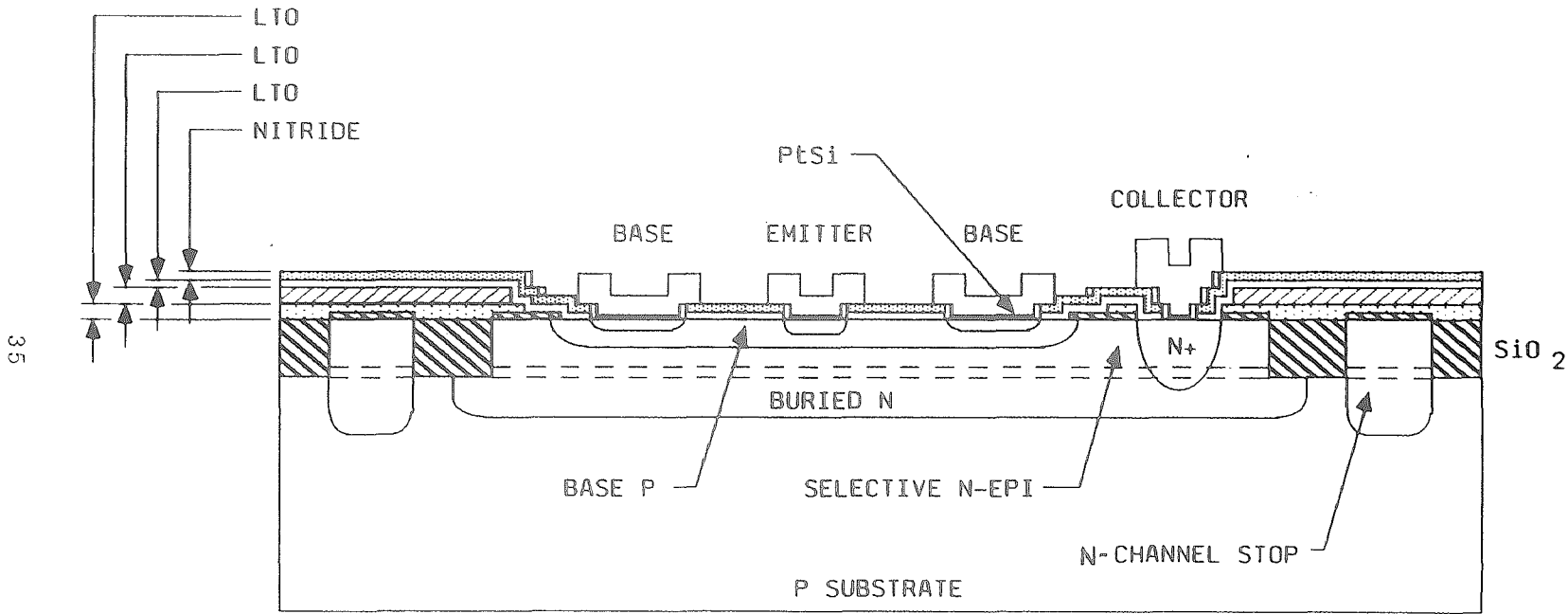


FIGURE 6 NPN Cross-sectional view

The PNP transistor in Figure 7 has all of the features of the NPN (except channel-stop) and two additional features: a lightly doped n-type region for collector isolation and a buried (ISOTUBN) n-type region for collector isolation from the p-substrate. This guarantees latch-free operation of the PNP at all possible bias conditions. Also, a reverse bias applied to the ISOTUBN layer through an epitaxial contact allows us to reduce collector-substrate (epi here) parasitic capacitance.

#### B. Process Description<sup>40</sup>

The first process step grows a thermal oxide on the lightly doped p-type substrate. The first photoresist (PR) step defines the three buried-n layers. The second PR step only opens the lightly doped ISOTUBN layer. Two PR steps then define features for the channel-stop and buried-n layer each followed by an implantation of boron and arsenic, respectively. Oxide grown during a subsequent anneal is then etched in areas where the n-type epitaxial film is to be deposited. A thin thermal oxide is grown to protect it from further nucleation during the p-type epitaxial deposition which is done after the p-buried layer is defined and implanted. Another thin thermal oxide is grown to preserve the integrity of the epi-oxide interface.

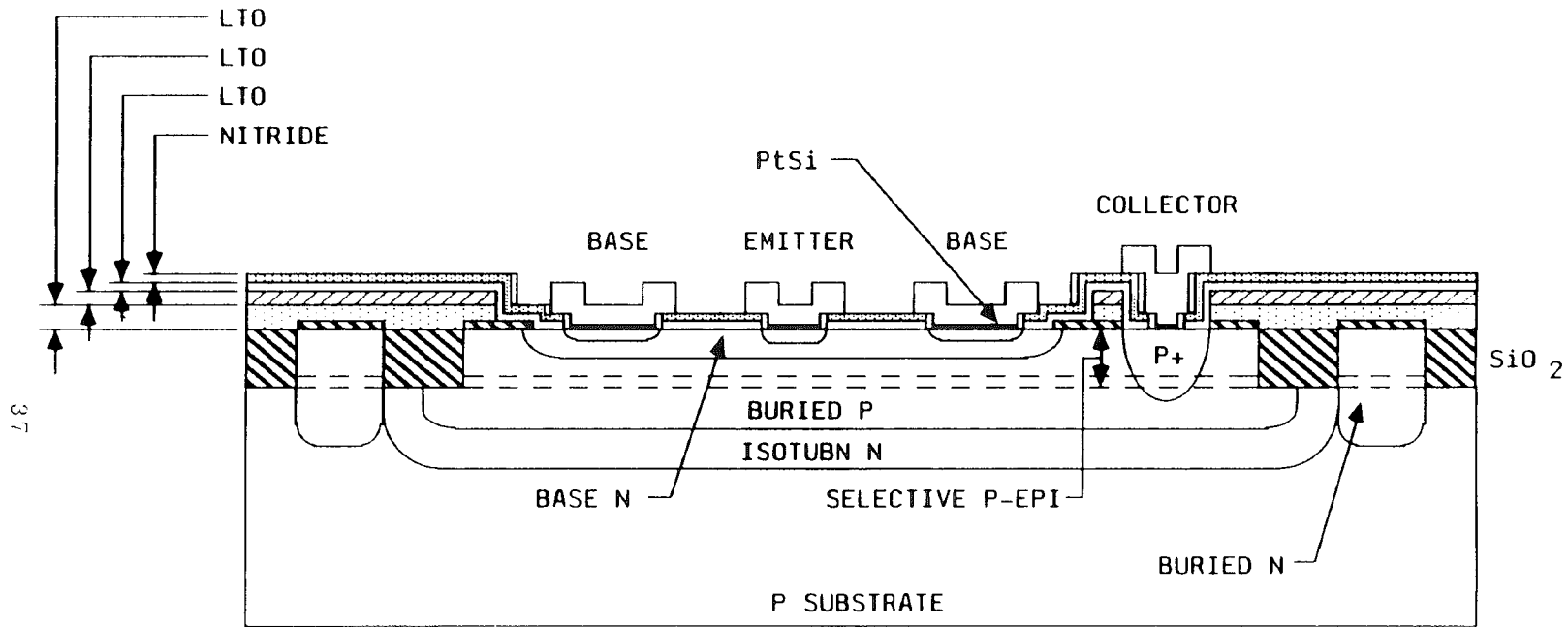


FIGURE 7 PNP Cross-sectional view

Heavily doped  $n^+$  and  $p^+$  deep collector regions are created in the next PR steps. A field oxide is deposited via a low temperature LPCVD process to minimize up-diffusion of the buried layers into the very thin epitaxial films. The n-base for the PNP and n-collector for the NPN is defined and implanted next and an n-base contact enhancement tub is formed to reduce the extrinsic base resistance ( $R_{BM}$ ) and improve  $f_{max}$  of the PNP. The NPN is processed similarly while the p-base tub is concurrently used for the low value 80  $\Omega$ /square diffused resistors. The final field oxide is deposited and the base box is defined. Thin layers of oxide and nitride are deposited before all of the contact windows are opened. Photoresist itself is used as a mask for the p and n-type emitters and an RTA sets the final gain.

Two levels of gold metallization, already proven in production on some of AT&T's slower speed processes, starts with PtSi formation in the contact windows with subsequent removal of unreacted platinum. A sandwich structure of Ti-TiN-Pt-Au-Pt is back sputtered for the first level of metallization and a low temperature LPCVD process is used to deposit the interlevel dielectric, SiN. Top metallization starts with a layer of Ti-TiN-Pt sputtered on the wafer and the following TOPMET PR step defines where Pt is chemically etched. PROTECT2 defines the pattern for gold plating of exposed Pt. A final layer of  $Si_3N_4$  for surface passivation is deposited and etched over bond pads in a SINCAP PR step.

With this high performance complementary bipolar process, a host of linear and digital circuits such as amplifiers with active loads, voltage regulators (low PSRR over wide bandwidth), voltage controlled oscillators, phase-locked loop circuits, D/A converters and other circuits will benefit from the availability of such a high speed substrate isolated PNP transistor. The lack of a high performance PNP often necessitates undesirable circuit tricks such as the use of a buried zener diode for passive level shifting or more elaborate output stages that provide level shift and gain. This typically requires a positive feedback scheme which is prone to oscillation. Excessive use of NPN transistors leads to higher power dissipation.

As one can see, complementary technology (CBIC or CMOS) has a number of distinct advantages over a non-complementary technology. While the CMOS inverter with its very small static power consumption is well known, the advantages of CBIC are not yet widely publicized. It is premium performance analog IC's that demand CBIC-V.



#### IV. IMPLEMENTATION OF A UNIFIED MODEL AND PARAMETER EXTRACTION

##### A. Unified Circuit Model Including Quasi-Saturation

The compact circuit model implemented in this work is a four terminal macro (subcircuit) model, the second of two models that have been developed in Ref. [35]. The main transistor represents the primary operation of the device including the base push-out (quasi-saturation) extension developed in section II-C. A partial Gummel-Poon model is specified to describe substrate injection. The actual macro model implemented here employs a full Gummel-Poon model of the opposite sex for parasitic action, but this simply burdens the simulation routines with some unnecessary computations that could be avoided if a true partial Gummel-Poon model were employed. When  $R_{C0}$  is set to zero (its default) in the PSpice simulator used, the main Gummel-Poon models reduce to bipolar transistor structures which do not exhibit quasi-saturation.

Automated parameter extraction programs are used at AT&T in Reading, Pennsylvania to extract and optimize the model parameters for the circuit simulator ADVICE. A complete description of these extraction programs is beyond the scope of this paper, but it is the optimized parameters for the ADVICE model which were translated into the PSpice implementation presented in this work. A brief discussion

on extraction procedures for the four parameters developed in section II-C and the reverse knee current parameter  $I_{KR}$  are described.

Transistor characteristics selected for our choice of  $R_{CO}$  and  $V_0$  are a set of  $I_C$  versus  $V_{CE}$  curves at constant emitter-base voltage. Referring back to Figure 5 in which ohmic and nonohmic quasi-saturation, as well as normal forward active mode are defined, points along the nonohmic and normal forward mode are chosen to represent operating conditions at which quasi-saturation effects have just become negligible. It can be difficult to determine the exact values of  $V_{bco}$  at the edge of this region from the terminal characteristics. However, if chosen at high enough current values such that  $|V_{bcw}| \gg |V_{bco}|$ , then the drop across the epitaxial region is large and one can approximate  $V_{bco} \approx 0$ . Consequently, (33) reduces to<sup>35</sup>

$$I_C = \frac{-V_{bcw}}{R_{CO} [1 + |V_{bcw}|/V_0]} \quad (40)$$

where  $V_{bcw} = [V_{BC} - I_b(R_{bx} + R_{bi}/q_b) + I_C R_C]$  and  $q_b$  is the normalized base charge. Parameters  $R_{CO}$  and  $V_0$  can be solved simultaneously at points along the nonohmic and forward active modes of operation.

Extraction of  $\Gamma$  and  $I_{KR}$  are carried out simultaneously as well. In order to optimize the accuracy of the unified model in the forward and quasi-saturation modes, a data

point deep in the ohmic region is used to represent a condition in which the transistor is operating at a high injection level with significant quasi-saturation effects. Equations (8), (18), (33), and the following equation describe the devices dc operating conditions:

$$q_b = \frac{I_b R_{bi}}{V_{BE} - I_b R_{bx} - (I_b + I_c) R_e - V_{be}} \quad (41)$$

which is a statement of Kirchoff's voltage law where  $q_b$  is expressed as a function of  $I_{KR}$ . These equations are solved simultaneously for four unknowns:  $V_{be}$ ,  $V_{bco}$ ,  $I_{KR}$ , and  $\Gamma$ .

Extraction of  $Q_{CO}$  requires a data point in the quasi-saturation region of a  $1/2\pi f_T$  versus  $1/I_C$  curve. This is the region where the  $1/2\pi f_T$  versus  $1/I_C$  curve bends upward. Assuming the parameter  $T_F$  is determined from a low injection level region of the curve, and the dc and capacitance model parameters are obtained,  $Q_{CO}$  is determined by solving these analytical expressions using an iterative technique.

A second and more serious modeling problem lies in the limitations of the basic three terminal representation of the BJT to model correctly the collector-base junction capacitance,  $C_{JC}$ . Commercially available SPICE 2G.6 based programs perform the fractional distribution of intrinsic and extrinsic portions of  $C_{JC}$  with the model parameter  $XCJC$  (see Figure 8). However, the specified distribution of  $C_{JC}$  around the intrinsic base reduces to the case of  $XCJC = 1$

when evaluated in the expression for gain-bandwidth<sup>41</sup>. An aggregate capacitance for  $C_{JC}$  multiplied by the  $(1 + g_m R_C)$  term results in substantially lower values of  $f_T$  if one attempts to model higher collector resistances correctly.

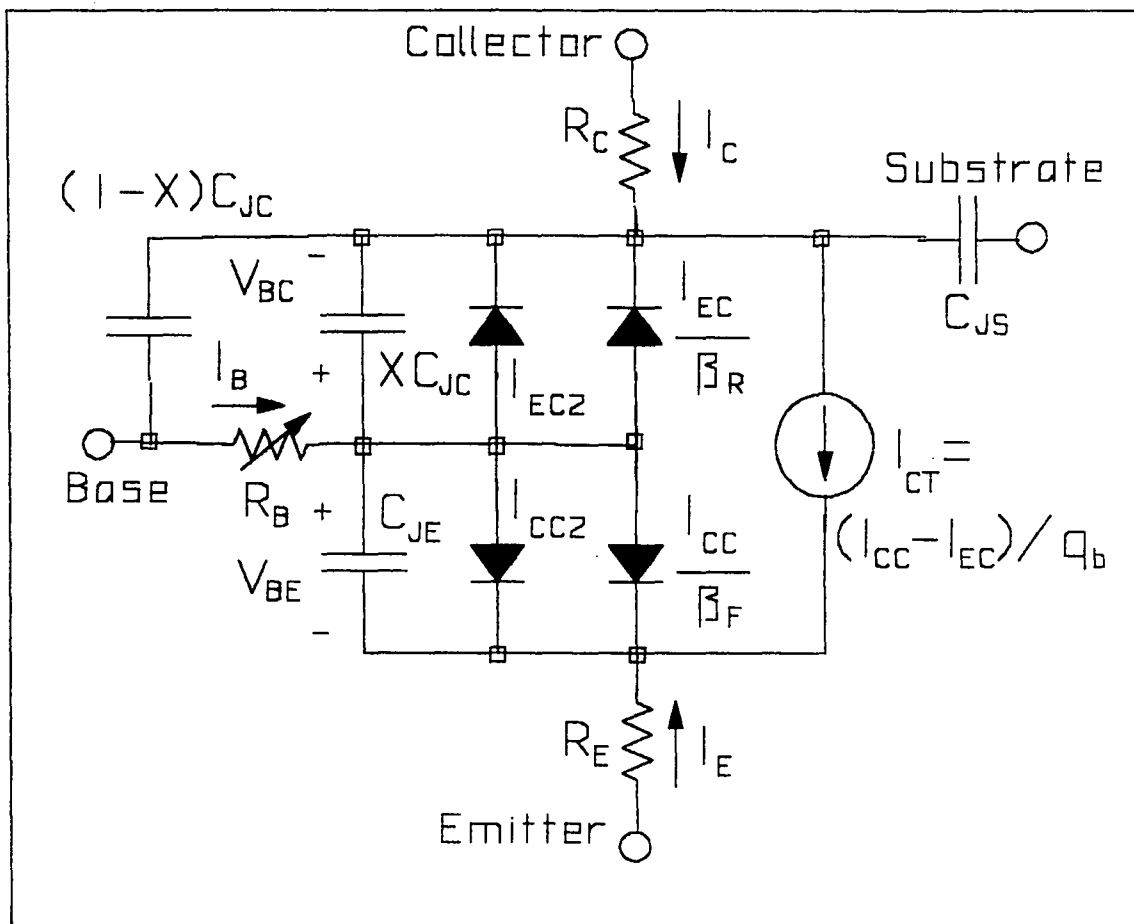


Figure 8. Equivalent circuit for model of transistor intrinsic to available SPICE programs

As a remedy, a subcircuit is used to separate  $C_{JC}$  and its parasitic counterpart,  $C_{JEP}$  (Figure 9). The subcircuit form of the transistor model overcomes the limitations described by specifying only the smaller portion of  $C_{JC}$  that is part of the active device and setting  $XCJC = 1$ . The remaining inactive sidewall capacitance associated with the

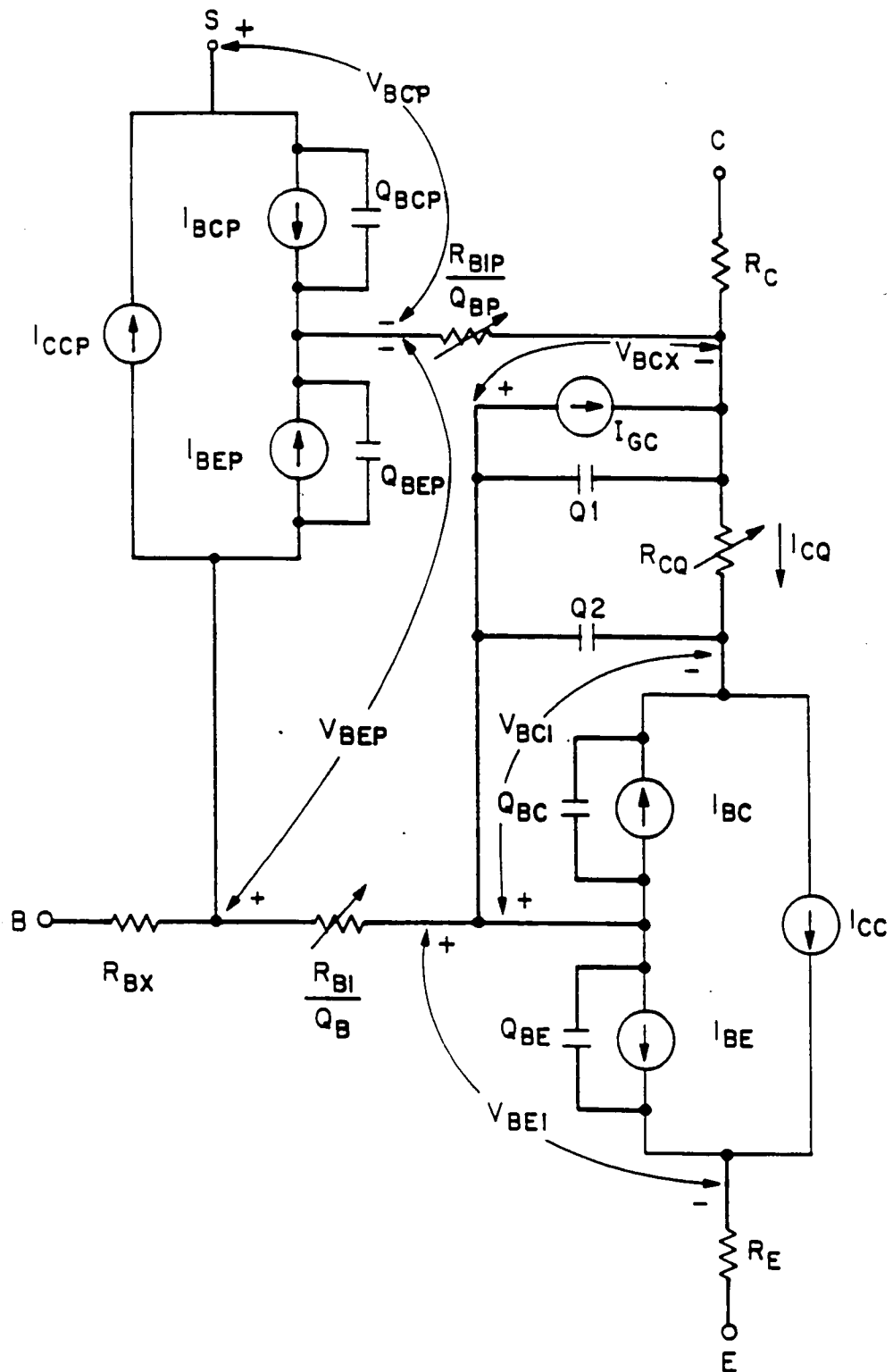


Figure 9. Equivalent circuit for Four-Terminal Extended BJT Model including quasi-sat effects 42

parasitic structure is physically apportioned to  $C_{JE}$  of the partial Gummel-Poon device representing the parasitic transistor. Appendix A shows a complete listing for a library of devices developed for AT&T's CBIC-V technology.

A transistor model using standard SPICE 2G.6 model parameters is also provided for each library component. Note that  $R_C$  is modeled extrinsically as a discrete resistor RCX, separate from the intrinsic transistor in SPICE. The extrinsic portion of the base resistance,  $R_{BM}$ , is modeled likewise with a discrete resistor RBX.  $R_{BM}$  in the intrinsic model is defined as some arbitrarily small value, but not zero to avoid the model parameter  $R_B$  from defaulting to a completely extrinsic representation of  $R_B$ . The model parameter  $I_{SC}$  is distributed between  $I_{SC}$  in the active transistor and  $I_{SE}$  in the parasitic transistor and all modeling parameters associated with  $C_{JS}$  have been moved to the collector-base junction of the parasitic device, since this now represents our fourth terminal.

Correctly modeling peak  $f_T$  in the SPICE implementation of the model required reducing the forward transit time,  $T_F$ , while scaling  $C_{JC}$  and  $R_C$  to their correct value for the four different transistor geometries available on AT&T's CBIC-V semi-custom array, the VB110. This leads to varying values of the  $T_F$  parameter for different transistor sizes which was simply a numerical attempt to control the contribution of each term in the denominator of the  $f_T$  expression:

$$f_T \approx 1/2\pi \frac{1}{T_F + [C_{JE} + (1 + g_m R_C) C_{JC}] \cdot 1/g_m} \quad (42)$$

This simplified expression for a three terminal BJT was derived for  $XCJC = 1$  but it can be shown that the case of  $XCJC < 1$  also reduces to (42). This means that the small signal bandwidth includes a time constant associated with the full value of the parameter  $C_{JC}$ , regardless of the specified  $XCJC$  split.

The small signal equivalent circuit for the BJT in Figure 8 has four capacitors producing four time constants as such<sup>41</sup>:

$$f_T = 1/2\pi \frac{g_m r_\pi}{R_{1o} C_{BE} + R_{2o} C_{BC} + R_{3o} C_{JS} + R_{4o} C_{BX}} \quad (43)$$

where the open circuit resistances are

$$\begin{aligned} R_{1o} &= r_\pi \\ R_{2o} &= r_\pi + (1 + g_m r_\pi)(R_C \parallel r_o) \approx r_\pi + (1 + g_m r_\pi)R_C \\ R_{3o} &= R_C \parallel r_o \approx R_C \\ R_{4o} &= R_B + R_{2o} \end{aligned} \quad (44)$$

with the assumption that  $r_o \gg R_C$  in the approximations for  $R_{2o}$  and  $R_{3o}$ . The base-emitter capacitance is composed of the diffusion capacitance,  $C_D$ , and the junction capacitance,  $C_{JE}$ , while the capacitances  $C_{BC}$  and  $C_{BX}$  are determined by the parameter  $XCJC$  according to their respective split

$$\begin{aligned} C_{BE} &= C_D + C_{JE} = g_m T_F + C_{JE} \\ C_{BC} &= XCJC \cdot C_{JC} \\ C_{BX} &= (1 - XCJC) \cdot C_{JC} \end{aligned} \quad (45)$$

We can simplify the expression by noting that the second and fourth poles in expression (43) can be reduced

$$\begin{aligned} R_{2o}XCJC \cdot C_{JC} + (R_B + R_{2o})(1 - XCJC) \cdot C_{JC} \\ = R_{2o}C_{JC} + R_B(1 - XCJC) \cdot C_{JC} \end{aligned} \quad (46)$$

to the three terminal equivalent circuit form with only the residual term  $R_B C_{BX}$  which has a negligible contribution to the time constant sum in (43). This eliminates the  $XCJC$  redistribution as far as the calculation of  $f_T$  is concerned. Substituting the time constants defined in (44) and (45) into expression (43), and applying the pole cancellation observed in (46) we obtain the following expression for gain-bandwidth product.

$$f_T \approx 1/2\pi \frac{g_m r_\pi}{r_\pi(g_m T_F + C_{JE}) + [r_\pi + (1 + g_m r_\pi)R_C]C_{JC} + R_C C_{JS}} \quad (47)$$

After some rearranging, equation (47) takes the form of the  $f_T$  expression in (42):

$$f_T \approx 1/2\pi \frac{1}{T_F + [C_{JE} + (1 + g_m R_C)C_{JC} + R_C/r_\pi \cdot C_{JS}] \cdot 1/g_m} \quad (48)$$

As was assumed in (42), the relative contribution of the third pole associated with  $C_{JS}$  is negligible since at low currents  $r_\pi \gg R_C$  and at higher currents  $f_T$  is dominated by the  $T_F$  parameter as the entire capacitive sum is divided down by a larger  $g_m$ . Hence equation (48) is equivalent to the  $f_T$  expression in (42).



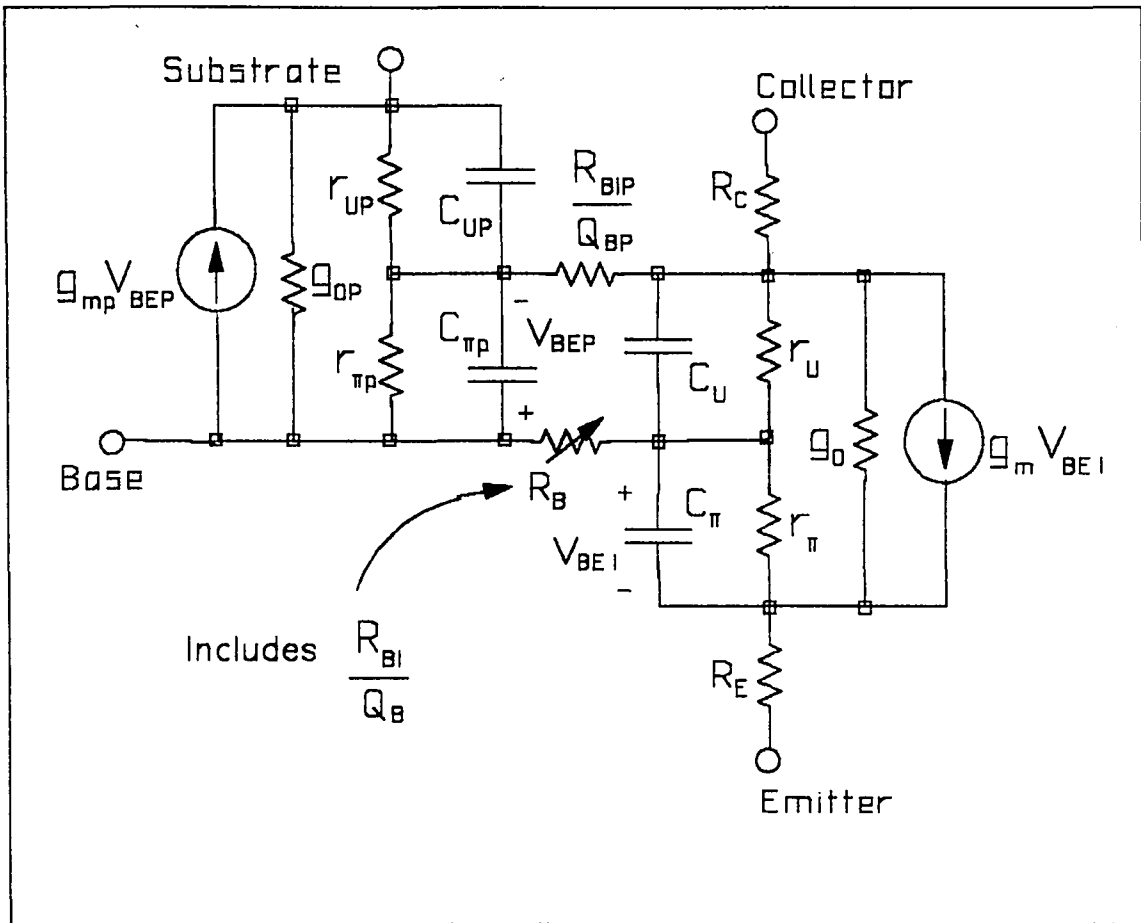


Figure 10. Small-Signal Equivalent circuit for the 4-Terminal Extended BJT model

The small signal equivalent circuit for the BJT in Figure 9 has four capacitors producing four time constants as in (43) except that  $C_{JS}$  and  $C_{BX}$  are represented by true junction capacitances in the parasitic device's collector-base,  $C_{JCP}$ , and base-emitter,  $C_{JEP}$ . Determining the open circuit resistances can be greatly simplified by realizing that the transconductance of the parasitic transistor,  $g_{mp}$ , is extremely small when the parasitic is off with the active transistor in the forward active mode. The parasitic base-emitter resistance is equivalently extremely large. These simplified open circuit resistances follow:

$$\begin{aligned}
R_{1o} &\approx r_{\pi} \parallel (R_B + r_{OP}) \approx r_{\pi} \\
R_{2o} &\approx r_{\pi} + (1 + g_m r_{\pi})(R_{CX} + R_{CI}) \\
R_{3o} &\approx (R_{CX} + R_{BIP}) \parallel r_O \approx R_{CX} + R_{BIP} \\
R_{4o} &\approx R_B + r_{\pi} + R_{CX} + R_{BIP}
\end{aligned} \tag{49}$$

Comparing these open circuit resistances with those obtained in (44) for the three terminal BJT reveals that  $R_{1o}$  is identical and  $R_{2o}$  is increased because of the replacement of  $R_C$  with  $R_{CX} + R_{CI}$ .  $R_{CI}$  is the intrinsic collector resistor specified by the parameter  $R_{CO}$ . Note, however, that the  $C_{JC}$  capacitance multiplier is much smaller in the four terminal model since it reflects only the intrinsic collector-base capacitance and excludes the extrinsic portion represented by  $C_{JEP}$  in the parasitic device. The  $C_{JEP}$  capacitance multiplier is applied to  $R_{4o}$ , which is much smaller than its three terminal form since  $R_{CX}$  is no longer multiplied by  $(1 + g_m r_{\pi})$ .  $R_{3o}$  is slightly larger in the four terminal model due to the additional resistance,  $R_{BIP}$ , but its contribution to  $f_T$  proved to be negligible previously.

Correctly modeling the distribution of the collector-base capacitance in the subcircuit or macro implementation of the model eliminates the need to "fudge" the forward transit time,  $T_F$ , while scaling  $C_{JC}$  and  $R_C$  to their correct values for different transistor sizes and geometries. Results indicate that correct values for collector-base capacitance and collector resistance can be specified without adversely affecting the defined  $f_T$ .

### B. Modeling of Avalanche Generation for Simulation

Avalanche breakdown, particularly in the collector-base junction, is a problem that crops up in the opposite extreme of operation from the saturation modeling discussed so far. The heavily doped and narrow profile of today's VHF devices magnify the problem as lower maximum sustaining voltages limit the potential applications of any new process development. A generally available and applicable implementation of this common phenomenon has continued to elude the CAD community. The simpler models, as used in this work, seem to work best if one is to achieve reasonable convergence success.

A current source  $I_c$  is included at the intrinsic collector-base terminals. This is accomplished in this work by use of the diode current law which makes use of the reverse exponential relation<sup>43</sup>

$$I_{\text{rev}} = IBV \cdot \exp[(-v_R + BV)/(NBV \cdot V_t)] \quad (50)$$

available in most versions of SPICE based simulators today. The parameter,  $NBV$ , is actually an extension available in PSpice 4.03, and was used to add the characteristic softness to the breakdown curve. The expression in (50) is used to simulate avalanche multiplication, instead of the classical multiplication factor in (37) because convergence using the classical factor has proven to be much more difficult and an exponential relation has been shown to provide a realistic description of avalanche multiplication<sup>44</sup>.  $I_c$  represents

the multiplication of the base transport current at the collector-base junction. This mechanism then interacts with the current gain characteristic of the transistor, resulting in the common-emitter  $BV_{CEO}$  breakdown evident in typical transistor terminal configurations.

Use of even the above mentioned modeling representation of avalanche breakdown presents problems for the numerical analysis used in network analysis programs, convergence is difficult and often impossible to obtain in large circuit applications. Network analysis programs such as SPICE may apply very large intermediate voltages while linearizing the matrix in its search for convergence; even though the final sustaining voltages may be quite reasonable. While the simulator is trying to solve for intermediate voltages, the exponential relation can cause runaway currents which will prevent a converging solution of the matrix. One remedy to this problem that proves useful with a subcircuit implementation of breakdown is the ease of removing the objectionably high currents from the source,  $I_C$ . The resulting model, without breakdown, can be used to obtain coarse DC operating points to be used, via .NODESET's, in subsequent simulations that do include breakdown modeling. The .NODESET command in SPICE provides a means of specifying the programs initial rough "guess" at the final operating point thereby speeding convergence to a solution. This technique proved useful

even with circuits of moderate size, particularly when operating some transistors near breakdown.

## V. RESULTS

The accuracy of the four-terminal representation in Figure 9 was tested for high speed transistors presented in section IV and results are presented in this section. As stated previously, the compact model consists of two Gummel-Poon transistors, two resistors and a diode (for breakdown). The architecture of this implementation lends itself to a subcircuit "macro-model" representation as presented in the Appendix, where Qs models the main operations of the device at a relatively low current level as the collector epitaxial region has little effect on device behavior. Qp models substrate injection in the saturation and reverse modes of operation. The compact model also includes conductivity modulated epitaxial collector resistance as implemented in PSpice 4.03 and above - with the exceptions noted in section IV pertaining to the splitting of XCJC, which is corrected in the subcircuit form presented in the thesis. Three additional elements - a current source and two charge storage elements - are part of the main transistor model in Qs.

Simulations made using the PSPICE<sup>43</sup> Circuit Simulator compare performance of a pure SPICE 2G.6 implementation with that of the compact model developed for AT&T's CBIC-V technology. Netlists suitable for computer simulation in PSpice are presented in Appendix B as they were used to generate characteristic plots illustrated in Figures 11 through 21

for both the NV231A01 and PV231A01 transistors. Accuracy of the model is also validated with physical measurements of nominal device performance. In each of the legends, "Q1" is the standard SPICE 2G.6 Gummel-Poon transistor compared with "X1", the subcircuit "macro-model". X's marked on the plots represent physical measurements of a nominal device fabricated on AT&T's VB110 linear array in 1990.

The first comparison is for Beta (or  $h_{FE}$ ) versus  $I_C$  and is illustrated in Figures 11 and 12. Shown is reverse bias of the collector-base junction at 2, 5 and 8 volts while the collector-substrate terminals are fixed at a reverse bias of 5 volts. Actual data points are presented at only the 2 V bias. For  $I_C$  of Q1 greater than 10 mA, the device starts to show the effects of quasi-saturation and the current gain is drastically reduced. The classic Gummel plot is presented in Figures 13 and 14 for the same reverse biases of the collector-base and collector-substrate terminals. Collector current as a function of base-emitter bias for  $V_{BE}$  greater than 0.85 V shows current gain degradation due to quasi-saturation. It should be noted that there is no serious substrate injection in either of these cases.

Quasi-saturation is clearly visible in an examination of the output characteristics of Figures 15 and 16. The collector current versus the sustaining voltage,  $V_{CE}$ , at three base-emitter biases (0.8, 0.85 and 0.9 V) reveals to varying degrees the two region saturation characteristic.

The  $I$ - $V$  characteristics clearly show three regions of operation: full saturation, quasi-saturation, and the normal forward active mode. At higher current levels (larger  $V_{BE}$ ), the non-linearity of the line indicates the effects of carrier velocity saturation. Some discrepancy at higher current levels is an artifact of Early voltage parameter extraction from low injection level  $I$ - $V$  curves. Figures 17 and 18 demonstrate how capable the compact model is for modeling the onset of substrate injection under the same conditions. The overall agreement between the compact model and the physical measurements is excellent.

The compact model was also tested for small-signal ac performance as indicated in Figures 19 and 20 for both the NPN and PNP transistors. Cutoff frequency playbacks in PSPICE with the zero-bias collector charge,  $Q_{CO}$ , estimate from epitaxial concentration shows a rapid falloff of  $f_T$  as the transistor goes into quasi-saturation. Measured data seems to indicate a more gradual falloff of  $f_T$  versus  $I_C$  as can be seen in Figure 19. A likely cause for this is the rapid increase in  $Q_0$  and  $Q_w$  when entering quasi-saturation. Due to the distributed nature of the epitaxial region, study<sup>45</sup> of this problem continues as we are reevaluating the partitioning of the stored charge,  $Q_{epi}$ , in very high frequency (VHF) applications of the model. Though, overall agreement is better using the compact model presented in this thesis.



Figure 11. NV231A01 Beta vs. Ic at Vcb = 2, 5 & 8 V

Temperature: 27.0

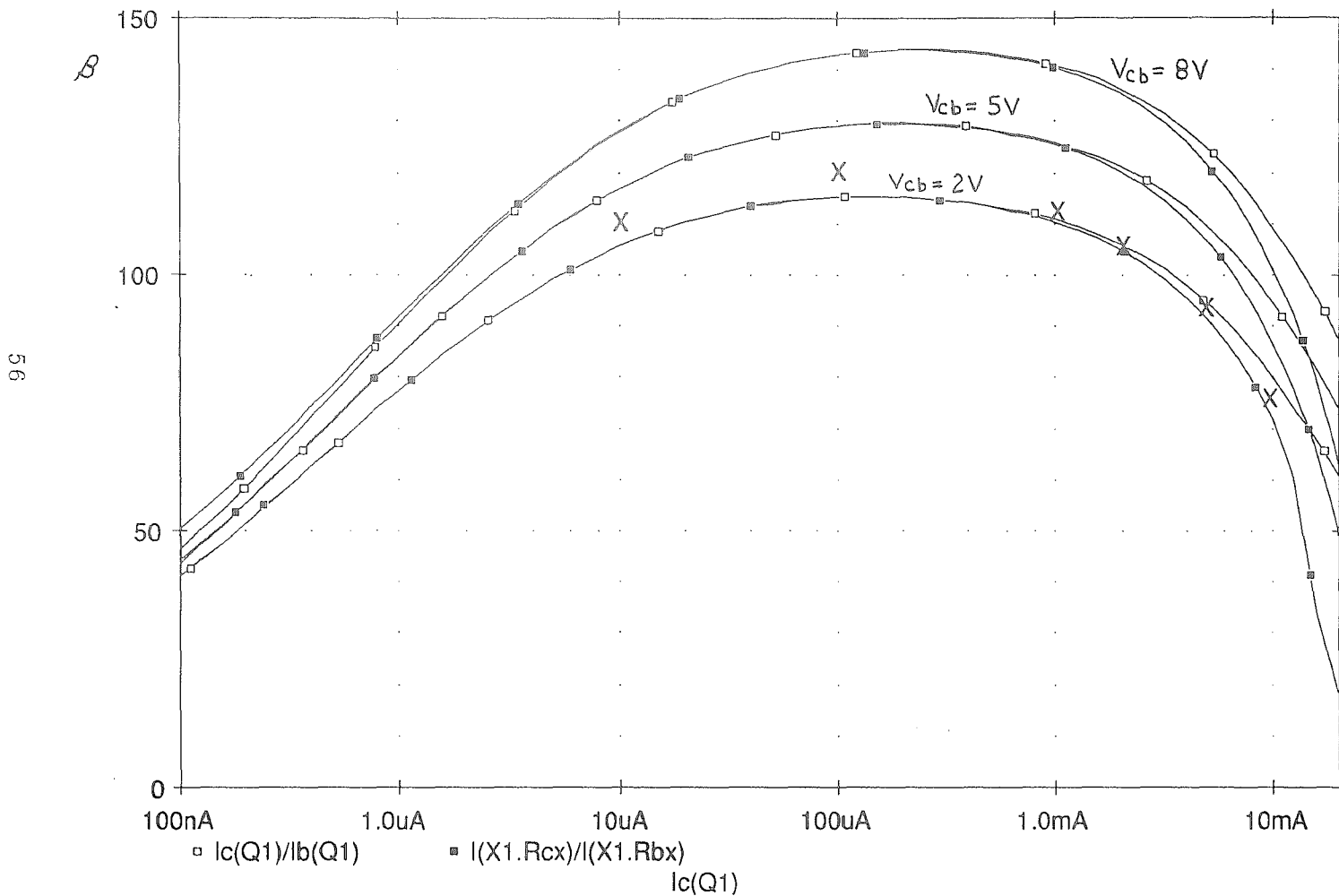


Figure 12. PV231A01 Beta vs. Ic at Vbc = 2, 5 & 8 V

Temperature: 27.0

57

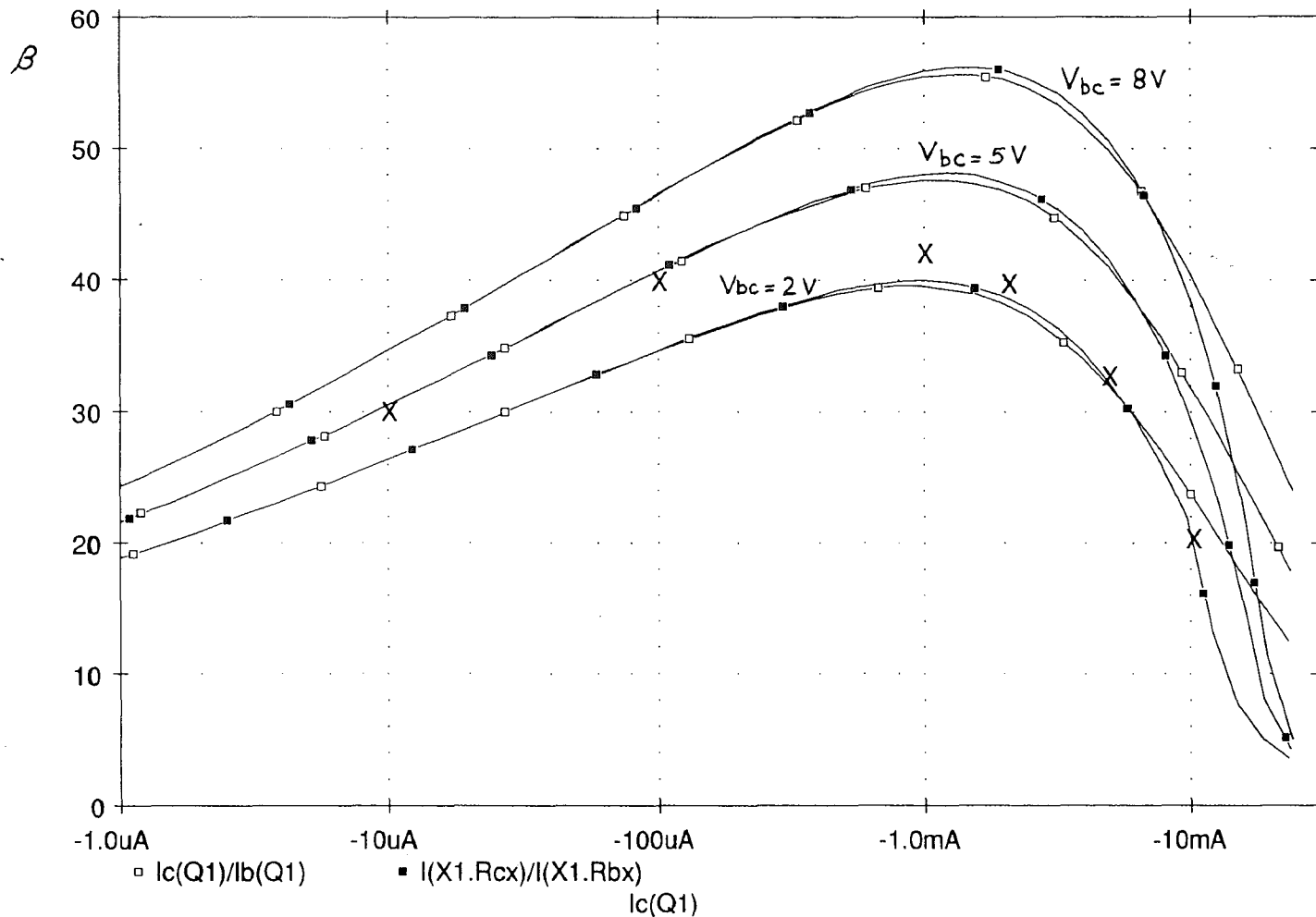


Figure 13. NV231A01  $I_c$  vs.  $V_{be}$  at  $V_{cb} = 2, 5 \text{ \& } 8 \text{ V}$

Temperature: 27.0

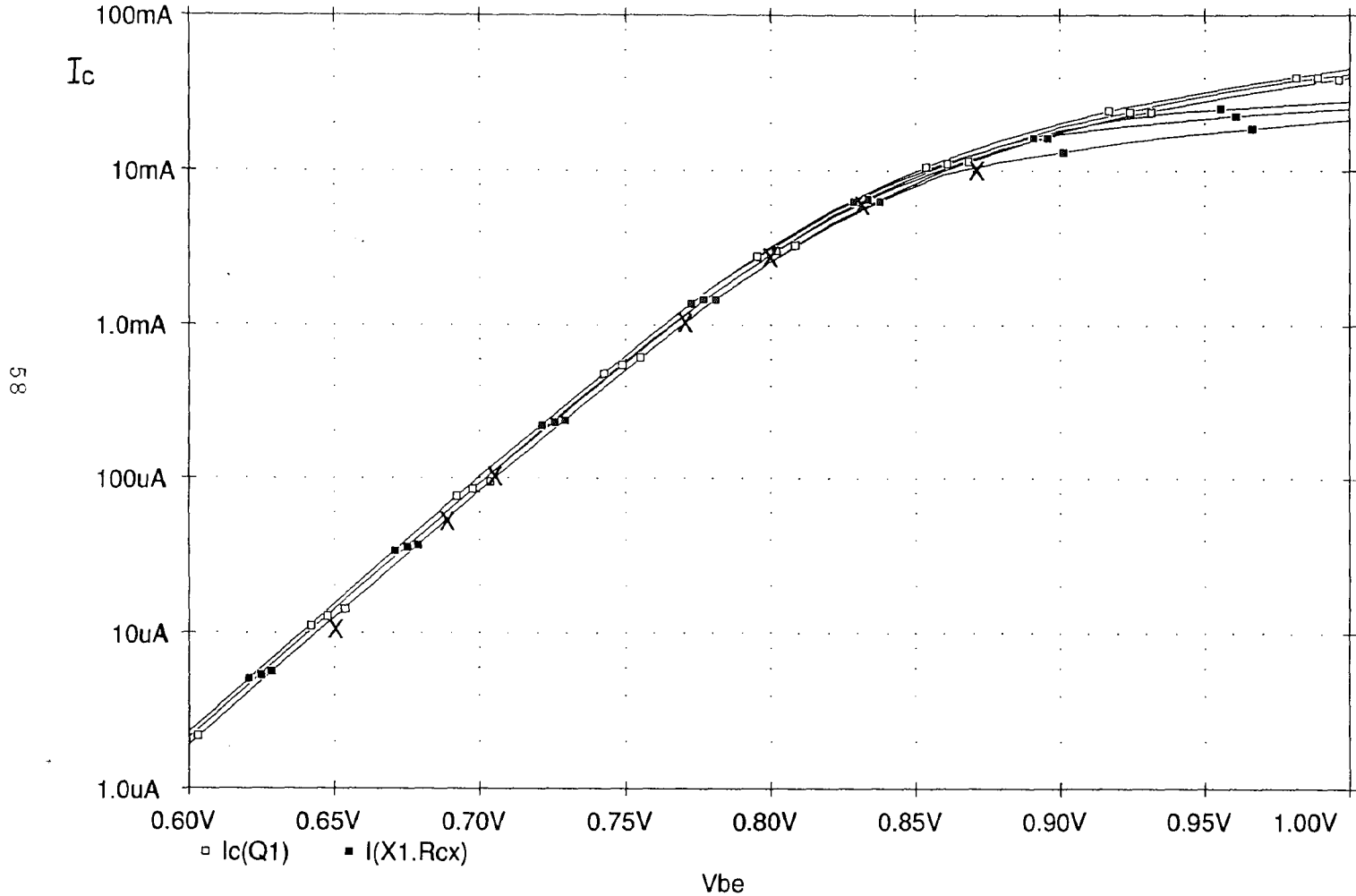


Figure 14. PV231A01  $I_c$  vs.  $V_{be}$  at  $V_{bc} = 2, 5 \text{ \& } 8 \text{ V}$

Temperature: 27.0

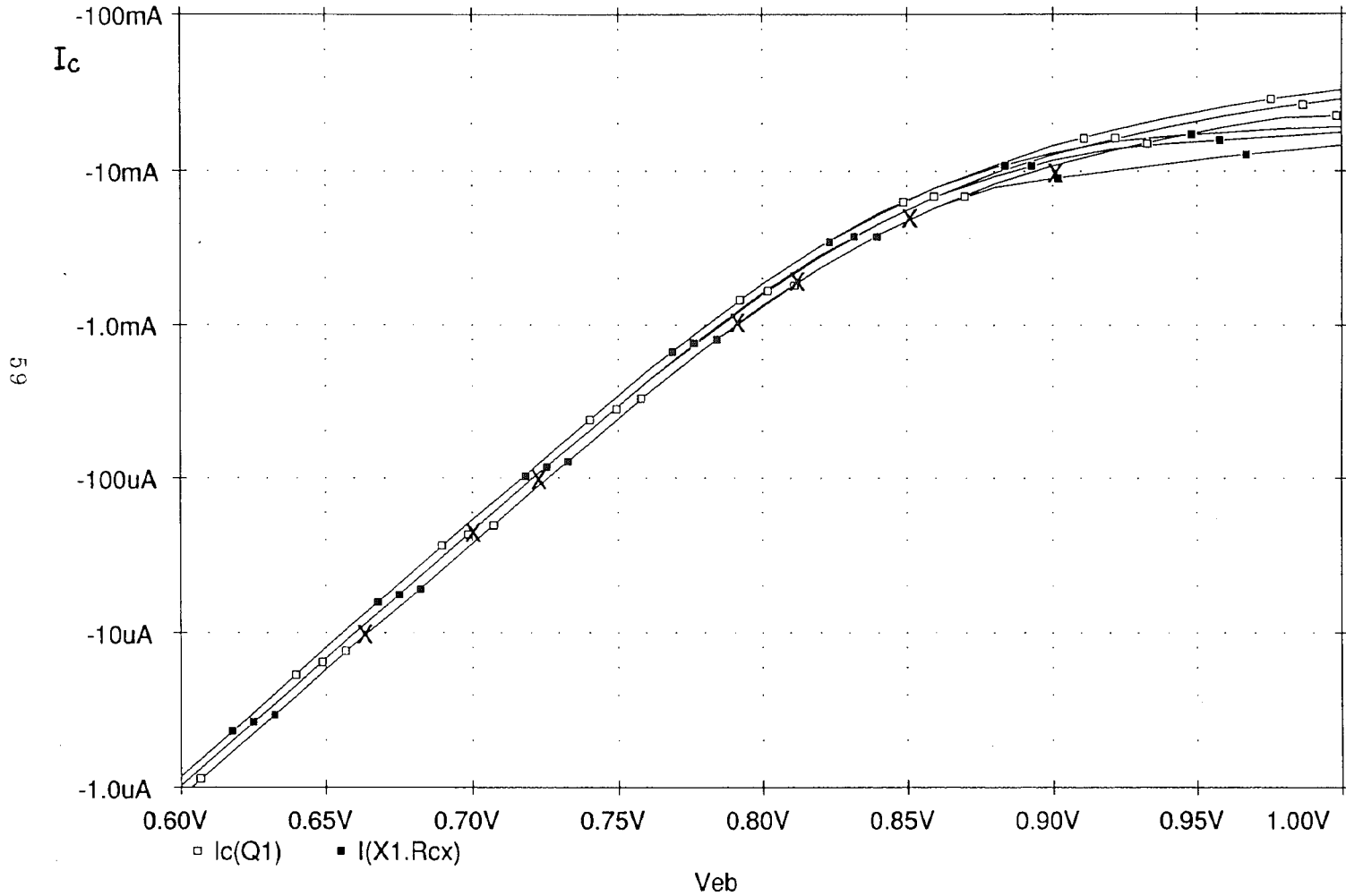


Figure 15. NV231A01  $I_c$  vs.  $V_{ce(sat)}$  at  $V_{be} = 0.8, 0.85$  &  $0.9$  V

Temperature: 27.0

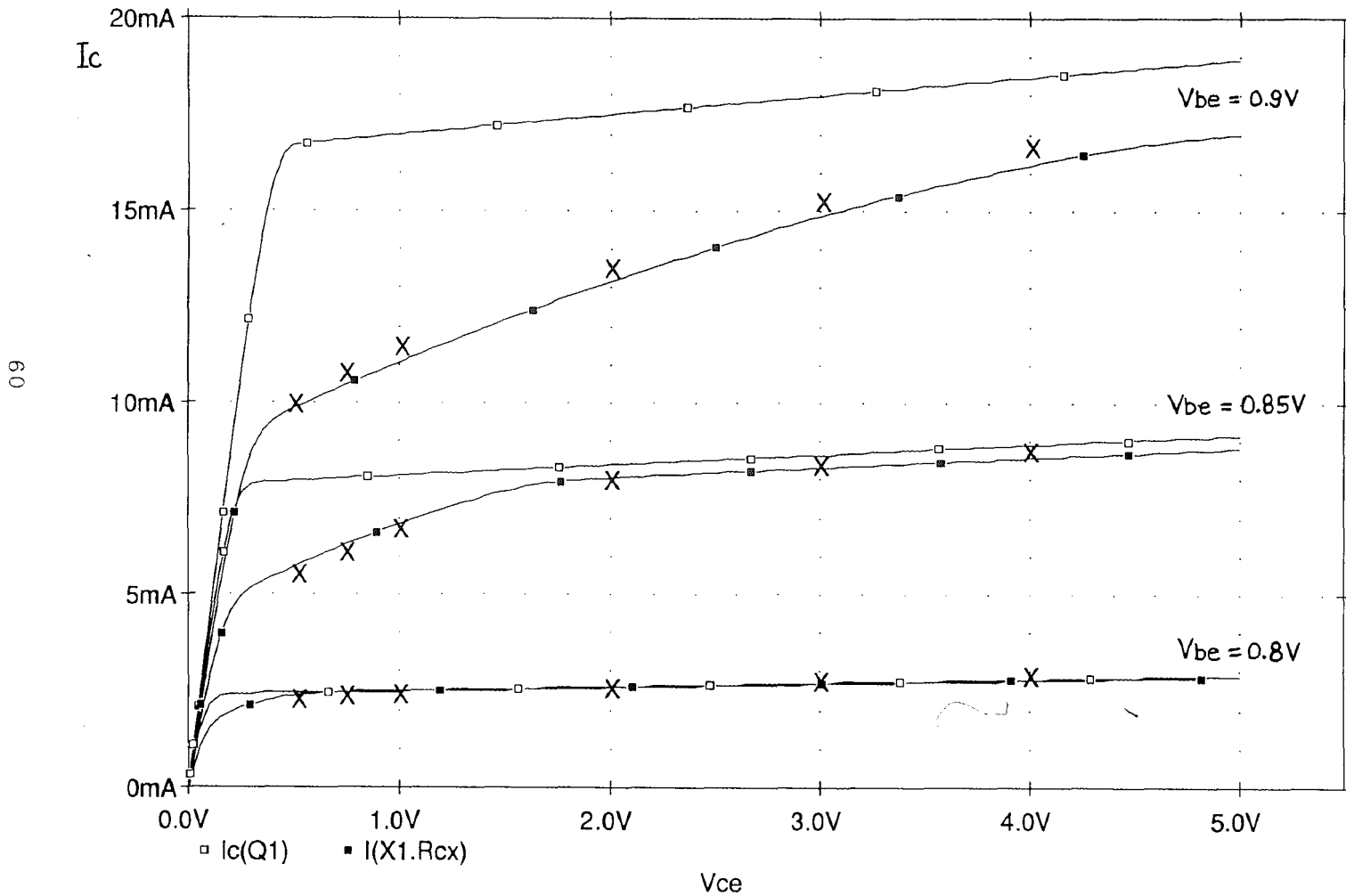


Figure 16. PV231A01  $I_c$  vs.  $V_{ce}(\text{sat})$  at  $V_{be} = 0.8, 0.85 \text{ \& } 0.9 \text{ V}$

Temperature: 27.0

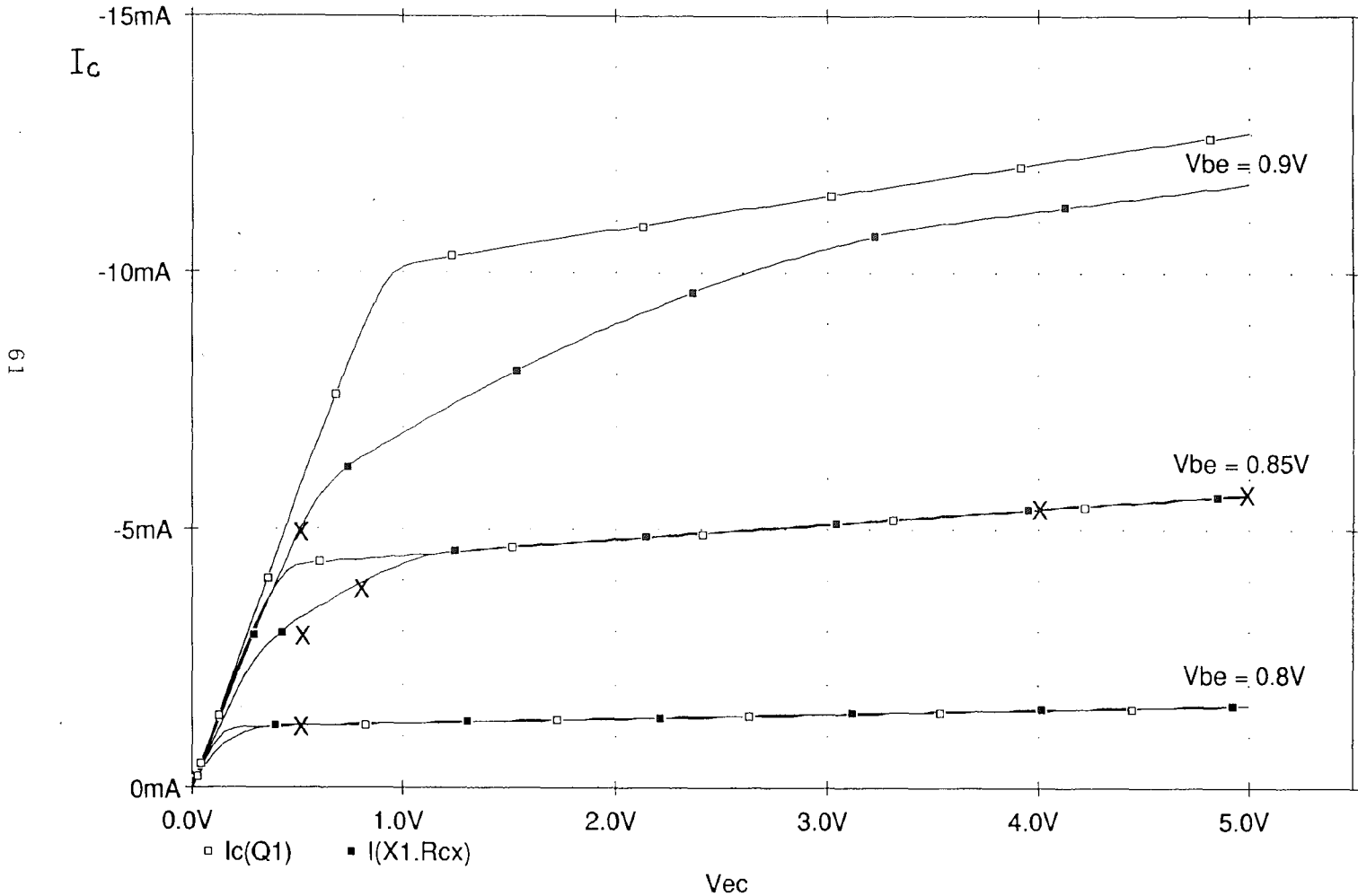


Figure 17. NV231A01 Substrate Current vs. Vce at Vbe = 0.8, 0.9 V

Temperature: 27.0

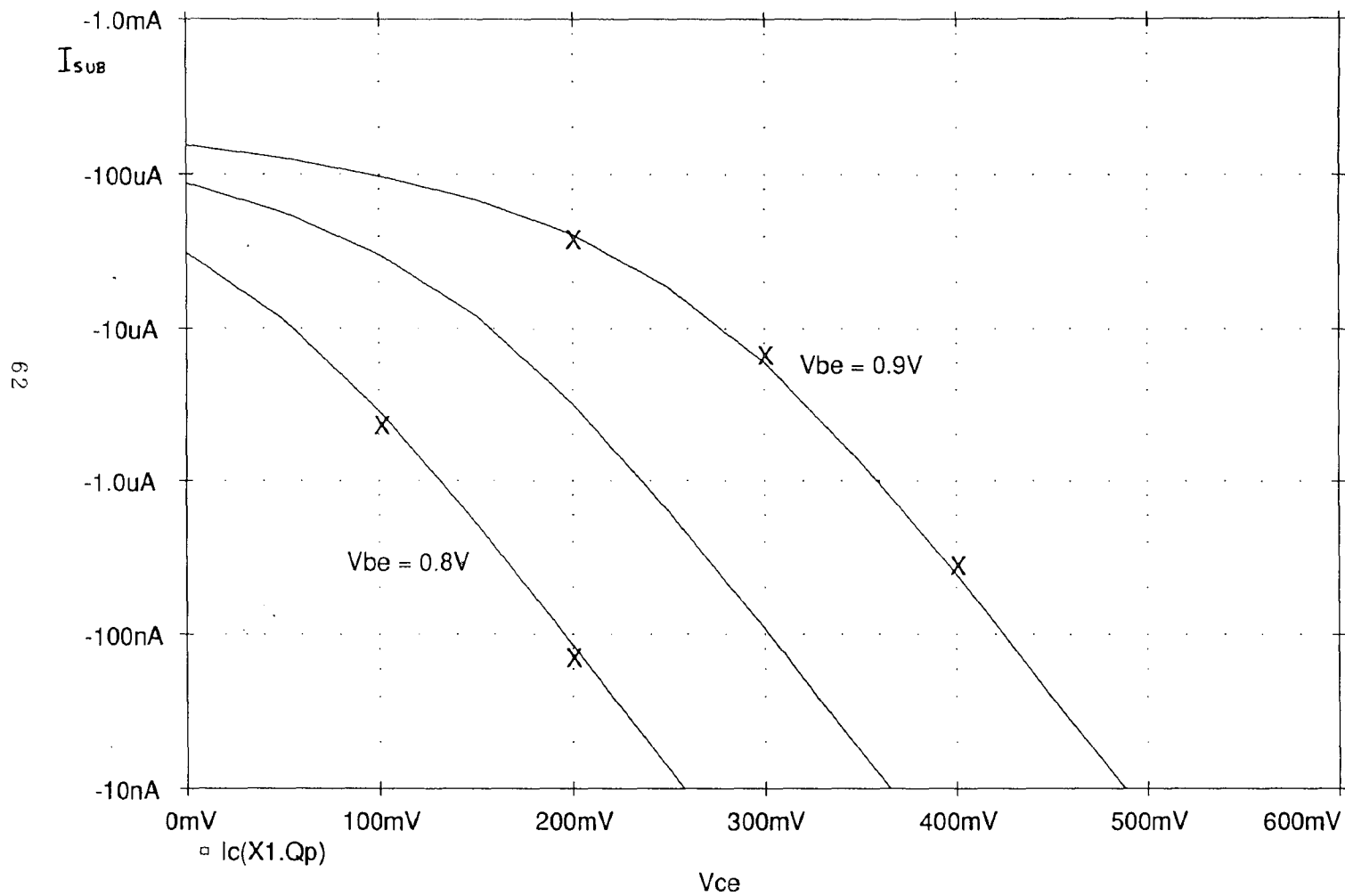


Figure 18. PV231A01 Substrate Current vs. Vce at Vbe = 0.8, 0.9 V

Temperature: 27.0

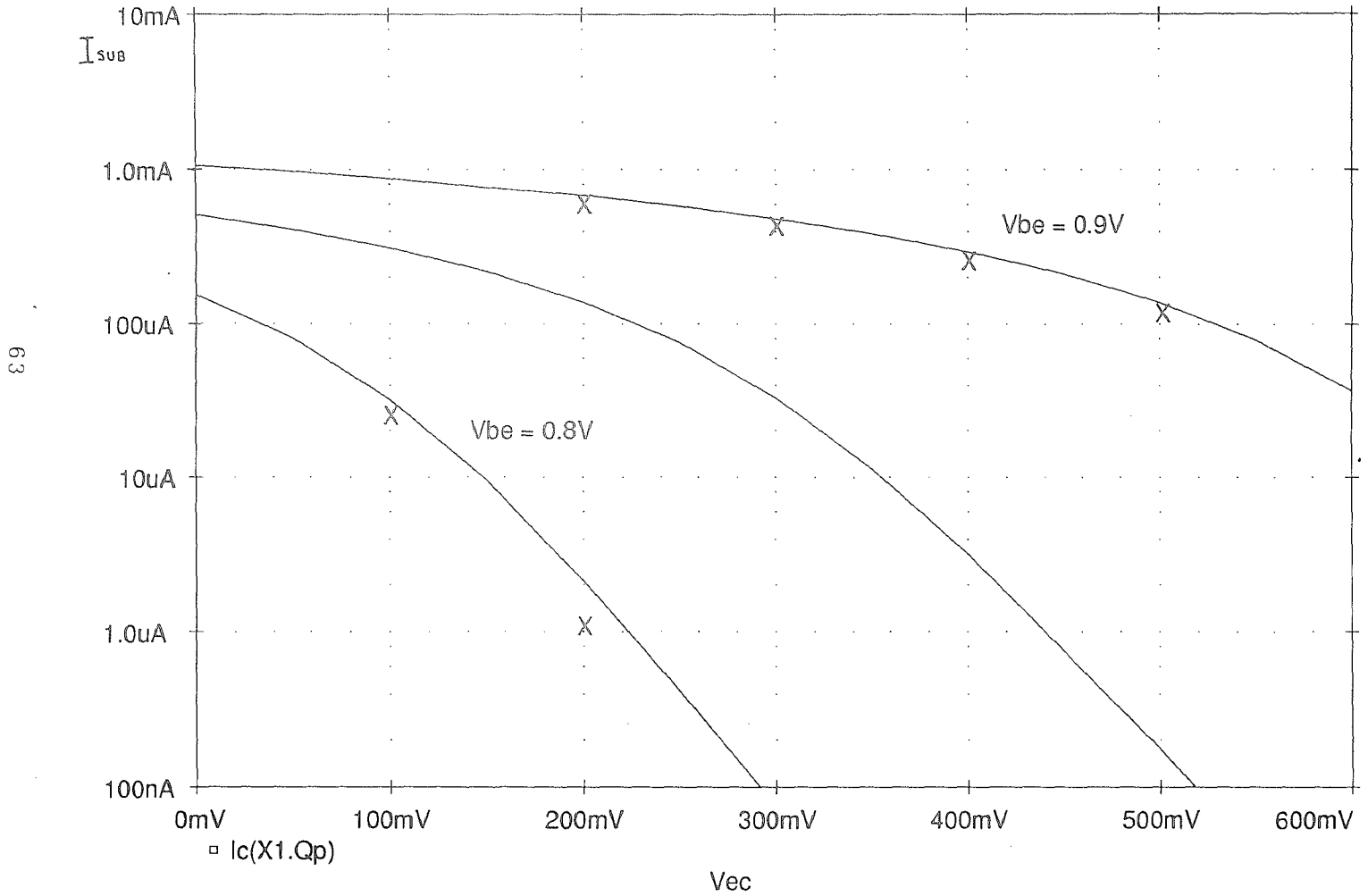




Figure 19. NV231A01 ft vs. Ic at Vce = 3 V

Temperature: 27.0

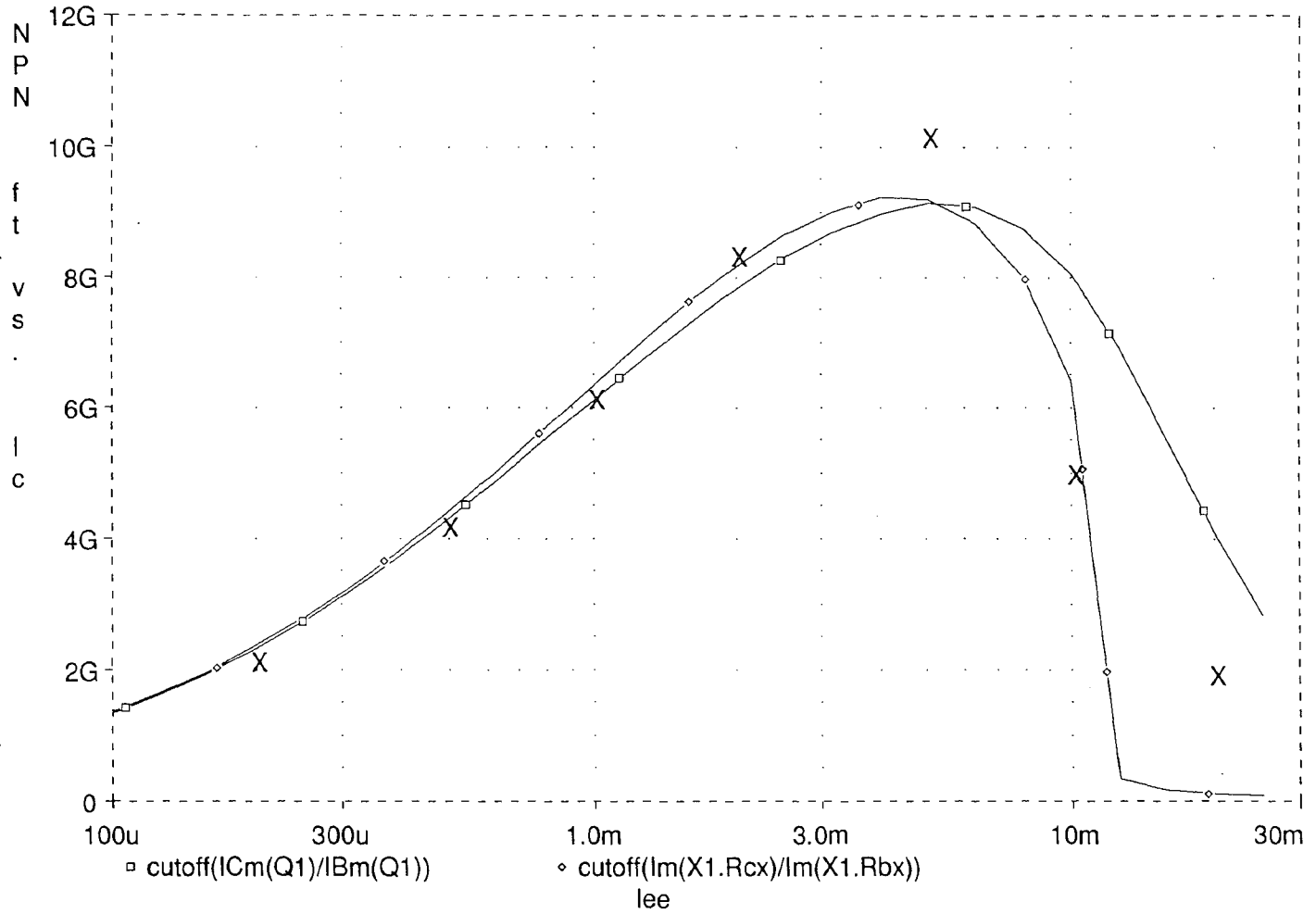
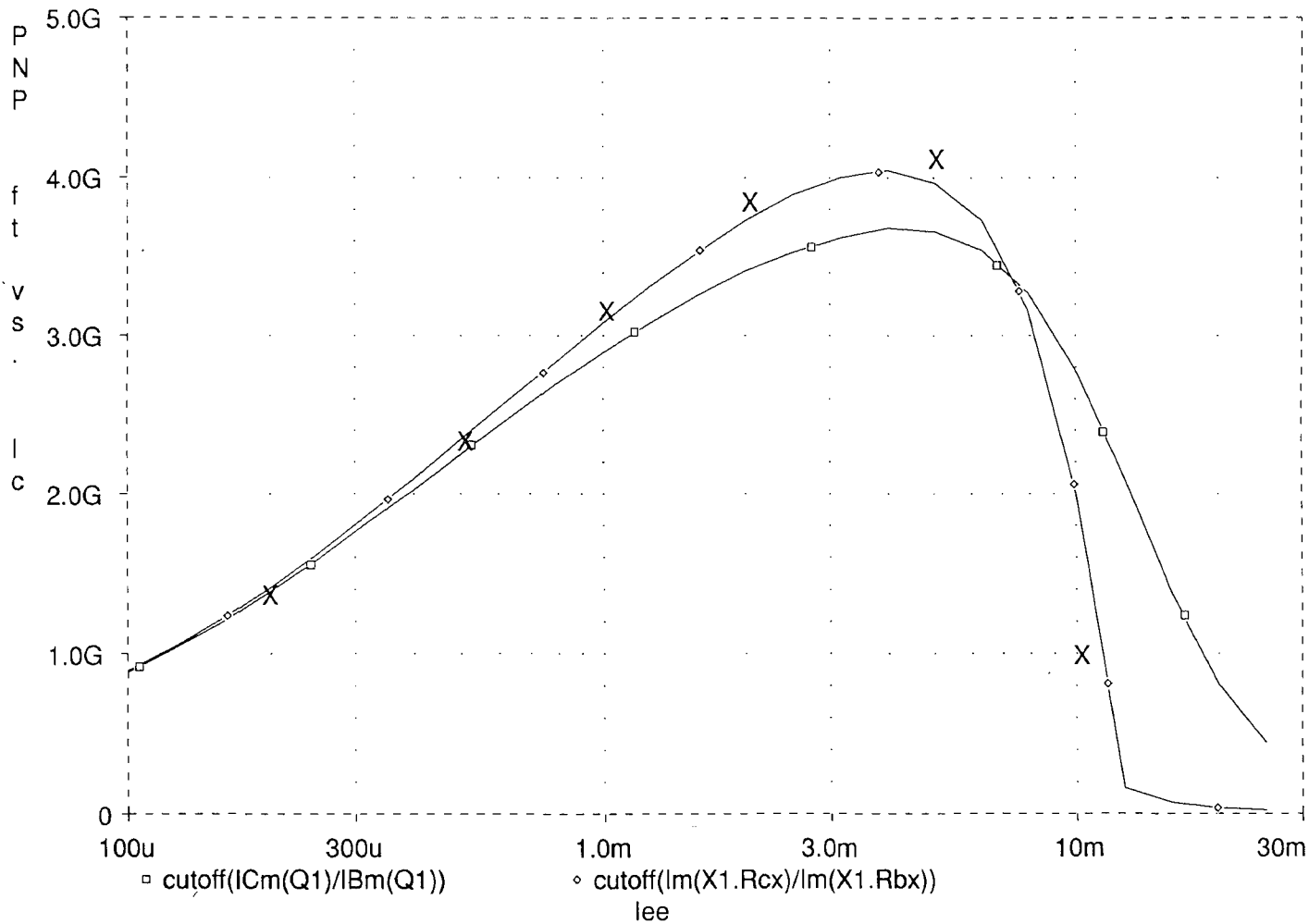


Figure 20. PV231A01 ft vs. lc at Vec = 3 V

Temperature: 27.0

6.9



Collector-emitter (or collector-base) breakdown was implemented in the compact model by adding a diode in parallel with the collector-base junction as indicated previously in section IV. A plot of collector current versus the sustaining voltage,  $V_{CE}$ , for several base current drives, as in Figure 21, is used to confirm both the Early voltage and  $BV_{CEX}$  parameters. The collector-substrate potential is set at a reverse bias of 15 volts to allow study of the reverse Early (or Late) voltage parameter,  $VAR$ . The  $NBV$  parameter, available in PSpice 4.03 and above, is used to approximate the shape of the breakdown portion of the curve as discussed previously in section IV. For other versions of SPICE not providing the  $NBV$  extension, this term which provides the characteristic softness to the curve can simply be left out. This results in a much sharper breakdown characteristic, but for an approximation of avalanche generated currents this may be sufficient. With the shallow junctions in AT&T's CBIC-V process being susceptible to a punch-through type of breakdown current generation, the  $NBV$  parameter provided a convenient means of fitting curves to the resulting characteristic data.

A sample/hold function consisting of two voltage follower type amplifiers was fabricated on AT&T's VB110 linear array shuttle. This provided a quick-turn capability to analyze the performance of the compact model in a circuit application. Initial findings of the dc characteristics are

Figure 21. NV231A01  $I_c$  vs.  $V_{ce}$  at  $I_b = 20, 40, 60, 80, 100 \mu A$

Temperature: 27.0

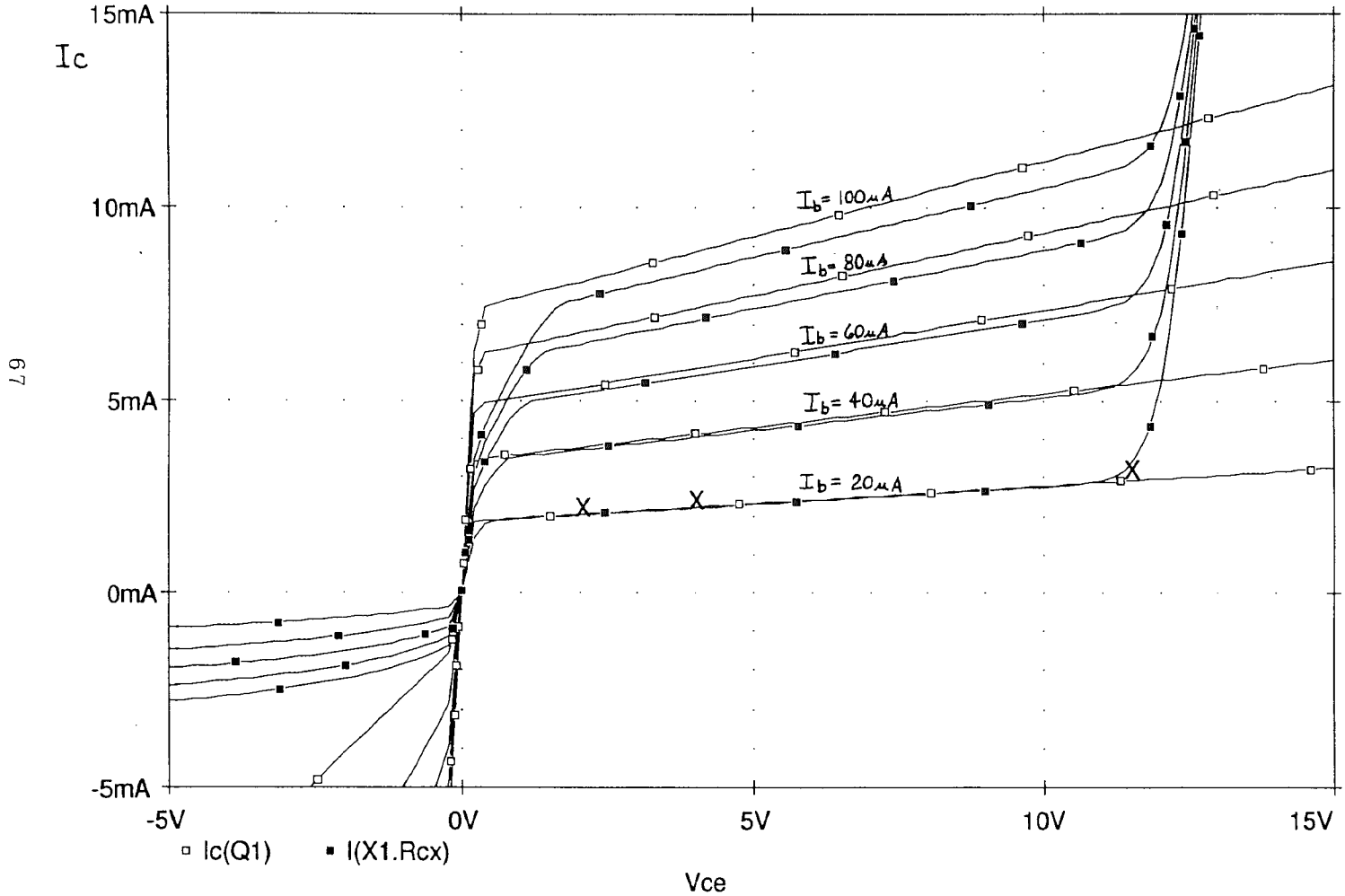
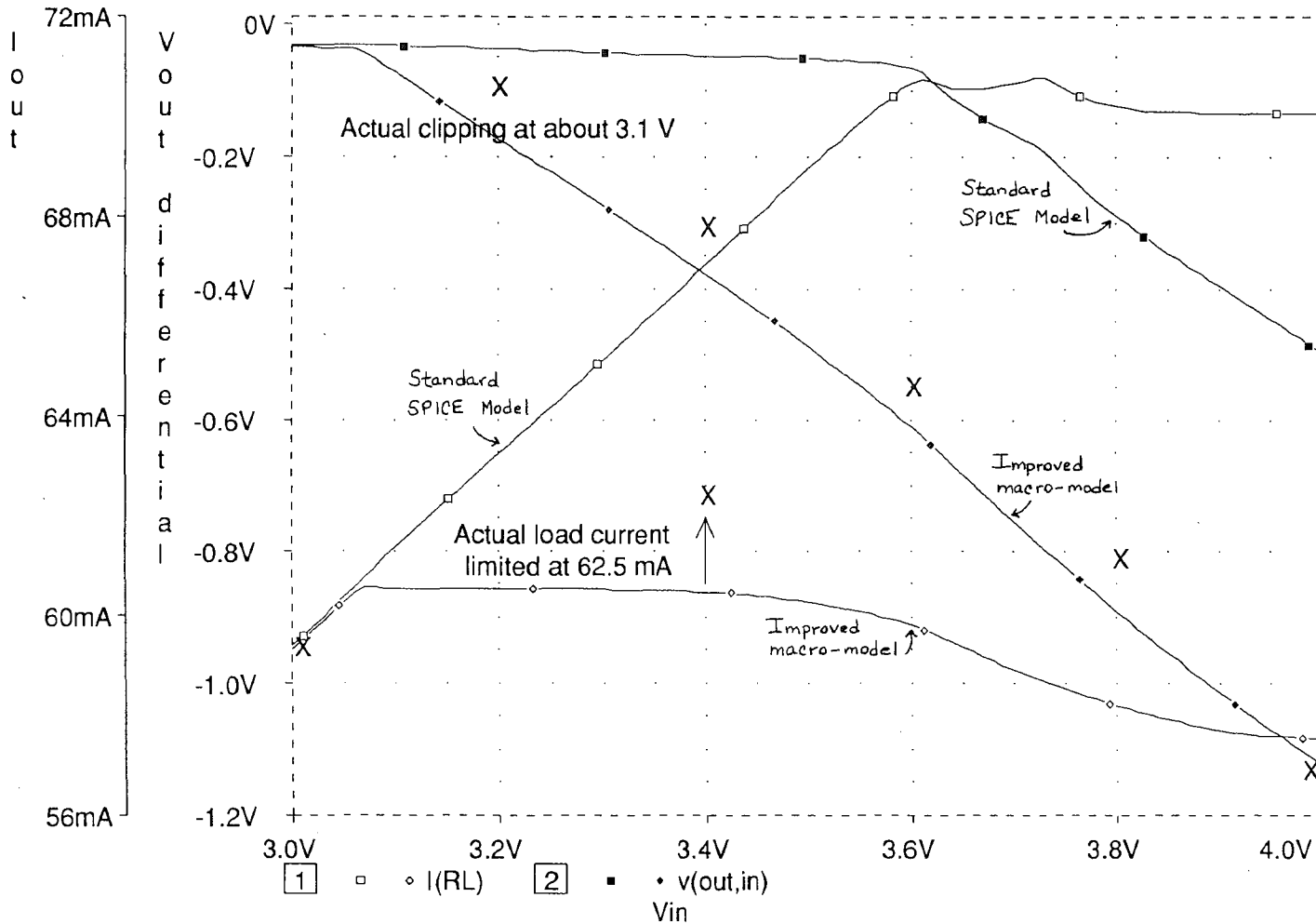


Figure 22. DC Transfer response to 4 V input swing on CBIC-V Sample/Hold Amp

Temperature: 27.0

88



reported here and presented in Figure 22. A block diagram of the Sample/Hold and a schematic for the output voltage follower can be found in Appendix C.

A dc sweep of the amplifier inputs for a  $\pm 4$  volt input swing shows the effects of quasi-saturation at the extremes of operation. With a 50 ohm load, the 6X NPN output transistor, Q89, is only capable of sustaining about 62 mA at  $V_{CE}$ 's less than 2 volts (at least on product fabricated for this study). With these current densities in the output stage, some level of quasi-saturation is inevitable, even at relatively high values for  $V_{CE}$ . Results show that the pure Gummel-Poon model inherent to SPICE is unable to reproduce the actual clipping at the prescribed 3.1 volts.

A comparison of run times shows the penalty associated with implementation of quasi-saturation modeling in the PSPICE simulator used. Table 3 presents the time associated with the various tasks as reported by PSpice's .OPTIONS ACCT command. All columns report results for an ac analysis of an eight transistor circuit, half of which employ the sub-circuit implementation of the compact model. The first column results are for a version of PSpice without the quasi-saturation code extension to the program (Version 4.02 - July 1989). The second column shows the results for the same circuit with quasi-saturation code implemented in the program (Version 4.03A - March 1990), but not active in the application circuit. The main difference in results is a

60% increase in the overhead associated with loading and checking in the additional code. Because this particular simulation was actually 25 separate ac analyses, this resulted in a 40% increase in total job time.

The third column shows the results for a PSpice job with quasi-saturation implemented in the subcircuit "macro models". Results show a 5 to 10 percent increase in run time across the board with the exceptions of setup, output and overhead. The increase in bias point calculation is due almost entirely to an increased number of iterations while attempting the ubiquitous dc operating point convergence. For transient jobs with long run times, overhead associated with the additional program code can be minimized and the resulting simulation time penalty should approach the 10% increase observed in this study.

TABLE 3 Comparative Analysis of Quasi-saturation in PSpice

	PSpice 4.02 SECONDS	4.03A w/o QS	4.03A w/ QSat	PCT. INCREASE
MATRIX SOLUTION	8.70	8.10	9.90	13.8%
MATRIX LOAD	10.50	12.50	13.13	25.0%
READIN	11.60	11.70	13.05	12.5%
SETUP	1.00	0.70	0.90	-10.0%
DC SWEEP	0.00	0.00	0.00	
BIAS POINT	94.20	98.50	101.33	7.6%
Normalized		98.50	94.67	0.5%
No. of Iterations	256	256	276	
AC and NOISE	167.00	172.80	182.50	9.3%
TRANSIENT ANALYSIS	0.00	0.00	0.00	
OUTPUT	0.20	0.10	0.10	-50.0%
OVERHEAD	80.20	209.60	208.50	160.0%
TOTAL JOB TIME	354.20	493.30	506.25	42.9%

## VI. CONCLUSIONS

The need for more accurate modeling of two regions of operation in Very High Frequency (VHF) technologies was established early in the thesis. With today's applications requiring IC technologies to push the extremes of breakdown and saturation, modeling in these regions can play a crucial role in the success or failure of circuits in their intended application. Through enhancements of the basic Gummel-Poon transistor model employed in SPICE, a "true" four-terminal Extended Gummel-Poon BJT model is realized without compromising the underpinnings of the integral charge-control relation (*ICCR*).

The study continues with a derivation of the model equations based on the underlying theoretical background. Several proposals for modeling quasi-saturation and breakdown are investigated and presented for consideration. A more complex two region saturation model employing both the low (*LFC*) and high field (*HFC*) cases is chosen to model quasi-saturation over a more empirical *B* factor implementation. Also, a description of qualitative techniques for parameter extraction is given. In contrast, a rather simple empirical model for collector-emitter breakdown ( $BV_{CEX}$  or  $BV_{CEO}$ ) is chosen in the hopes of minimizing convergence difficulties notoriously encountered in these attempts. Both mechanisms are realized in a subcircuit "macro-model".



Several advantages of a subcircuit form of the model include its flexibility as a "true" four-terminal Extended Gummel-Poon BJT model. Demonstrated improvements in the ability to model  $f_T$  versus  $I_C$  and  $V_{CEsat}$  curves show this versatility as we strive for a model for all occasions. Avalanche breakdown, not available in most SPICE based simulators, even in its most basic form can provide useful feedback to designers of demanding integrated circuit applications.

Additional work can yield improvements in the Early effect for technologies with very low Early voltage. The basic equations for the normalized base charge,  $q_b$ , as implemented in SPICE need to be revisited. A solution needs to address the loose approximation of  $q_b$  as implemented while avoiding the singularities of a more physical representation. One solution undertaken in AT&T's ADVICE simulator is the numerical integration of that portion associated with  $q_1$ . This solution has its penalties though, simulation run time being the most noticeable.

Another area of continued study will result in a better understanding of the distributed nature of stored charge in the epitaxial collector. The lumped apportionment of  $Q_{C0}$  as two charge storage elements in this implementation has been observed to result in abrupt current gain and  $f_T$  rolloff for VHF transistors such as those found in CBIC-V. Here again,

the complexity of a solution needs to be weighed against the obvious penalty of simulation run time.

The bipolar transistor model presented here includes a possible unified approach to quasi-saturation and breakdown effects. Portions of this have been successfully used to model several Complementary Bipolar Integrated Circuit (CBIC) technologies at AT&T Microelectronics in Reading, PA where it is incorporated into the ADVICE simulator. This thesis presents a detailed description of the model through figures and tabulations in Appendix A. A detailed verification of the model shows graphical proof of the improved accuracy of the compact model when compared with physical measurements of actual devices.

## APPENDICES

```

*****
* AT&T Microelectronics CBIC-V Technology - Spice Models   June 1991 *
* "NPNNOM.LIB" - NPN Transistors - Nominal                 *
*****
* - From ADVICE usrmod Models and Data                     *
* Full-Scale Revision by JHB 1/15/90: DC, AC Characteristics, T-Depend *
* Models Compiled by KEG 4/20/90                           *
*                                                           *
* NOTE: Reference Temperature is 27 C                       *
*****
*                   Nominal Beta and ft CBIC-V NPN Transistor Models *
*****
**
* TWO 1.5 BY 15 MICRON STRIPES :      NOM  MODEL          ** VB110 **
.MODEL NV231A01 NPN
+ IS = 2.367E-16 BF = 1.961E+02 NF = 1.000E+00 VAF = 3.875E+01
+ IKF = 5.330E-02 ISE = 7.330E-14 NE = 2.000E+00 BR = 1.553E+02
+ NR = 1.000E+00 VAR = 1.683E+00 IKR = 3.000E-02 ISC = 3.451E-14
+ NC = 1.653E+00 RB = 5.283E+01 IRB = 0.000E+00 RBM = 2.500E+01
+ RE = 1.923E+00 RC = 1.854E+01 CJE = 1.242E-13 VJE = 7.414E-01
+ MJE = 4.950E-01 TF = 1.176E-11 XTF = 2.000E+01 VTF = 7.618E+00
+ ITF = 2.643E-01 PTF = 0.000E+00 CJC = 1.241E-13 VJC = 6.465E-01
+ MJC = 4.509E-01 XCJC= 2.248E-01 TR = 7.070E-11 CJS = 1.178E-13
+ VJS = 5.286E-01 MJS = 4.389E-01 XTB = 1.071E+00 EG = 1.184E+00
+ XTI = 2.000E+00 KF = 0.000E+00 AF = 1.000E+00 FC = 8.150E-01
*
* From ADVICE usrmod=NEB1 Extended Bipolar Model with Quasi-sat
.SUBCKT NV231A01 (1, 2, 3, 4)
Qs  10 20 3 NV231Q01
Qp  4  10 20 NV231P01
Dbv 20 10 NBVBC
RCX 1  10 18.54
RBX 2  20 25.00
.MODEL NV231Q01 NPN
+ IS = 2.367E-16 BF = 1.961E+02 NF = 1.000E+00 VAF = 3.875E+01
+ IKF = 5.830E-02 ISE = 7.330E-14 NE = 2.000E+00 BR = 1.553E+02
+ NR = 1.000E+00 VAR = 1.683E+00 IKR = 3.000E-02 ISC = 1.943E-20
+ NC = 1.653E+00 RB = 2.783E+01 IRB = 0.000E+00 RBM = 1E-4
+ RE = 1.923E+00 RC = 0.          CJE = 1.242E-13 VJE = 7.414E-01
+ MJE = 4.950E-01 TF = 7.290E-12 XTF = 2.000E+01 VTF = 7.618E+00
+ ITF = 2.643E-01 PTF = 0.000E+00 CJC = 2.790E-14 VJC = 6.465E-01
+ MJC = 4.509E-01 XCJC= 1.        TR = 7.070E-11 CJS = 0.
+ VJS = 5.286E-01 MJS = 0.        XTB = 1.071E+00 EG = 1.184E+00
+ XTI = 2.000E+00 KF = 0.000E+00 AF = 1.000E+00 FC = 8.150E-01
* Quasi-saturation Effect available in PSpice 4.03 and above only
+ QCO = 5.233E-14 RCO = 1.531E+02 VO = 6.195E+00 GAMMA= 2.497E-11
.MODEL NV231P01 PNP RB = 8.000E+01 IRB = 0.000E+00 RBM = 1E-4
+ IS = 1.834E-18 BF = 6.242E-01 ISE = 3.451E-14 NE = 1.953E+00
+ IKF = 2.206E-04 CJE = 9.621E-14 VJE = 6.465E-01 MJE = 4.509E-01
+ BR = 1.322E-02 CJC = 1.178E-13 VJC = 5.286E-01 MJC = 4.389E-01
+ XTB = 0.          EG = 1.184E+00 XTI = 3.000E+00 FC = 8.150E-01
.ENDS

```

```

**
* FOUR 1.5 BY 15 MICRON STRIPES :      NOM  MODEL      ** VB110 **
.MODEL NV431A01 NPN
+ IS = 4.734E-16  BF = 1.961E+02  NF = 1.000E+00  VAF = 3.875E+01
+ IKF = 1.067E-01  ISE = 1.466E-13  NE = 2.000E+00  BR = 1.625E+02
+ NR = 1.000E+00  VAR = 1.683E+00  IKR = 6.000E-02  ISC = 6.087E-14
+ NC = 1.653E+00  RB = 2.641E+01  IRB = 0.000E+00  RBM = 1.250E+01
+ RE = 9.615E-01  RC = 2.662E+01  CJE = 2.485E-13  VJE = 7.414E-01
+ MJE = 4.950E-01  TF = 1.152E-11  XTF = 2.000E+01  VTF = 7.618E+00
+ ITF = 5.286E-01  PTF = 0.000E+00  CJC = 2.212E-13  VJC = 6.465E-01
+ MJC = 4.509E-01  XCJC= 2.522E-01  TR = 7.070E-11  CJS = 1.722E-13
+ VJS = 5.286E-01  MJS = 4.389E-01  XTB = 1.071E+00  EG = 1.184E+00
+ XTI = 2.000E+00  KF = 0.000E+00  AF = 1.000E+00  FC = 8.150E-01
*
* From ADVICE usrmod=NEB1 Extended Bipolar Model with Quasi-sat
.SUBCKT NV431A01 (1, 2, 3, 4)
Qs  10 20 3  NV431Q01
Qp  4  10 20 NV431P01
Dbv 20 10  NBVBC 2
RCX  1  10  26.62
RBX  2  20  12.50
.MODEL NV431Q01 NPN
+ IS = 4.734E-16  BF = 1.961E+02  NF = 1.000E+00  VAF = 3.875E+01
+ IKF = 1.167E-01  ISE = 1.466E-13  NE = 2.000E+00  BR = 1.625E+02
+ NR = 1.000E+00  VAR = 1.683E+00  IKR = 6.000E-02  ISC = 3.885E-20
+ NC = 1.653E+00  RB = 1.391E+01  IRB = 0.000E+00  RBM = 1E-4
+ RE = 9.615E-01  RC = 0.          CJE = 2.485E-13  VJE = 7.414E-01
+ MJE = 4.950E-01  TF = 7.290E-12  XTF = 2.000E+01  VTF = 7.618E+00
+ ITF = 5.286E-01  PTF = 0.000E+00  CJC = 5.580E-14  VJC = 6.465E-01
+ MJC = 4.509E-01  XCJC= 1.          TR = 7.070E-11  CJS = 0.
+ VJS = 5.286E-01  MJS = 0.          XTB = 1.071E+00  EG = 1.184E+00
+ XTI = 2.000E+00  KF = 0.000E+00  AF = 1.000E+00  FC = 8.150E-01
* Quasi-saturation Effect available in PSpice 4.03 and above only
+ QCO = 5.233E-14  RCO = 7.657E+01  VO = 6.195E+00  GAMMA= 2.497E-11
.MODEL NV431P01 PNP RB = 4.653E+01  IRB = 0.000E+00  RBM = 1E-4
+ IS = 3.234E-18  BF = 6.242E-01  ISE = 6.087E-14  NE = 1.953E+00
+ IKF = 3.890E-04  CJE = 1.654E-13  VJE = 6.465E-01  MJE = 4.509E-01
+ BR = 1.322E-02  CJC = 1.722E-13  VJC = 5.286E-01  MJC = 4.389E-01
+ XTB = 0.          EG = 1.184E+00  XTI = 3.000E+00  FC = 8.150E-01
.ENDS

```

```

**
* THREE 1.5 BY 30 MICRON STRIPES :      NOM  MODEL      ** VB110 **
.MODEL NV362A01 NPN
+ IS = 7.101E-16  BF = 1.961E+02  NF = 1.000E+00  VAF = 3.875E+01
+ IKF = 1.601E-01  ISE = 2.199E-13  NE = 2.000E+00  BR = 1.675E+02
+ NR = 1.000E+00  VAR = 1.683E+00  IKR = 9.000E-02  ISC = 8.376E-14
+ NC = 1.653E+00  RB = 1.761E+01  IRB = 0.000E+00  RBM = 8.333E+00
+ RE = 6.410E-01  RC = 4.820E+00  CJE = 3.727E-13  VJE = 7.414E-01
+ MJE = 4.950E-01  TF = 1.142E-11  XTF = 2.000E+01  VTF = 7.618E+00
+ ITF = 7.929E-01  PTF = 0.000E+00  CJC = 3.069E-13  VJC = 6.465E-01
+ MJC = 4.509E-01  XCJC= 2.727E-01  TR = 7.070E-11  CJS = 2.914E-13
+ VJS = 5.286E-01  MJS = 4.389E-01  XTB = 1.071E+00  EG = 1.184E+00
+ XTI = 2.000E+00  KF = 0.000E+00  AF = 1.000E+00  FC = 8.150E-01

```

```

*
* From ADVICE usrmod=NEB1 Extended Bipolar Model with Quasi-sat

```

```

.SUBCKT NV362A01 (1, 2, 3, 4)

```

```

Qs 10 20 3 NV362Q01

```

```

Qp 4 10 20 NV362P01

```

```

Dbv 20 10 NBVBC 3

```

```

RCX 1 10 4.820

```

```

RBX 2 20 8.333

```

```

.MODEL NV362Q01 NPN

```

```

+ IS = 7.101E-16  BF = 1.961E+02  NF = 1.000E+00  VAF = 3.875E+01
+ IKF = 1.751E-01  ISE = 2.199E-13  NE = 2.000E+00  BR = 1.675E+02
+ NR = 1.000E+00  VAR = 1.683E+00  IKR = 9.000E-02  ISC = 5.828E-20
+ NC = 1.653E+00  RB = 9.277E+00  IRB = 0.000E+00  RBM = 1E-4
+ RE = 6.410E-01  RC = 0.          CJE = 3.727E-13  VJE = 7.414E-01
+ MJE = 4.950E-01  TF = 7.290E-12  XTF = 2.000E+01  VTF = 7.618E+00
+ ITF = 7.929E-01  PTF = 0.000E+00  CJC = 8.370E-14  VJC = 6.465E-01
+ MJC = 4.509E-01  XCJC= 1.          TR = 7.070E-11  CJS = 0.
+ VJS = 5.286E-01  MJS = 0.          XTB = 1.071E+00  EG = 1.184E+00
+ XTI = 2.000E+00  KF = 0.000E+00  AF = 1.000E+00  FC = 8.150E-01

```

```

* Quasi-saturation Effect available in PSpice 4.03 and above only

```

```

+ QCO = 1.028E-13  RCO = 5.105E+01  VO = 6.195E+00  GAMMA= 2.497E-11

```

```

.MODEL NV362P01 PNP RB = 3.449E+01  IRB = 0.000E+00  RBM = 1E-4

```

```

+ IS = 4.450E-18  BF = 6.242E-01  ISE = 8.376E-14  NE = 1.953E+00

```

```

+ IKF = 5.354E-04  CJE = 2.232E-13  VJE = 6.465E-01  MJE = 4.509E-01

```

```

+ BR = 1.322E-02  CJC = 2.914E-13  VJC = 5.286E-01  MJC = 4.389E-01

```

```

+ XTB = 0.          EG = 1.184E+00  XTI = 3.000E+00  FC = 8.150E-01

```

```

.ENDS

```

```

**
* SIX 1.5 BY 30 MICRON STRIPES :      NOM  MODEL      ** VB110 **
.MODEL NV663A01 NPN
+ IS = 1.420E-15  BF = 1.961E+02  NF = 1.000E+00  VAF = 3.875E+01
+ IKF = 3.202E-01  ISE = 4.397E-13  NE = 2.000E+00  BR = 1.722E+02
+ NR = 1.000E+00  VAR = 1.683E+00  IKR = 1.800E-01  ISC = 1.531E-13
+ NC = 1.653E+00  RB = 8.805E+00  IRB = 0.000E+00  RBM = 4.167E+00
+ RE = 3.205E-01  RC = 2.409E+00  CJE = 7.455E-13  VJE = 7.414E-01
+ MJE = 4.950E-01  TF = 1.121E-11  XTF = 2.000E+01  VTF = 7.618E+00
+ ITF = 1.586E+00  PTF = 0.000E+00  CJC = 5.663E-13  VJC = 6.465E-01
+ MJC = 4.509E-01  XCJC= 2.956E-01  TR = 7.070E-11  CJS = 4.288E-13
+ VJS = 5.286E-01  MJS = 4.389E-01  XTB = 1.071E+00  EG = 1.184E+00
+ XTI = 2.000E+00  KF = 0.000E+00  AF = 1.000E+00  FC = 8.150E-01

```

```

*
* From ADVICE usrmod=NEB1 Extended Bipolar Model with Quasi-sat
.SUBCKT NV663A01 (1, 2, 3, 4)

```

```

Qs  10 20 3  NV663Q01
Qp  4  10 20 NV663P01
Dbv 20 10  NBVBC 6
RCX 1  10  2.409
RBX 2  20  4.167

```

```

.MODEL NV663Q01 NPN
+ IS = 1.420E-15  BF = 1.961E+02  NF = 1.000E+00  VAF = 3.875E+01
+ IKF = 3.502E-01  ISE = 4.397E-13  NE = 2.000E+00  BR = 1.722E+02
+ NR = 1.000E+00  VAR = 1.683E+00  IKR = 1.800E-01  ISC = 1.166E-19
+ NC = 1.653E+00  RB = 4.638E+00  IRB = 0.000E+00  RBM = 1E-4
+ RE = 3.205E-01  RC = 0.          CJE = 7.455E-13  VJE = 7.414E-01
+ MJE = 4.950E-01  TF = 7.290E-12  XTF = 2.000E+01  VTF = 7.618E+00
+ ITF = 1.586E+00  PTF = 0.000E+00  CJC = 1.674E-13  VJC = 6.465E-01
+ MJC = 4.509E-01  XCJC= 1.          TR = 7.070E-11  CJS = 0.
+ VJS = 5.286E-01  MJS = 0.          XTB = 1.071E+00  EG = 1.184E+00
+ XTI = 2.000E+00  KF = 0.000E+00  AF = 1.000E+00  FC = 8.150E-01

```

```

* Quasi-saturation Effect available in PSpice 4.03 and above only
+ QCO = 1.028E-13  RCO = 2.552E+01  VO = 6.195E+00  GAMMA= 2.497E-11
.MODEL NV663P01 PNP RB = 1.930E+01  IRB = 0.000E+00  RBM = 1E-4
+ IS = 8.137E-18  BF = 6.242E-01  ISE = 1.531E-13  NE = 1.953E+00
+ IKF = 9.789E-04  CJE = 3.989E-13  VJE = 6.465E-01  MJE = 4.509E-01
+ BR = 1.322E-02  CJC = 4.288E-13  VJC = 5.286E-01  MJC = 4.389E-01
+ XTB = 0.          EG = 1.184E+00  XTI = 3.000E+00  FC = 8.150E-01

```

```

.ENDS

```

```

**
* Collector-Base Avalanche Breakdown Diode
.MODEL NBVBC D
+ BV = 1.150E+01  IBV = 1.000E-04  IS = 1.000E-21  RS = 0.

```

```

* Low-level reverse breakdown available in PSpice 4.03 and above only
+ NBV = 1.000E+01  TBV1=-4.000E-02  TBV2= 0.

```

```

*****
* AT&T Microelectronics CBIC-V Technology - Spice Models   June 1991 *
* "NPNLOW.LIB" - NPN Transistors - Low                      *
*****
* - From ADVICE usrmod Models and Data                      *
* Full-Scale Revision by JHB 1/15/90: DC, AC Characteristics, T-Depend
* Models Compiled by KEG 4/20/90                            *
*
* NOTE: Reference Temperature is 27 C                        *
*****
*               Low Beta and fT CBIC-V NPN Transistor Models *
*****
**
* TWO 1.5 BY 15 MICRON STRIPES :      LOW  MODEL          ** VB110 **
.MODEL NV231A01 NPN
+ IS = 7.051E-17 BF = 5.636E+01 NF = 1.000E+00 VAF = 6.236E+01
+ IKF = 5.389E-02 ISE = 1.884E-13 NE = 2.000E+00 BR = 4.625E+01
+ NR = 1.000E+00 VAR = 2.889E+00 IKR = 3.000E-02 ISC = 3.451E-14
+ NC = 1.653E+00 RB = 4.053E+01 IRB = 0.000E+00 RBM = 3.000E+01
+ RE = 1.109E+00 RC = 2.004E+01 CJE = 1.567E-13 VJE = 7.414E-01
+ MJE = 4.950E-01 TF = 1.432E-11 XTF = 2.380E+01 VTF = 9.000E+00
+ ITF = 2.080E-01 PTF = 0.000E+00 CJC = 1.433E-13 VJC = 6.465E-01
+ MJC = 4.509E-01 XCJC= 2.029E-01 TR = 7.575E-11 CJS = 1.348E-13
+ VJS = 5.286E-01 MJS = 4.389E-01 XTB = 1.193E+00 EG = 1.184E+00
+ XTI = 2.000E+00 KF = 0.000E+00 AF = 1.000E+00 FC = 8.500E-01
*
* From ADVICE usrmod=NEB1 Extended Bipolar Model with Quasi-sat
.SUBCKT NV231A01 (1, 2, 3, 4)
Qs  10 20 3 NV231Q01
Qp  4  10 20 NV231P01
Dbv 20 10 NBVBC
RCX  1  10 20.04
RBX  2  20 30.00
.MODEL NV231Q01 NPN
+ IS = 7.051E-17 BF = 5.636E+01 NF = 1.000E+00 VAF = 6.236E+01
+ IKF = 5.889E-02 ISE = 1.884E-13 NE = 2.000E+00 BR = 4.625E+01
+ NR = 1.000E+00 VAR = 2.889E+00 IKR = 3.000E-02 ISC = 1.943E-20
+ NC = 1.653E+00 RB = 1.053E+01 IRB = 0.000E+00 RBM = 1E-4
+ RE = 1.109E+00 RC = 0.          CJE = 1.567E-13 VJE = 7.414E-01
+ MJE = 4.950E-01 TF = 8.800E-12 XTF = 2.380E+01 VTF = 9.000E+00
+ ITF = 2.080E-01 PTF = 0.000E+00 CJC = 2.970E-14 VJC = 6.465E-01
+ MJC = 4.509E-01 XCJC= 1.        TR = 7.575E-11 CJS = 0.
+ VJS = 5.286E-01 MJS = 0.        XTB = 1.193E+00 EG = 1.184E+00
+ XTI = 2.000E+00 KF = 0.000E+00 AF = 1.000E+00 FC = 8.500E-01
* Quasi-saturation Effect available in PSpice 4.03 and above only
+ QCO = 5.233E-14 RCO = 1.884E+02 VO = 6.619E+00 GAMMA= 2.497E-11
.MODEL NV231P01 PNP RB = 8.000E+01 IRB = 0.000E+00 RBM = 1E-4
+ IS = 1.834E-18 BF = 6.242E-01 ISE = 3.451E-14 NE = 1.953E+00
+ IKF = 2.206E-04 CJE = 1.136E-13 VJE = 6.465E-01 MJE = 4.509E-01
+ BR = 1.322E-02 CJC = 1.348E-13 VJC = 5.286E-01 MJC = 4.389E-01
+ XTB = 0.          EG = 1.184E+00 XTI = 3.000E+00 FC = 8.500E-01
.ENDS

```



```

**
* FOUR 1.5 BY 15 MICRON STRIPES :      LOW MODEL      ** VB110 **
.MODEL NV431A01 NPN
+ IS = 1.411E-16  BF = 5.636E+01  NF = 1.000E+00  VAF = 6.236E+01
+ IKF = 1.078E-01  ISE = 3.768E-13  NE = 2.000E+00  BR = 4.843E+01
+ NR = 1.000E+00  VAR = 2.889E+00  IKR = 6.000E-02  ISC = 6.087E-14
+ NC = 1.653E+00  RB = 2.026E+01  IRB = 0.000E+00  RBM = 1.500E+01
+ RE = 5.545E-01  RC = 2.877E+01  CJE = 3.134E-13  VJE = 7.414E-01
+ MJE = 4.950E-01  TF = 1.390E-11  XTF = 2.380E+01  VTF = 9.000E+00
+ ITF = 4.160E-01  PTF = 0.000E+00  CJC = 2.547E-13  VJC = 6.465E-01
+ MJC = 4.509E-01  XCJC= 2.332E-01  TR = 7.575E-11  CJS = 1.972E-13
+ VJS = 5.286E-01  MJS = 4.389E-01  XTB = 1.193E+00  EG = 1.184E+00
+ XTI = 2.000E+00  KF = 0.000E+00  AF = 1.000E+00  FC = 8.500E-01
*
* From ADVICE usrmod=NEB1 Extended Bipolar Model with Quasi-sat
.SUBCKT NV431A01 (1, 2, 3, 4)
Qs  10 20 3  NV431Q01
Qp  4  10 20  NV431P01
Dbv 20 10  NBVBC 2
RCX  1  10 28.77
RBX  2  20 15.00
.MODEL NV431Q01 NPN
+ IS = 1.411E-16  BF = 5.636E+01  NF = 1.000E+00  VAF = 6.236E+01
+ IKF = 1.178E-01  ISE = 3.768E-13  NE = 2.000E+00  BR = 4.843E+01
+ NR = 1.000E+00  VAR = 2.889E+00  IKR = 6.000E-02  ISC = 3.885E-20
+ NC = 1.653E+00  RB = 5.265E+00  IRB = 0.000E+00  RBM = 1E-4
+ RE = 5.545E-01  RC = 0.          CJE = 3.134E-13  VJE = 7.414E-01
+ MJE = 4.950E-01  TF = 8.800E-12  XTF = 2.380E+01  VTF = 9.000E+00
+ ITF = 4.160E-01  PTF = 0.000E+00  CJC = 5.939E-14  VJC = 6.465E-01
+ MJC = 4.509E-01  XCJC= 1.          TR = 7.575E-11  CJS = 0.
+ VJS = 5.286E-01  MJS = 0.          XTB = 1.193E+00  EG = 1.184E+00
+ XTI = 2.000E+00  KF = 0.000E+00  AF = 1.000E+00  FC = 8.500E-01
* Quasi-saturation Effect available in PSpice 4.03 and above only
+ QCO = 5.233E-14  RCO = 9.420E+01  VO = 6.619E+00  GAMMA= 2.497E-11
.MODEL NV431P01 PNP
+ IS = 3.234E-18  BF = 6.242E-01  ISE = 6.087E-14  NE = 1.953E+00
+ IKF = 3.890E-04  CJE = 1.953E-13  VJE = 6.465E-01  MJE = 4.509E-01
+ BR = 1.322E-02  CJC = 1.972E-13  VJC = 5.286E-01  MJC = 4.389E-01
+ XTB = 0.          EG = 1.184E+00  XTI = 3.000E+00  FC = 8.500E-01
.ENDS

```

```

**
* THREE 1.5 BY 30 MICRON STRIPES :      LOW MODEL      ** VB110 **
.MODEL NV362A01 NPN
+ IS = 2.115E-16  BF = 5.636E+01  NF = 1.000E+00  VAF = 6.236E+01
+ IKF = 1.617E-01  ISE = 5.652E-13  NE = 2.000E+00  BR = 4.990E+01
+ NR = 1.000E+00  VAR = 2.889E+00  IKR = 9.000E-02  ISC = 8.376E-14
+ NC = 1.653E+00  RB = 1.351E+01  IRB = 0.000E+00  RBM = 1.000E+01
+ RE = 3.697E-01  RC = 5.212E+00  CJE = 4.701E-13  VJE = 7.414E-01
+ MJE = 4.950E-01  TF = 1.378E-11  XTF = 2.380E+01  VTF = 9.000E+00
+ ITF = 6.240E-01  PTF = 0.000E+00  CJC = 3.526E-13  VJC = 6.465E-01
+ MJC = 4.509E-01  XCJC= 2.527E-01  TR = 7.575E-11  CJS = 3.338E-13
+ VJS = 5.286E-01  MJS = 4.389E-01  XTB = 1.193E+00  EG = 1.184E+00
+ XTI = 2.000E+00  KF = 0.000E+00  AF = 1.000E+00  FC = 8.500E-01
*
* From ADVICE usrmod=NEB1 Extended Bipolar Model with Quasi-sat
.SUBCKT NV362A01 (1, 2, 3, 4)
Qs  10 20 3  NV362Q01
Qp  4  10 20 NV362P01
Dbv 20 10  NBVBC 3
RCX 1  10  5.212
RBX 2  20  10.00
.MODEL NV362Q01 NPN
+ IS = 2.115E-16  BF = 5.636E+01  NF = 1.000E+00  VAF = 6.236E+01
+ IKF = 1.767E-01  ISE = 5.652E-13  NE = 2.000E+00  BR = 4.990E+01
+ NR = 1.000E+00  VAR = 2.889E+00  IKR = 9.000E-02  ISC = 5.828E-20
+ NC = 1.653E+00  RB = 3.510E+00  IRB = 0.000E+00  RBM = 1E-4
+ RE = 3.697E-01  RC = 0.          CJE = 4.701E-13  VJE = 7.414E-01
+ MJE = 4.950E-01  TF = 8.800E-12  XTF = 2.380E+01  VTF = 9.000E+00
+ ITF = 6.240E-01  PTF = 0.000E+00  CJC = 8.909E-14  VJC = 6.465E-01
+ MJC = 4.509E-01  XCJC= 1.          TR = 7.575E-11  CJS = 0.
+ VJS = 5.286E-01  MJS = 0.          XTB = 1.193E+00  EG = 1.184E+00
+ XTI = 2.000E+00  KF = 0.000E+00  AF = 1.000E+00  FC = 8.500E-01
* Quasi-saturation Effect available in PSpice 4.03 and above only
+ QCO = 1.028E-13  RCO = 6.280E+01  VO = 6.619E+00  GAMMA= 2.497E-11
.MODEL NV362P01 PNP RB = 3.449E+01  IRB = 0.000E+00  RBM = 1E-4
+ IS = 4.450E-18  BF = 6.242E-01  ISE = 8.376E-14  NE = 1.953E+00
+ IKF = 5.354E-04  CJE = 2.635E-13  VJE = 6.465E-01  MJE = 4.509E-01
+ BR = 1.322E-02  CJC = 3.338E-13  VJC = 5.286E-01  MJC = 4.389E-01
+ XTB = 0.          EG = 1.184E+00  XTI = 3.000E+00  FC = 8.500E-01
.ENDS

```

```

**
* SIX 1.5 BY 30 MICRON STRIPES :      LOW MODEL      ** VB110 **
.MODEL NV663A01 NPN
+ IS = 4.231E-16  BF = 5.636E+01  NF = 1.000E+00  VAF = 6.236E+01
+ IKF = 3.235E-01  ISE = 1.130E-12  NE = 2.000E+00  BR = 5.131E+01
+ NR = 1.000E+00  VAR = 2.889E+00  IKR = 1.800E-01  ISC = 1.531E-13
+ NC = 1.653E+00  RB = 6.755E+00  IRB = 0.000E+00  RBM = 5.000E+00
+ RE = 1.848E-01  RC = 2.604E+00  CJE = 9.403E-13  VJE = 7.414E-01
+ MJE = 4.950E-01  TF = 1.353E-11  XTF = 2.380E+01  VTF = 9.000E+00
+ ITF = 1.248E+00  PTF = 0.000E+00  CJC = 6.491E-13  VJC = 6.465E-01
+ MJC = 4.509E-01  XCJC= 2.745E-01  TR = 7.575E-11  CJS = 4.910E-13
+ VJS = 5.286E-01  MJS = 4.389E-01  XTB = 1.193E+00  EG = 1.184E+00
+ XTI = 2.000E+00  KF = 0.000E+00  AF = 1.000E+00  FC = 8.500E-01
*
* From ADVICE usrmod=NEB1 Extended Bipolar Model with Quasi-sat
.SUBCKT NV663A01 (1, 2, 3, 4)
Qs  10 20 3  NV663Q01
Qp  4  10 20 NV663P01
Dbv 20 10  NBVBC 6
RCX  1  10  2.604
RBX  2  20  5.000
.MODEL NV663Q01 NPN
+ IS = 4.231E-16  BF = 5.636E+01  NF = 1.000E+00  VAF = 6.236E+01
+ IKF = 3.535E-01  ISE = 1.130E-12  NE = 2.000E+00  BR = 5.131E+01
+ NR = 1.000E+00  VAR = 2.889E+00  IKR = 1.800E-01  ISC = 1.166E-19
+ NC = 1.653E+00  RB = 1.755E+00  IRB = 0.000E+00  RBM = 1E-4
+ RE = 1.848E-01  RC = 0.          CJE = 9.403E-13  VJE = 7.414E-01
+ MJE = 4.950E-01  TF = 8.800E-12  XTF = 2.380E+01  VTF = 9.000E+00
+ ITF = 1.248E+00  PTF = 0.000E+00  CJC = 1.782E-13  VJC = 6.465E-01
+ MJC = 4.509E-01  XCJC= 1.          TR = 7.575E-11  CJS = 0.
+ VJS = 5.286E-01  MJS = 0.          XTB = 1.193E+00  EG = 1.184E+00
+ XTI = 2.000E+00  KF = 0.000E+00  AF = 1.000E+00  FC = 8.500E-01
* Quasi-saturation Effect available in PSpice 4.03 and above only
+ QCO = 1.028E-13  RCO = 3.140E+01  VO = 6.619E+00  GAMMA= 2.497E-11
.MODEL NV663P01 PNP RB = 1.930E+01  IRB = 0.000E+00  RBM = 1E-4
+ IS = 8.137E-18  BF = 6.242E-01  ISE = 1.531E-13  NE = 1.953E+00
+ IKF = 9.789E-04  CJE = 4.709E-13  VJE = 6.465E-01  MJE = 4.509E-01
+ BR = 1.322E-02  CJC = 4.910E-13  VJC = 5.286E-01  MJC = 4.389E-01
+ XTB = 0.          EG = 1.184E+00  XTI = 3.000E+00  FC = 8.500E-01
.ENDS

**
* Collector-Base Avalanche Breakdown Diode
.MODEL NBVBC D
+ BV = 1.800E+01  IBV = 1.000E-04  IS = 1.000E-21  RS = 0.
* Low-level reverse breakdown available in PSpice 4.03 and above only
+ NBV = 1.000E+01  TBV1=-4.000E-02  TBV2= 0.

```

```

*****
* AT&T Microelectronics CBIC-V Technology - Spice Models   June 1991 *
* "NPNHI.LIB" - NPN Transistors - High                    *
*****
* - From ADVICE usrmod Models and Data                    *
* Full-Scale Revision by JHB 1/15/90: DC, AC Characteristics, T-Depend *
* Models Compiled by KEG 4/20/90                          *
*                                                          *
* NOTE: Reference Temperature is 27 C                      *
*****
*                   High Beta and fT CBIC-V NPN Transistor Models      *
*****
**
* TWO 1.5 BY 15 MICRON STRIPES :      HIGH MODEL          ** VB110 **
.MODEL NV231A01 NPN
+ IS = 7.051E-16 BF = 7.038E+02 NF = 1.000E+00 VAF = 5.003E+01
+ IKF = 3.693E-02 ISE = 8.108E-14 NE = 2.000E+00 BR = 4.628E+02
+ NR = 1.000E+00 VAR = 1.027E+00 IKR = 3.000E-02 ISC = 3.451E-14
+ NC = 1.653E+00 RB = 8.493E+01 IRB = 0.000E+00 RBM = 2.000E+01
+ RE = 1.923E+00 RC = 1.704E+01 CJE = 9.419E-14 VJE = 7.414E-01
+ MJE = 4.950E-01 TF = 1.000E-11 XTF = 1.600E+01 VTF = 6.200E+00
+ ITF = 3.000E-01 PTF = 0.000E+00 CJC = 1.111E-13 VJC = 6.465E-01
+ MJC = 4.509E-01 XCJC= 2.270E-01 TR = 6.625E-11 CJS = 1.006E-13
+ VJS = 5.286E-01 MJS = 4.389E-01 XTB = 1.181E+00 EG = 1.184E+00
+ XTI = 2.000E+00 KF = 0.000E+00 AF = 1.000E+00 FC = 7.800E-01
*
* From ADVICE usrmod=NEB1 Extended Bipolar Model with Quasi-sat
.SUBCKT NV231A01 (1, 2, 3, 4)
Qs  10 20 3 NV231Q01
Qp  4  10 20 NV231P01
Dbv 20 10 NBVBC
RCX  1  10 17.04
RBX  2  20 20.00
.MODEL NV231Q01 NPN
+ IS = 7.051E-16 BF = 7.038E+02 NF = 1.000E+00 VAF = 5.003E+01
+ IKF = 4.193E-02 ISE = 8.108E-14 NE = 2.000E+00 BR = 4.628E+02
+ NR = 1.000E+00 VAR = 1.027E+00 IKR = 3.000E-02 ISC = 1.943E-20
+ NC = 1.653E+00 RB = 6.493E+01 IRB = 0.000E+00 RBM = 1E-4
+ RE = 1.923E+00 RC = 0.          CJE = 9.419E-14 VJE = 7.414E-01
+ MJE = 4.950E-01 TF = 6.200E-12 XTF = 1.600E+01 VTF = 6.200E+00
+ ITF = 3.000E-01 PTF = 0.000E+00 CJC = 2.522E-14 VJC = 6.465E-01
+ MJC = 4.509E-01 XCJC= 1.        TR = 6.625E-11 CJS = 0.
+ VJS = 5.286E-01 MJS = 0.        XTB = 1.181E+00 EG = 1.184E+00
+ XTI = 2.000E+00 KF = 0.000E+00 AF = 1.000E+00 FC = 7.800E-01
* Quasi-saturation Effect available in PSpice 4.03 and above only
+ QCO = 5.233E-14 RCO = 1.179E+02 VO = 5.791E+00 GAMMA= 2.497E-11
.MODEL NV231P01 PNP RB = 8.000E+01 IRB = 0.000E+00 RBM = 1E-4
+ IS = 1.834E-18 BF = 6.242E-01 ISE = 3.451E-14 NE = 1.953E+00
+ IKF = 2.206E-04 CJE = 8.586E-14 VJE = 6.465E-01 MJE = 4.509E-01
+ BR = 1.322E-02 CJC = 1.006E-13 VJC = 5.286E-01 MJC = 4.389E-01
+ XTB = 0.          EG = 1.184E+00 XTI = 3.000E+00 FC = 7.800E-01
.ENDS

```

```

**
* FOUR 1.5 BY 15 MICRON STRIPES :      HIGH MODEL      ** VB110 **
.MODEL NV431A01 NPN
+ IS = 1.411E-15  BF = 7.038E+02  NF = 1.000E+00  VAF = 5.003E+01
+ IKF = 7.386E-02  ISE = 1.621E-13  NE = 2.000E+00  BR = 4.844E+02
+ NR = 1.000E+00  VAR = 1.027E+00  IKR = 6.000E-02  ISC = 6.087E-14
+ NC = 1.653E+00  RB = 4.246E+01  IRB = 0.000E+00  RBM = 1.000E+01
+ RE = 9.615E-01  RC = 2.446E+01  CJE = 1.884E-13  VJE = 7.414E-01
+ MJE = 4.950E-01  TF = 9.796E-12  XTF = 1.600E+01  VTF = 6.200E+00
+ ITF = 6.000E-01  PTF = 0.000E+00  CJC = 1.981E-13  VJC = 6.465E-01
+ MJC = 4.509E-01  XCJC= 2.547E-01  TR = 6.625E-11  CJS = 1.471E-13
+ VJS = 5.286E-01  MJS = 4.389E-01  XTB = 1.181E+00  EG = 1.184E+00
+ XTI = 2.000E+00  KF = 0.000E+00  AF = 1.000E+00  FC = 7.800E-01
*
* From ADVICE usrmod=NEB1 Extended Bipolar Model with Quasi-sat
.SUBCKT NV431A01 (1, 2, 3, 4)
Qs  10 20 3  NV431Q01
Qp  4  10 20 NV431P01
Dbv 20 10  NBVBC 2
RCX  1  10 24.46
RBX  2  20 10.00
.MODEL NV431Q01 NPN
+ IS = 1.411E-15  BF = 7.038E+02  NF = 1.000E+00  VAF = 5.003E+01
+ IKF = 8.386E-02  ISE = 1.621E-13  NE = 2.000E+00  BR = 4.844E+02
+ NR = 1.000E+00  VAR = 1.027E+00  IKR = 6.000E-02  ISC = 3.885E-20
+ NC = 1.653E+00  RB = 3.246E+01  IRB = 0.000E+00  RBM = 1E-4
+ RE = 9.615E-01  RC = 0.          CJE = 1.884E-13  VJE = 7.414E-01
+ MJE = 4.950E-01  TF = 6.200E-12  XTF = 1.600E+01  VTF = 6.200E+00
+ ITF = 6.000E-01  PTF = 0.000E+00  CJC = 5.045E-14  VJC = 6.465E-01
+ MJC = 4.509E-01  XCJC= 1.          TR = 6.625E-11  CJS = 0.
+ VJS = 5.286E-01  MJS = 0.          XTB = 1.181E+00  EG = 1.184E+00
+ XTI = 2.000E+00  KF = 0.000E+00  AF = 1.000E+00  FC = 7.800E-01
* Quasi-saturation Effect available in PSpice 4.03 and above only
+ QCO = 5.233E-14  RCO = 5.893E+01  VO = 5.791E+00  GAMMA= 2.497E-11
.MODEL NV431P01 PNP RB = 4.653E+01  IRB = 0.000E+00  RBM = 1E-4
+ IS = 3.234E-18  BF = 6.242E-01  ISE = 6.087E-14  NE = 1.953E+00
+ IKF = 3.890E-04  CJE = 1.476E-13  VJE = 6.465E-01  MJE = 4.509E-01
+ BR = 1.322E-02  CJC = 1.471E-13  VJC = 5.286E-01  MJC = 4.389E-01
+ XTB = 0.          EG = 1.184E+00  XTI = 3.000E+00  FC = 7.800E-01
.ENDS

```

```

**
* THREE 1.5 BY 30 MICRON STRIPES :      HIGH MODEL      ** VB110 **
.MODEL NV362A01 NPN
+ IS = 2.115E-15 BF = 7.038E+02 NF = 1.000E+00 VAF = 5.003E+01
+ IKF = 1.109E-01 ISE = 2.433E-13 NE = 2.000E+00 BR = 4.990E+02
+ NR = 1.000E+00 VAR = 1.027E+00 IKR = 9.000E-02 ISC = 8.376E-14
+ NC = 1.653E+00 RB = 2.831E+01 IRB = 0.000E+00 RBM = 6.667E+00
+ RE = 6.410E-01 RC = 4.432E+00 CJE = 2.826E-13 VJE = 7.414E-01
+ MJE = 4.950E-01 TF = 9.710E-12 XTF = 1.600E+01 VTF = 6.200E+00
+ ITF = 9.000E-01 PTF = 0.000E+00 CJC = 2.749E-13 VJC = 6.465E-01
+ MJC = 4.509E-01 XCJC= 2.753E-01 TR = 6.625E-11 CJS = 2.491E-13
+ VJS = 5.286E-01 MJS = 4.389E-01 XTB = 1.181E+00 EG = 1.184E+00
+ XTI = 2.000E+00 KF = 0.000E+00 AF = 1.000E+00 FC = 7.800E-01
*
* From ADVICE usrmod=NEB1 Extended Bipolar Model with Quasi-sat
.SUBCKT NV362A01 (1, 2, 3, 4)
Qs 10 20 3 NV362Q01
Qp 4 10 20 NV362P01
Dbv 20 10 NBVBC 3
RCX 1 10 4.432
RBX 2 20 6.667
.MODEL NV362Q01 NPN
+ IS = 2.115E-15 BF = 7.038E+02 NF = 1.000E+00 VAF = 5.003E+01
+ IKF = 1.259E-01 ISE = 2.433E-13 NE = 2.000E+00 BR = 4.990E+02
+ NR = 1.000E+00 VAR = 1.027E+00 IKR = 9.000E-02 ISC = 5.828E-20
+ NC = 1.653E+00 RB = 2.164E+01 IRB = 0.000E+00 RBM = 1E-4
+ RE = 6.410E-01 RC = 0. CJE = 2.826E-13 VJE = 7.414E-01
+ MJE = 4.950E-01 TF = 6.200E-12 XTF = 1.600E+01 VTF = 6.200E+00
+ ITF = 9.000E-01 PTF = 0.000E+00 CJC = 7.567E-14 VJC = 6.465E-01
+ MJC = 4.509E-01 XCJC= 1. TR = 6.625E-11 CJS = 0.
+ VJS = 5.286E-01 MJS = 0. XTB = 1.181E+00 EG = 1.184E+00
+ XTI = 2.000E+00 KF = 0.000E+00 AF = 1.000E+00 FC = 7.800E-01
* Quasi-saturation Effect available in PSpice 4.03 and above only
+ QCO = 1.028E-13 RCO = 3.929E+01 VO = 5.791E+00 GAMMA= 2.497E-11
.MODEL NV362P01 PNP RB = 3.449E+01 IRB = 0.000E+00 RBM = 1E-4
+ IS = 4.450E-18 BF = 6.242E-01 ISE = 8.376E-14 NE = 1.953E+00
+ IKF = 5.354E-04 CJE = 1.992E-13 VJE = 6.465E-01 MJE = 4.509E-01
+ BR = 1.322E-02 CJC = 2.491E-13 VJC = 5.286E-01 MJC = 4.389E-01
+ XTB = 0. EG = 1.184E+00 XTI = 3.000E+00 FC = 7.800E-01
.ENDS

```

```

**
* SIX 1.5 BY 30 MICRON STRIPES :      HIGH MODEL      ** VB110 **
.MODEL NV663A01 NPN
+ IS = 4.231E-15  BF = 7.038E+02  NF = 1.000E+00  VAF = 5.003E+01
+ IKF = 2.218E-01  ISE = 4.865E-13  NE = 2.000E+00  BR = 5.131E+02
+ NR = 1.000E+00  VAR = 1.027E+00  IKR = 1.800E-01  ISC = 1.531E-13
+ NC = 1.653E+00  RB = 1.415E+01  IRB = 0.000E+00  RBM = 3.333E+00
+ RE = 3.205E-01  RC = 2.214E+00  CJE = 5.651E-13  VJE = 7.414E-01
+ MJE = 4.950E-01  TF = 9.534E-12  XTF = 1.600E+01  VTF = 6.200E+00
+ ITF = 1.800E+00  PTF = 0.000E+00  CJC = 5.074E-13  VJC = 6.465E-01
+ MJC = 4.509E-01  XCJC= 2.984E-01  TR = 6.625E-11  CJS = 3.664E-13
+ VJS = 5.286E-01  MJS = 4.389E-01  XTB = 1.181E+00  EG = 1.184E+00
+ XTI = 2.000E+00  KF = 0.000E+00  AF = 1.000E+00  FC = 7.800E-01

```

```

*
* From ADVICE usrmod=NEB1 Extended Bipolar Model with Quasi-sat

```

```

.SUBCKT NV663A01 (1, 2, 3, 4)

```

```

Qs 10 20 3 NV663Q01

```

```

Qp 4 10 20 NV663P01

```

```

Dbv 20 10 NBVBC 6

```

```

RCX 1 10 2.214

```

```

RBX 2 20 3.333

```

```

.MODEL NV663Q01 NPN

```

```

+ IS = 4.231E-15  BF = 7.038E+02  NF = 1.000E+00  VAF = 5.003E+01
+ IKF = 2.518E-01  ISE = 4.865E-13  NE = 2.000E+00  BR = 5.131E+02
+ NR = 1.000E+00  VAR = 1.027E+00  IKR = 1.800E-01  ISC = 1.166E-19
+ NC = 1.653E+00  RB = 1.082E+01  IRB = 0.000E+00  RBM = 1E-4
+ RE = 3.205E-01  RC = 0.          CJE = 5.651E-13  VJE = 7.414E-01
+ MJE = 4.950E-01  TF = 6.200E-12  XTF = 1.600E+01  VTF = 6.200E+00
+ ITF = 1.800E+00  PTF = 0.000E+00  CJC = 1.514E-13  VJC = 6.465E-01
+ MJC = 4.509E-01  XCJC= 1.          TR = 6.625E-11  CJS = 0.
+ VJS = 5.286E-01  MJS = 0.          XTB = 1.181E+00  EG = 1.184E+00
+ XTI = 2.000E+00  KF = 0.000E+00  AF = 1.000E+00  FC = 7.800E-01

```

```

* Quasi-saturation Effect available in PSpice 4.03 and above only

```

```

+ QCO = 1.028E-13  RCO = 1.964E+01  VO = 5.791E+00  GAMMA= 2.497E-11

```

```

.MODEL NV663P01 PNP RB = 1.930E+01  IRB = 0.000E+00  RBM = 1E-4

```

```

+ IS = 8.137E-18  BF = 6.242E-01  ISE = 1.531E-13  NE = 1.953E+00

```

```

+ IKF = 9.789E-04  CJE = 3.560E-13  VJE = 6.465E-01  MJE = 4.509E-01

```

```

+ BR = 1.322E-02  CJC = 3.664E-13  VJC = 5.286E-01  MJC = 4.389E-01

```

```

+ XTB = 0.          EG = 1.184E+00  XTI = 3.000E+00  FC = 7.800E-01

```

```

.ENDS

```

```

**
* Collector-Base Avalanche Breakdown Diode

```

```

.MODEL NBVBC D

```

```

+ BV = 6.000E+00  IBV = 1.000E-04  IS = 1.000E-21  RS = 0.

```

```

* Low-level reverse breakdown available in PSpice 4.03 and above only

```

```

+ NBV = 1.000E+01  TBV1=-4.000E-02  TBV2= 0.

```

```

*****
* AT&T Microelectronics CBIC-V Technology - Spice Models   June 1991 *
* "PNPNOM.LIB" - PNP Transistors - Nominal                 *
*****
* - From ADVICE usrmod=PEB1 Extended Bipolar Model with Quasi-sat *
* Full-Scale Revision by JHB 1/15/90: DC, AC Characteristics, T-Depend
* Models Compiled by KEG 4/20/90                             *
*
* NOTE: Reference Temperature is 27 C                       *
*****
*                   Nominal CBIC-V Beta and fT PNP Transistor Models *
*****
**

```

```

* TWO 1.5 BY 15 MICRON STRIPES :      NOM  MODEL                ** VB110 **
.MODEL PV231A01 PNP
+ IS = 9.672E-17 BF = 1.092E+02 NF = 1.000E+00 VAF = 2.150E+01
+ IKF = 1.580E-02 ISE = 5.662E-16 NE = 1.287E+00 BR = 5.894E+02
+ NR = 1.000E+00 VAR = 1.927E+00 IKR = 1.000E-01 ISC = 3.476E-14
+ NC = 1.634E+00 RB = 4.008E+01 IRB = 0.000E+00 RBM = 1.925E+01
+ RE = 1.261E+00 RC = 8.354E+01 CJE = 1.224E-13 VJE = 7.320E-01
+ MJE = 4.930E-01 TF = 2.094E-11 XTF = 3.500E+01 VTF = 7.553E+00
+ ITF = 4.010E-01 PTF = 0.000E+00 CJC = 1.993E-13 VJC = 7.743E-01
+ MJC = 5.185E-01 XCJC= 1.562E-01 TR = 6.500E-11 CJS = 5.935E-13
+ VJS = 9.058E-01 MJS = 4.931E-01 XTB = 2.452E+00 EG = 1.184E+00
+ XTI = 2.000E+00 KF = 0.000E+00 AF = 1.000E+00 FC = 9.000E-01

```

```

*
* From ADVICE usrmod=PEB1 Extended Bipolar Model with Quasi-sat
.SUBCKT PV231A01 (1, 2, 3, 4)
Qs 10 20 3 PV231Q01
Qp 4 10 20 PV231P01
Dbv 10 20 PBVBC
RCX 1 10 83.54
RBX 2 20 19.25

```

```

.MODEL PV231Q01 PNP
+ IS = 9.672E-17 BF = 1.092E+02 NF = 1.000E+00 VAF = 2.150E+01
+ IKF = 2.080E-02 ISE = 5.662E-16 NE = 1.287E+00 BR = 5.894E+02
+ NR = 1.000E+00 VAR = 1.927E+00 IKR = 1.000E-01 ISC = 2.502E-16
+ NC = 1.634E+00 RB = 2.083E+01 IRB = 0.000E+00 RBM = 1E-4
+ RE = 1.261E+00 RC = 0. CJE = 1.224E-13 VJE = 7.320E-01
+ MJE = 4.930E-01 TF = 1.217E-11 XTF = 3.500E+01 VTF = 7.553E+00
+ ITF = 4.010E-01 PTF = 0.000E+00 CJC = 3.114E-14 VJC = 7.743E-01
+ MJC = 5.185E-01 XCJC= 0. TR = 6.500E-11 CJS = 0.
+ VJS = 9.058E-01 MJS = 0. XTB = 2.452E+00 EG = 1.184E+00
+ XTI = 2.000E+00 KF = 0.000E+00 AF = 1.000E+00 FC = 9.000E-01

```

```

* Quasi-saturation Effect available in PSpice 4.03 and above only
+ QCO = 1.006E-25 RCO = 1.227E+02 VO = 2.931E+00 GAMMA= 3.298E-12
.MODEL PV231P01 NPN RB = 8.000E+01 IRB = 0.000E+00 RBM = 1E-4
+ IS = 8.097E-18 BF = 1.140E+01 ISE = 3.451E-14 NE = 1.953E+00
+ IKF = 1.154E-03 CJE = 1.682E-13 VJE = 7.743E-01 MJE = 5.185E-01
+ BR = 5.837E-02 CJC = 5.935E-13 VJC = 9.058E-01 MJC = 4.931E-01
+ XTB = 0. EG = 1.184E+00 XTI = 3.000E+00 FC = 9.000E-01

```

```

.ENDS

```



```

**
* FOUR 1.5 BY 15 MICRON STRIPES :      NOM  MODEL      ** VB110 **
.MODEL PV432A01 PNP
+ IS = 1.934E-16  BF = 1.092E+02  NF = 1.000E+00  VAF = 2.150E+01
+ IKF = 3.159E-02  ISE = 1.132E-15  NE = 1.287E+00  BR = 6.161E+02
+ NR = 1.000E+00  VAR = 1.927E+00  IKR = 2.000E-01  ISC = 6.137E-14
+ NC = 1.634E+00  RB = 2.004E+01  IRB = 0.000E+00  RBM = 9.625E+00
+ RE = 6.305E-01  RC = 4.177E+01  CJE = 2.447E-13  VJE = 7.320E-01
+ MJE = 4.930E-01  TF = 2.044E-11  XTF = 3.500E+01  VTF = 7.553E+00
+ ITF = 8.020E-01  PTF = 0.000E+00  CJC = 3.515E-13  VJC = 7.743E-01
+ MJC = 5.185E-01  XCJC= 1.772E-01  TR = 6.500E-11  CJS = 1.033E-12
+ VJS = 9.058E-01  MJS = 4.931E-01  XTB = 2.452E+00  EG = 1.184E+00
+ XTI = 2.000E+00  KF = 0.000E+00  AF = 1.000E+00  FC = 9.000E-01
*
* From ADVICE usrmod=PEB1 Extended Bipolar Model with Quasi-sat
.SUBCKT PV432A01 (1, 2, 3, 4)
Qs  10 20 3  PV432Q01
Qp  4  10 20 PV432P01
Dbv 10 20  PBVBC 2
RCX  1  10 41.77
RBX  2  20  9.625
.MODEL PV432Q01 PNP
+ IS = 1.934E-16  BF = 1.092E+02  NF = 1.000E+00  VAF = 2.150E+01
+ IKF = 4.159E-02  ISE = 1.132E-15  NE = 1.287E+00  BR = 6.161E+02
+ NR = 1.000E+00  VAR = 1.927E+00  IKR = 2.000E-01  ISC = 5.003E-16
+ NC = 1.634E+00  RB = 1.041E+01  IRB = 0.000E+00  RBM = 1E-4
+ RE = 6.305E-01  RC = 0.          CJE = 2.447E-13  VJE = 7.320E-01
+ MJE = 4.930E-01  TF = 1.217E-11  XTF = 3.500E+01  VTF = 7.553E+00
+ ITF = 8.020E-01  PTF = 0.000E+00  CJC = 6.228E-14  VJC = 7.743E-01
+ MJC = 5.185E-01  XCJC= 1.          TR = 6.500E-11  CJS = 0.
+ VJS = 9.058E-01  MJS = 0.          XTB = 2.452E+00  EG = 1.184E+00
+ XTI = 2.000E+00  KF = 0.000E+00  AF = 1.000E+00  FC = 9.000E-01
* Quasi-saturation Effect available in PSpice 4.03 and above only
+ QCO = 1.006E-25  RCO = 6.137E+01  VO = 2.931E+00  GAMMA= 3.298E-12
.MODEL PV432P01 NPN RB = 4.653E+01  IRB = 0.000E+00  RBM = 1E-4
+ IS = 1.427E-17  BF = 1.140E+01  ISE = 6.087E-14  NE = 1.953E+00
+ IKF = 2.035E-03  CJE = 2.892E-13  VJE = 7.743E-01  MJE = 5.185E-01
+ BR = 5.837E-02  CJC = 1.033E-12  VJC = 9.058E-01  MJC = 4.931E-01
+ XTB = 0.          EG = 1.184E+00  XTI = 3.000E+00  FC = 9.000E-01
.ENDS

```

```

**
* THREE 1.5 BY 45 MICRON STRIPES :      NOM  MODEL      ** VB110 **
.MODEL PV392A01 PNP
+ IS = 4.352E-16  BF = 1.092E+02  NF = 1.000E+00  VAF = 2.150E+01
+ IKF = 7.110E-02  ISE = 2.548E-15  NE = 1.287E+00  BR = 6.446E+02
+ NR = 1.000E+00  VAR = 1.927E+00  IKR = 4.500E-01  ISC = 1.210E-13
+ NC = 1.634E+00  RB = 8.906E+00  IRB = 0.000E+00  RBM = 4.278E+00
+ RE = 2.802E-01  RC = 2.038E+01  CJE = 5.507E-13  VJE = 7.320E-01
+ MJE = 4.930E-01  TF = 1.996E-11  XTF = 3.500E+01  VTF = 7.553E+00
+ ITF = 1.805E+00  PTF = 0.000E+00  CJC = 6.916E-13  VJC = 7.743E-01
+ MJC = 5.185E-01  XCJC= 2.026E-01  TR = 6.500E-11  CJS = 1.868E-12
+ VJS = 9.058E-01  MJS = 4.931E-01  XTB = 2.452E+00  EG = 1.184E+00
+ XTI = 2.000E+00  KF = 0.000E+00  AF = 1.000E+00  FC = 9.000E-01
*
* From ADVICE usrmod=PEB1 Extended Bipolar Model with Quasi-sat
.SUBCKT PV392A01 (1, 2, 3, 4)
Qs  10 20 3  PV392Q01
Qp  4  10 20 PV392P01
Dbv 10 20  PBVBC 4.5
RCX  1  10  20.38
RBX  2  20  4.278
.MODEL PV392Q01 PNP
+ IS = 4.352E-16  BF = 1.092E+02  NF = 1.000E+00  VAF = 2.150E+01
+ IKF = 9.360E-02  ISE = 2.548E-15  NE = 1.287E+00  BR = 6.446E+02
+ NR = 1.000E+00  VAR = 1.927E+00  IKR = 4.500E-01  ISC = 1.126E-15
+ NC = 1.634E+00  RB = 4.628E+00  IRB = 0.000E+00  RBM = 1E-4
+ RE = 2.802E-01  RC = 0.          CJE = 5.507E-13  VJE = 7.320E-01
+ MJE = 4.930E-01  TF = 1.217E-11  XTF = 3.500E+01  VTF = 7.553E+00
+ ITF = 1.805E+00  PTF = 0.000E+00  CJC = 1.401E-13  VJC = 7.743E-01
+ MJC = 5.185E-01  XCJC= 1.          TR = 6.500E-11  CJS = 0.
+ VJS = 9.058E-01  MJS = 0.          XTB = 2.452E+00  EG = 1.184E+00
+ XTI = 2.000E+00  KF = 0.000E+00  AF = 1.000E+00  FC = 9.000E-01
* Quasi-saturation Effect available in PSpice 4.03 and above only
+ QCO = 2.079E-25  RCO = 2.728E+01  VO = 2.931E+00  GAMMA= 3.298E-12
.MODEL PV392P01 NPN RB = 2.440E+01  IRB = 0.000E+00  RBM = 1E-4
+ IS = 2.811E-17  BF = 1.140E+01  ISE = 1.199E-13  NE = 1.953E+00
+ IKF = 4.007E-03  CJE = 5.515E-13  VJE = 7.743E-01  MJE = 5.185E-01
+ BR = 5.837E-02  CJC = 1.868E-12  VJC = 9.058E-01  MJC = 4.931E-01
+ XTB = 0.          EG = 1.184E+00  XTI = 3.000E+00  FC = 9.000E-01
.ENDS

```

```

**
* SIX 1.5 BY 45 MICRON STRIPES :      NOM  MODEL      ** VB110 **
.MODEL PV693A01 PNP
+ IS = 8.704E-16  BF = 1.092E+02  NF = 1.000E+00  VAF = 2.150E+01
+ IKF = 1.422E-01  ISE = 5.096E-15  NE = 1.287E+00  BR = 6.616E+02
+ NR = 1.000E+00  VAR = 1.927E+00  IKR = 9.000E-01  ISC = 2.214E-13
+ NC = 1.634E+00  RB = 4.453E+00  IRB = 0.000E+00  RBM = 2.139E+00
+ RE = 1.401E-01  RC = 1.019E+01  CJE = 1.101E-12  VJE = 7.320E-01
+ MJE = 4.930E-01  TF = 1.968E-11  XTF = 3.500E+01  VTF = 7.553E+00
+ ITF = 3.609E+00  PTF = 0.000E+00  CJC = 1.265E-12  VJC = 7.743E-01
+ MJC = 5.185E-01  XCJC= 2.216E-01  TR = 6.500E-11  CJS = 3.877E-12
+ VJS = 9.058E-01  MJS = 4.931E-01  XTB = 2.452E+00  EG = 1.184E+00
+ XTI = 2.000E+00  KF = 0.000E+00  AF = 1.000E+00  FC = 9.000E-01

```

```

*
* From ADVICE usrmod=PEB1 Extended Bipolar Model with Quasi-sat
.SUBCKT PV693A01 (1, 2, 3, 4)
Qs  10 20 3  PV693Q01
Qp  4  10 20 PV693P01
Dbv 10 20  PBVBC 9
RCX  1  10 10.19
RBX  2  20  2.139

```

```

.MODEL PV693Q01 PNP
+ IS = 8.704E-16  BF = 1.092E+02  NF = 1.000E+00  VAF = 2.150E+01
+ IKF = 1.872E-01  ISE = 5.096E-15  NE = 1.287E+00  BR = 6.616E+02
+ NR = 1.000E+00  VAR = 1.927E+00  IKR = 9.000E-01  ISC = 2.251E-15
+ NC = 1.634E+00  RB = 2.314E+00  IRB = 0.000E+00  RBM = 1E-4
+ RE = 1.401E-01  RC = 0.          CJE = 1.101E-12  VJE = 7.320E-01
+ MJE = 4.930E-01  TF = 1.217E-11  XTF = 3.500E+01  VTF = 7.553E+00
+ ITF = 3.609E+00  PTF = 0.000E+00  CJC = 2.802E-13  VJC = 7.743E-01
+ MJC = 5.185E-01  XCJC= 1.          TR = 6.500E-11  CJS = 0.
+ VJS = 9.058E-01  MJS = 0.          XTB = 2.452E+00  EG = 1.184E+00
+ XTI = 2.000E+00  KF = 0.000E+00  AF = 1.000E+00  FC = 9.000E-01

```

```

* Quasi-saturation Effect available in PSpice 4.03 and above only
+ QCO = 2.079E-25  RCO = 1.364E+01  VO = 2.931E+00  GAMMA= 3.298E-12
.MODEL PV693P01 NPN RB = 1.367E+01  IRB = 0.000E+00  RBM = 1E-4
+ IS = 5.140E-17  BF = 1.140E+01  ISE = 2.191E-13  NE = 1.953E+00
+ IKF = 7.326E-03  CJE = 9.845E-13  VJE = 7.743E-01  MJE = 5.185E-01
+ BR = 5.837E-02  CJC = 3.877E-12  VJC = 9.058E-01  MJC = 4.931E-01
+ XTB = 0.          EG = 1.184E+00  XTI = 3.000E+00  FC = 9.000E-01
.ENDS

```

```

**
* Collector-Base Avalanche Breakdown Diode
.MODEL PBVBC D
+ BV = 1.500E+01  IBV = 1.000E-04  IS = 1.000E-21  RS = 0.
* Low-level reverse breakdown available in PSpice 4.03 and above only
+ NBV = 1.000E+01  TBV1=-4.000E-02  TBV2= 0.

```

```

*****
* AT&T Microelectronics CBIC-V Technology - Spice Models   June 1991 *
* "PNPLOW.LIB" - PNP Transistors - Low                      *
*****
* - From ADVICE usrmod=PEB1 Extended Bipolar Model with Quasi-sat *
* Full-Scale Revision by JHB 1/15/90: DC, AC Characteristics, T-Depend
* Models Compiled by KEG 4/20/90                             *
*
* NOTE: Reference Temperature is 27 C                       *
*****
*                   Low CBIC-V Beta and fT PNP Transistor Models *
*****
**
* TWO 1.5 BY 15 MICRON STRIPES :      LOW  MODEL          ** VB110 **
.MODEL PV231A01 PNP
+ IS = 3.116E-17 BF = 5.680E+01 NF = 1.000E+00 VAF = 2.949E+01
+ IKF = 1.680E-02 ISE = 4.294E-16 NE = 1.287E+00 BR = 1.900E+02
+ NR = 1.000E+00 VAR = 3.194E+00 IKR = 1.000E-01 ISC = 3.476E-14
+ NC = 1.634E+00 RB = 3.394E+01 IRB = 0.000E+00 RBM = 2.353E+01
+ RE = 1.261E+00 RC = 1.172E+02 CJE = 1.446E-13 VJE = 7.320E-01
+ MJE = 4.930E-01 TF = 2.693E-11 XTF = 3.677E+01 VTF = 7.327E+00
+ ITF = 2.724E-01 PTF = 0.000E+00 CJC = 2.234E-13 VJC = 7.743E-01
+ MJC = 5.185E-01 XCJC= 1.562E-01 TR = 7.500E-11 CJS = 6.936E-13
+ VJS = 9.058E-01 MJS = 4.931E-01 XTB = 3.117E+00 EG = 1.184E+00
+ XTI = 2.000E+00 KF = 0.000E+00 AF = 1.000E+00 FC = 9.000E-01
*
* From ADVICE usrmod=PEB1 Extended Bipolar Model with Quasi-sat
.SUBCKT PV231A01 (1, 2, 3, 4)
Qs  10 20 3 PV231Q01
Qp  4  10 20 PV231P01
Dbv 10 20 PBVBC
RCX  1  10 117.2
RBX  2  20 23.53
.MODEL PV231Q01 PNP
+ IS = 3.116E-17 BF = 5.680E+01 NF = 1.000E+00 VAF = 2.949E+01
+ IKF = 2.180E-02 ISE = 4.294E-16 NE = 1.287E+00 BR = 1.900E+02
+ NR = 1.000E+00 VAR = 3.194E+00 IKR = 1.000E-01 ISC = 2.502E-16
+ NC = 1.634E+00 RB = 1.041E+01 IRB = 0.000E+00 RBM = 1E-4
+ RE = 1.261E+00 RC = 0.          CJE = 1.446E-13 VJE = 7.320E-01
+ MJE = 4.930E-01 TF = 1.450E-11 XTF = 3.677E+01 VTF = 7.327E+00
+ ITF = 2.724E-01 PTF = 0.000E+00 CJC = 3.490E-14 VJC = 7.743E-01
+ MJC = 5.185E-01 XCJC= 1.        TR = 7.500E-11 CJS = 0.
+ VJS = 9.058E-01 MJS = 0.        XTB = 3.117E+00 EG = 1.184E+00
+ XTI = 2.000E+00 KF = 0.000E+00 AF = 1.000E+00 FC = 9.000E-01
* Quasi-saturation Effect available in PSpice 4.03 and above only
+ QCO = 1.006E-25 RCO = 1.631E+02 VO = 3.234E+00 GAMMA= 1.495E-12
.MODEL PV231P01 NPN RB = 8.000E+01 IRB = 0.000E+00 RBM = 1E-4
+ IS = 5.479E-18 BF = 7.719E+00 ISE = 3.451E-14 NE = 1.953E+00
+ IKF = 1.154E-03 CJE = 1.885E-13 VJE = 7.743E-01 MJE = 5.185E-01
+ BR = 3.950E-02 CJC = 6.936E-13 VJC = 9.058E-01 MJC = 4.931E-01
+ XTB = 0.          EG = 1.184E+00 XTI = 3.000E+00 FC = 9.000E-01
.ENDS

```

```

**
* FOUR 1.5 BY 15 MICRON STRIPES :      LOW  MODEL          ** VB110 **
.MODEL PV432A01 PNP
+ IS = 6.233E-17 BF = 5.680E+01 NF = 1.000E+00 VAF = 2.949E+01
+ IKF = 3.361E-02 ISE = 8.587E-16 NE = 1.287E+00 BR = 1.985E+02
+ NR = 1.000E+00 VAR = 3.194E+00 IKR = 2.000E-01 ISC = 6.137E-14
+ NC = 1.634E+00 RB = 1.698E+01 IRB = 0.000E+00 RBM = 1.177E+01
+ RE = 6.305E-01 RC = 5.860E+01 CJE = 2.892E-13 VJE = 7.320E-01
+ MJE = 4.930E-01 TF = 2.635E-11 XTF = 3.677E+01 VTF = 7.327E+00
+ ITF = 5.448E-01 PTF = 0.000E+00 CJC = 3.938E-13 VJC = 7.743E-01
+ MJC = 5.185E-01 XCJC= 1.772E-01 TR = 7.500E-11 CJS = 1.208E-12
+ VJS = 9.058E-01 MJS = 4.931E-01 XTB = 3.117E+00 EG = 1.184E+00
+ XTI = 2.000E+00 KF = 0.000E+00 AF = 1.000E+00 FC = 9.000E-01
*
* From ADVICE usrmod=PEB1 Extended Bipolar Model with Quasi-sat
.SUBCKT PV432A01 (1, 2, 3, 4)
Qs  10 20 3  PV432Q01
Qp  4  10 20 PV432P01
Dbv 10 20  PBVBC 2
RCX  1  10  58.60
RBX  2  20  11.77
.MODEL PV432Q01 PNP
+ IS = 6.233E-17 BF = 5.680E+01 NF = 1.000E+00 VAF = 2.949E+01
+ IKF = 4.361E-02 ISE = 8.587E-16 NE = 1.287E+00 BR = 1.985E+02
+ NR = 1.000E+00 VAR = 3.194E+00 IKR = 2.000E-01 ISC = 5.003E-16
+ NC = 1.634E+00 RB = 5.205E+00 IRB = 0.000E+00 RBM = 1E-4
+ RE = 6.305E-01 RC = 0.          CJE = 2.892E-13 VJE = 7.320E-01
+ MJE = 4.930E-01 TF = 1.450E-11 XTF = 3.677E+01 VTF = 7.327E+00
+ ITF = 5.448E-01 PTF = 0.000E+00 CJC = 6.979E-14 VJC = 7.743E-01
+ MJC = 5.185E-01 XCJC= 1.          TR = 7.500E-11 CJS = 0.
+ VJS = 9.058E-01 MJS = 0.          XTB = 3.117E+00 EG = 1.184E+00
+ XTI = 2.000E+00 KF = 0.000E+00 AF = 1.000E+00 FC = 9.000E-01
* Quasi-saturation Effect available in PSpice 4.03 and above only
+ QCO = 1.006E-25 RCO = 8.153E+01 VO = 3.234E+00 GAMMA= 1.495E-12
.MODEL PV432P01 NPN RB = 4.653E+01 IRB = 0.000E+00 RBM = 1E-4
+ IS = 9.663E-18 BF = 7.719E+00 ISE = 6.087E-14 NE = 1.953E+00
+ IKF = 2.035E-03 CJE = 3.240E-13 VJE = 7.743E-01 MJE = 5.185E-01
+ BR = 3.950E-02 CJC = 1.208E-12 VJC = 9.058E-01 MJC = 4.931E-01
+ XTB = 0.          EG = 1.184E+00 XTI = 3.000E+00 FC = 9.000E-01
.ENDS

```

```

**
* THREE 1.5 BY 45 MICRON STRIPES :      LOW  MODEL      ** VB110 **
.MODEL PV392A01 PNP
+ IS = 1.403E-16  BF = 5.680E+01  NF = 1.000E+00  VAF = 2.949E+01
+ IKF = 7.561E-02  ISE = 1.932E-15  NE = 1.287E+00  BR = 2.077E+02
+ NR = 1.000E+00  VAR = 3.194E+00  IKR = 4.500E-01  ISC = 1.210E-13
+ NC = 1.634E+00  RB = 7.542E+00  IRB = 0.000E+00  RBM = 5.229E+00
+ RE = 2.802E-01  RC = 2.860E+01  CJE = 6.507E-13  VJE = 7.320E-01
+ MJE = 4.930E-01  TF = 2.579E-11  XTF = 3.677E+01  VTF = 7.327E+00
+ ITF = 1.226E+00  PTF = 0.000E+00  CJC = 7.751E-13  VJC = 7.743E-01
+ MJC = 5.185E-01  XCJC= 2.026E-01  TR = 7.500E-11  CJS = 2.183E-12
+ VJS = 9.058E-01  MJS = 4.931E-01  XTB = 3.117E+00  EG = 1.184E+00
+ XTI = 2.000E+00  KF = 0.000E+00  AF = 1.000E+00  FC = 9.000E-01
*
* From ADVICE usrmod=PEB1 Extended Bipolar Model with Quasi-sat
.SUBCKT PV392A01 (1, 2, 3, 4)
Qs  10 20 3  PV392Q01
Qp  4  10 20 PV392P01
Dbv 10 20  PBVBC 4.5
RCX  1  10 28.60
RBX  2  20  5.229
.MODEL PV392Q01 PNP
+ IS = 1.403E-16  BF = 5.680E+01  NF = 1.000E+00  VAF = 2.949E+01
+ IKF = 9.811E-02  ISE = 1.932E-15  NE = 1.287E+00  BR = 2.077E+02
+ NR = 1.000E+00  VAR = 3.194E+00  IKR = 4.500E-01  ISC = 1.126E-15
+ NC = 1.634E+00  RB = 2.314E+00  IRB = 0.000E+00  RBM = 1E-4
+ RE = 2.802E-01  RC = 0.          CJE = 6.507E-13  VJE = 7.320E-01
+ MJE = 4.930E-01  TF = 1.450E-11  XTF = 3.677E+01  VTF = 7.327E+00
+ ITF = 1.226E+00  PTF = 0.000E+00  CJC = 1.571E-13  VJC = 7.743E-01
+ MJC = 5.185E-01  XCJC= 1.          TR = 7.500E-11  CJS = 0.
+ VJS = 9.058E-01  MJS = 0.          XTB = 3.117E+00  EG = 1.184E+00
+ XTI = 2.000E+00  KF = 0.000E+00  AF = 1.000E+00  FC = 9.000E-01
* Quasi-saturation Effect available in PSpice 4.03 and above only
+ QCO = 2.079E-25  RCO = 3.624E+01  VO = 3.234E+00  GAMMA= 1.495E-12
.MODEL PV392P01 NPN RB = 2.440E+01  IRB = 0.000E+00  RBM = 1E-4
+ IS = 1.903E-17  BF = 7.719E+00  ISE = 1.199E-13  NE = 1.953E+00
+ IKF = 4.007E-03  CJE = 6.180E-13  VJE = 7.743E-01  MJE = 5.185E-01
+ BR = 3.950E-02  CJC = 2.183E-12  VJC = 9.058E-01  MJC = 4.931E-01
+ XTB = 0.          EG = 1.184E+00  XTI = 3.000E+00  FC = 9.000E-01
.ENDS

```

```

**
* SIX 1.5 BY 45 MICRON STRIPES :      LOW  MODEL          ** VB110 **
.MODEL PV693A01 PNP
+ IS = 2.805E-16  BF = 5.680E+01  NF = 1.000E+00  VAF = 2.949E+01
+ IKF = 1.516E-01  ISE = 3.864E-15  NE = 1.287E+00  BR = 2.131E+02
+ NR = 1.000E+00  VAR = 3.194E+00  IKR = 9.000E-01  ISC = 2.214E-13
+ NC = 1.634E+00  RB = 3.771E+00  IRB = 0.000E+00  RBM = 2.614E+00
+ RE = 1.401E-01  RC = 1.430E+01  CJE = 1.302E-12  VJE = 7.320E-01
+ MJE = 4.930E-01  TF = 2.547E-11  XTF = 3.677E+01  VTF = 7.327E+00
+ ITF = 2.452E+00  PTF = 0.000E+00  CJC = 1.417E-12  VJC = 7.743E-01
+ MJC = 5.185E-01  XCJC= 2.216E-01  TR = 7.500E-11  CJS = 4.531E-12
+ VJS = 9.058E-01  MJS = 4.931E-01  XTB = 3.117E+00  EG = 1.184E+00
+ XTI = 2.000E+00  KF = 0.000E+00  AF = 1.000E+00  FC = 9.000E-01
*
* From ADVICE usrmod=PEB1 Extended Bipolar Model with Quasi-sat
.SUBCKT PV693A01 (1, 2, 3, 4)
Qs  10 20 3  PV693Q01
Qp  4  10 20 PV693P01
Dbv 10 20  PBVBC 9
RCX 1  10 14.30
RBX 2  20 2.614
.MODEL PV693Q01 PNP
+ IS = 2.805E-16  BF = 5.680E+01  NF = 1.000E+00  VAF = 2.949E+01
+ IKF = 1.966E-01  ISE = 3.864E-15  NE = 1.287E+00  BR = 2.131E+02
+ NR = 1.000E+00  VAR = 3.194E+00  IKR = 9.000E-01  ISC = 2.251E-15
+ NC = 1.634E+00  RB = 1.157E+00  IRB = 0.000E+00  RBM = 1E-4
+ RE = 1.401E-01  RC = 0.          CJE = 1.302E-12  VJE = 7.320E-01
+ MJE = 4.930E-01  TF = 1.450E-11  XTF = 3.677E+01  VTF = 7.327E+00
+ ITF = 2.452E+00  PTF = 0.000E+00  CJC = 3.141E-13  VJC = 7.743E-01
+ MJC = 5.185E-01  XCJC= 1.        TR = 7.500E-11  CJS = 0.
+ VJS = 9.058E-01  MJS = 0.        XTB = 3.117E+00  EG = 1.184E+00
+ XTI = 2.000E+00  KF = 0.000E+00  AF = 1.000E+00  FC = 9.000E-01
* Quasi-saturation Effect available in PSpice 4.03 and above only
+ QCO = 2.079E-25  RCO = 1.812E+01  VO = 3.234E+00  GAMMA= 1.495E-12
.MODEL PV693P01 NPN RB = 1.367E+01  IRB = 0.000E+00  RBM = 1E-4
+ IS = 3.479E-17  BF = 7.719E+00  ISE = 2.191E-13  NE = 1.953E+00
+ IKF = 7.326E-03  CJE = 1.103E-12  VJE = 7.743E-01  MJE = 5.185E-01
+ BR = 3.950E-02  CJC = 4.531E-12  VJC = 9.058E-01  MJC = 4.931E-01
+ XTB = 0.        EG = 1.184E+00  XTI = 3.000E+00  FC = 9.000E-01
.ENDS

**
* Collector-Base Avalanche Breakdown Diode
.MODEL PBVBC D
+ BV = 2.100E+01  IBV = 1.000E-04  IS = 1.000E-21  RS = 0.
* Low-level reverse breakdown available in PSpice 4.03 and above only
+ NBV = 1.000E+01  TBV1=-4.000E-02  TBV2= 0.

```

```

*****
* AT&T Microelectronics CBIC-V Technology - Spice Models   June 1991 *
* "PNPHI.LIB" - PNP Transistors - High                      *
*****
* - From ADVICE usrmod=PEB1 Extended Bipolar Model with Quasi-sat *
* Full-Scale Revision by JHB 1/15/90: DC, AC Characteristics, T-Depend *
* Models Compiled by KEG 4/20/90                               *
*                                                               *
* NOTE: Reference Temperature is 27 C                         *
*****
*               High CBIC-V Beta and fT PNP Transistor Models *
*****
**
* TWO 1.5 BY 15 MICRON STRIPES :    HIGH MODEL                ** VB110 **
.MODEL PV231A01 PNP
+ IS = 3.278E-16 BF = 3.943E+02 NF = 1.000E+00 VAF = 2.697E+01
+ IKF = 1.934E-02 ISE = 6.836E-16 NE = 1.287E+00 BR = 1.715E+03
+ NR = 1.000E+00 VAR = 1.198E+00 IKR = 1.000E-01 ISC = 3.476E-14
+ NC = 1.634E+00 RB = 5.663E+01 IRB = 0.000E+00 RBM = 1.497E+01
+ RE = 1.261E+00 RC = 6.445E+01 CJE = 1.101E-13 VJE = 7.320E-01
+ MJE = 4.930E-01 TF = 1.496E-11 XTF = 2.423E+01 VTF = 5.355E+00
+ ITF = 4.728E-01 PTF = 0.000E+00 CJC = 1.183E-13 VJC = 7.743E-01
+ MJC = 5.185E-01 XCJC= 2.318E-01 TR = 5.500E-11 CJS = 4.934E-13
+ VJS = 9.058E-01 MJS = 4.931E-01 XTB = 2.200E+00 EG = 1.184E+00
+ XTI = 2.000E+00 KF = 0.000E+00 AF = 1.000E+00 FC = 8.800E-01
*
* From ADVICE usrmod=PEB1 Extended Bipolar Model with Quasi-sat
.SUBCKT PV231A01 (1, 2, 3, 4)
Qs  10 20 3 PV231Q01
Qp  4  10 20 PV231P01
Dbv 10 20 PBVBC
RCX  1  10 64.45
RBX  2  20 14.97
.MODEL PV231Q01 PNP
+ IS = 3.278E-16 BF = 3.943E+02 NF = 1.000E+00 VAF = 2.697E+01
+ IKF = 2.434E-02 ISE = 6.836E-16 NE = 1.287E+00 BR = 1.715E+03
+ NR = 1.000E+00 VAR = 1.198E+00 IKR = 1.000E-01 ISC = 2.502E-16
+ NC = 1.634E+00 RB = 4.166E+01 IRB = 0.000E+00 RBM = 1E-4
+ RE = 1.261E+00 RC = 0.          CJE = 1.101E-13 VJE = 7.320E-01
+ MJE = 4.930E-01 TF = 9.840E-12 XTF = 2.423E+01 VTF = 5.355E+00
+ ITF = 4.728E-01 PTF = 0.000E+00 CJC = 2.742E-14 VJC = 7.743E-01
+ MJC = 5.185E-01 XCJC= 1.      TR = 5.500E-11 CJS = 0.
+ VJS = 9.058E-01 MJS = 0.      XTB = 2.200E+00 EG = 1.184E+00
+ XTI = 2.000E+00 KF = 0.000E+00 AF = 1.000E+00 FC = 8.800E-01
* Quasi-saturation Effect available in PSpice 4.03 and above only
+ QCO = 1.006E-25 RCO = 8.303E+01 VO = 2.627E+00 GAMMA= 5.101E-12
.MODEL PV231P01 NPN RB = 8.000E+01 IRB = 0.000E+00 RBM = 1E-4
+ IS = 1.071E-17 BF = 1.509E+01 ISE = 3.451E-14 NE = 1.953E+00
+ IKF = 1.154E-03 CJE = 9.087E-14 VJE = 7.743E-01 MJE = 5.185E-01
+ BR = 7.722E-02 CJC = 4.934E-13 VJC = 9.058E-01 MJC = 4.931E-01
+ XTB = 0.          EG = 1.184E+00 XTI = 3.000E+00 FC = 8.800E-01
.ENDS

```



```

**
* FOUR 1.5 BY 15 MICRON STRIPES :      HIGH MODEL      ** VB110 **
.MODEL PV432A01 PNP
+ IS = 6.555E-16  BF = 3.943E+02  NF = 1.000E+00  VAF = 2.697E+01
+ IKF = 3.867E-02  ISE = 1.367E-15  NE = 1.287E+00  BR = 1.816E+03
+ NR = 1.000E+00  VAR = 1.198E+00  IKR = 2.000E-01  ISC = 6.137E-14
+ NC = 1.634E+00  RB = 2.832E+01  IRB = 0.000E+00  RBM = 7.485E+00
+ RE = 6.305E-01  RC = 3.222E+01  CJE = 2.203E-13  VJE = 7.320E-01
+ MJE = 4.930E-01  TF = 1.446E-11  XTF = 2.423E+01  VTF = 5.355E+00
+ ITF = 9.456E-01  PTF = 0.000E+00  CJC = 2.110E-13  VJC = 7.743E-01
+ MJC = 5.185E-01  XCJC= 2.599E-01  TR = 5.500E-11  CJS = 8.588E-13
+ VJS = 9.058E-01  MJS = 4.931E-01  XTB = 2.200E+00  EG = 1.184E+00
+ XTI = 2.000E+00  KF = 0.000E+00  AF = 1.000E+00  FC = 8.800E-01
*
* From ADVICE usrmod=PEB1 Extended Bipolar Model with Quasi-sat
.SUBCKT PV432A01 (1, 2, 3, 4)
Qs  10 20 3  PV432Q01
Qp  4  10 20 PV432P01
Dbv 10 20  PBVBC 2
RCX  1  10  32.22
RBX  2  20  7.485
.MODEL PV432Q01 PNP
+ IS = 6.555E-16  BF = 3.943E+02  NF = 1.000E+00  VAF = 2.697E+01
+ IKF = 4.867E-02  ISE = 1.367E-15  NE = 1.287E+00  BR = 1.816E+03
+ NR = 1.000E+00  VAR = 1.198E+00  IKR = 2.000E-01  ISC = 5.003E-16
+ NC = 1.634E+00  RB = 2.083E+01  IRB = 0.000E+00  RBM = 1E-4
+ RE = 6.305E-01  RC = 0.          CJE = 2.203E-13  VJE = 7.320E-01
+ MJE = 4.930E-01  TF = 9.840E-12  XTF = 2.423E+01  VTF = 5.355E+00
+ ITF = 9.456E-01  PTF = 0.000E+00  CJC = 5.484E-14  VJC = 7.743E-01
+ MJC = 5.185E-01  XCJC= 1.          TR = 5.500E-11  CJS = 0.
+ VJS = 9.058E-01  MJS = 0.          XTB = 2.200E+00  EG = 1.184E+00
+ XTI = 2.000E+00  KF = 0.000E+00  AF = 1.000E+00  FC = 8.800E-01
* Quasi-saturation Effect available in PSpice 4.03 and above only
+ QCO = 1.006E-25  RCO = 4.151E+01  VO = 2.627E+00  GAMMA= 5.101E-12
.MODEL PV432P01 NPN RB = 4.653E+01  IRB = 0.000E+00  RBM = 1E-4
+ IS = 1.889E-17  BF = 1.509E+01  ISE = 6.087E-14  NE = 1.953E+00
+ IKF = 2.035E-03  CJE = 1.562E-13  VJE = 7.743E-01  MJE = 5.185E-01
+ BR = 7.722E-02  CJC = 8.588E-13  VJC = 9.058E-01  MJC = 4.931E-01
+ XTB = 0.          EG = 1.184E+00  XTI = 3.000E+00  FC = 8.800E-01
.ENDS

```

```

**
* THREE 1.5 BY 45 MICRON STRIPES :      HIGH MODEL      ** VB110 **
.MODEL PV392A01 PNP
+ IS = 1.475E-15  BF = 3.943E+02  NF = 1.000E+00  VAF = 2.697E+01
+ IKF = 8.703E-02  ISE = 3.076E-15  NE = 1.287E+00  BR = 1.927E+03
+ NR = 1.000E+00  VAR = 1.198E+00  IKR = 4.500E-01  ISC = 1.210E-13
+ NC = 1.634E+00  RB = 1.258E+01  IRB = 0.000E+00  RBM = 3.326E+00
+ RE = 2.802E-01  RC = 1.573E+01  CJE = 4.956E-13  VJE = 7.320E-01
+ MJE = 4.930E-01  TF = 1.397E-11  XTF = 2.423E+01  VTF = 5.355E+00
+ ITF = 2.128E+00  PTF = 0.000E+00  CJC = 4.215E-13  VJC = 7.743E-01
+ MJC = 5.185E-01  XCJC= 2.928E-01  TR = 5.500E-11  CJS = 1.553E-12
+ VJS = 9.058E-01  MJS = 4.931E-01  XTB = 2.200E+00  EG = 1.184E+00
+ XTI = 2.000E+00  KF = 0.000E+00  AF = 1.000E+00  FC = 8.800E-01
*
* From ADVICE usrmod=PEB1 Extended Bipolar Model with Quasi-sat
.SUBCKT PV392A01 (1, 2, 3, 4)
Qs  10 20 3  PV392Q01
Qp  4  10 20 PV392P01
Dbv 10 20  PBVBC 4.5
RCX  1  10 15.73
RBX  2  20  3.326
.MODEL PV392Q01 PNP
+ IS = 1.475E-15  BF = 3.943E+02  NF = 1.000E+00  VAF = 2.697E+01
+ IKF = 1.095E-01  ISE = 3.076E-15  NE = 1.287E+00  BR = 1.927E+03
+ NR = 1.000E+00  VAR = 1.198E+00  IKR = 4.500E-01  ISC = 1.126E-15
+ NC = 1.634E+00  RB = 9.258E+00  IRB = 0.000E+00  RBM = 1E-4
+ RE = 2.802E-01  RC = 0.          CJE = 4.956E-13  VJE = 7.320E-01
+ MJE = 4.930E-01  TF = 9.840E-12  XTF = 2.423E+01  VTF = 5.355E+00
+ ITF = 2.128E+00  PTF = 0.000E+00  CJC = 1.234E-13  VJC = 7.743E-01
+ MJC = 5.185E-01  XCJC= 1.          TR = 5.500E-11  CJS = 0.
+ VJS = 9.058E-01  MJS = 0.          XTB = 2.200E+00  EG = 1.184E+00
+ XTI = 2.000E+00  KF = 0.000E+00  AF = 1.000E+00  FC = 8.800E-01
* Quasi-saturation Effect available in PSpice 4.03 and above only
+ QCO = 2.079E-25  RCO = 1.845E+01  VO = 2.627E+00  GAMMA= 5.101E-12
.MODEL PV392P01 NPN RB = 2.440E+01  IRB = 0.000E+00  RBM = 1E-4
+ IS = 3.720E-17  BF = 1.509E+01  ISE = 1.199E-13  NE = 1.953E+00
+ IKF = 4.007E-03  CJE = 2.981E-13  VJE = 7.743E-01  MJE = 5.185E-01
+ BR = 7.722E-02  CJC = 1.553E-12  VJC = 9.058E-01  MJC = 4.931E-01
+ XTB = 0.          EG = 1.184E+00  XTI = 3.000E+00  FC = 8.800E-01
.ENDS

```

```

**
* SIX 1.5 BY 45 MICRON STRIPES :      HIGH MODEL      ** VB110 **
.MODEL PV693A01 PNP
+ IS = 2.950E-15  BF = 3.943E+02  NF = 1.000E+00  VAF = 2.697E+01
+ IKF = 1.741E-01  ISE = 6.152E-15  NE = 1.287E+00  BR = 1.995E+03
+ NR = 1.000E+00  VAR = 1.198E+00  IKR = 9.000E-01  ISC = 2.214E-13
+ NC = 1.634E+00  RB = 6.292E+00  IRB = 0.000E+00  RBM = 1.663E+00
+ RE = 1.401E-01  RC = 7.865E+00  CJE = 9.911E-13  VJE = 7.320E-01
+ MJE = 4.930E-01  TF = 1.369E-11  XTF = 2.423E+01  VTF = 5.355E+00
+ ITF = 4.255E+00  PTF = 0.000E+00  CJC = 7.787E-13  VJC = 7.743E-01
+ MJC = 5.185E-01  XCJC= 3.169E-01  TR = 5.500E-11  CJS = 3.223E-12
+ VJS = 9.058E-01  MJS = 4.931E-01  XTB = 2.200E+00  EG = 1.184E+00
+ XTI = 2.000E+00  KF = 0.000E+00  AF = 1.000E+00  FC = 8.800E-01

```

```

*
* From ADVICE usrmod=PEB1 Extended Bipolar Model with Quasi-sat
.SUBCKT PV693A01 (1, 2, 3, 4)

```

```

Qs  10 20 3  PV693Q01
Qp  4  10 20 PV693P01
Dbv 10 20  PBVBC 9
RCX  1  10  7.865
RBX  2  20  1.663

```

```

.MODEL PV693Q01 PNP
+ IS = 2.950E-15  BF = 3.943E+02  NF = 1.000E+00  VAF = 2.697E+01
+ IKF = 2.191E-01  ISE = 6.152E-15  NE = 1.287E+00  BR = 1.995E+03
+ NR = 1.000E+00  VAR = 1.198E+00  IKR = 9.000E-01  ISC = 2.251E-15
+ NC = 1.634E+00  RB = 4.629E+00  IRB = 0.000E+00  RBM = 1E-4
+ RE = 1.401E-01  RC = 0.          CJE = 9.911E-13  VJE = 7.320E-01
+ MJE = 4.930E-01  TF = 9.840E-12  XTF = 2.423E+01  VTF = 5.355E+00
+ ITF = 4.255E+00  PTF = 0.000E+00  CJC = 2.468E-13  VJC = 7.743E-01
+ MJC = 5.185E-01  XCJC= 1.          TR = 5.500E-11  CJS = 0.
+ VJS = 9.058E-01  MJS = 0.          XTB = 2.200E+00  EG = 1.184E+00
+ XTI = 2.000E+00  KF = 0.000E+00  AF = 1.000E+00  FC = 8.800E-01

```

```

* Quasi-saturation Effect available in PSpice 4.03 and above only
+ QCO = 2.079E-25  RCO = 9.226E+00  VO = 2.627E+00  GAMMA= 5.101E-12

```

```

.MODEL PV693P01 NPN RB = 1.367E+01  IRB = 0.000E+00  RBM = 1E-4
+ IS = 6.802E-17  BF = 1.509E+01  ISE = 2.191E-13  NE = 1.953E+00
+ IKF = 7.326E-03  CJE = 5.319E-13  VJE = 7.743E-01  MJE = 5.185E-01
+ BR = 7.722E-02  CJC = 3.223E-12  VJC = 9.058E-01  MJC = 4.931E-01
+ XTB = 0.          EG = 1.184E+00  XTI = 3.000E+00  FC = 8.800E-01
.ENDS

```

```

**
* Collector-Base Avalanche Breakdown Diode
.MODEL PBVBC D

```

```

+ BV = 6.000E+00  IBV = 1.000E-04  IS = 1.000E-21  RS = 0.
* Low-level reverse breakdown available in PSpice 4.03 and above only
+ NBV = 1.000E+01  TBV1=-4.000E-02  TBV2= 0.

```

## Appendix B

## NPN Test Circuits

```

VB110 - nv231,431,362,663a01 Nominal Vbe Case
* Voltage-driven Base
* Ic vs. Vbe , gm vs. f
*
Vce 5 0 5v
Q1 5 1 0 0 nv231a01
X1 5 1 0 0 nv231a01
Q2 5 1 0 0 nv431a01
X2 5 1 0 0 nv431a01
Q3 5 1 0 0 nv362a01
X3 5 1 0 0 nv362a01
Q6 5 1 0 0 nv663a01
X6 5 1 0 0 nv663a01
Vbe 1 0 DC 0.75v
.Lib NPNNOM.LIB
.DC Vbe 0.3 1.0 0.02 Vce 2 9 3
.Print DC Ic(Q1) I(X1.Rcx)
.Probe
.End
VB110 - nv231a01 Nominal Beta Case
* Current-driven Emitter
* Beta vs. Ic , Beta vs. f
*
Vcb 5 0 5v
Q1 5 0 1 1 nv231a01
X1 5 0 x x nv231a01
Iee e 0 DC 1mA
Vee 1 e DC 0v
Fex x 0 Vee 1.0
.Lib NPNNOM.LIB
.DC DEC Iee 10nA 20mA 10 Vcb 2 9 3
.Print DC Ic(Q1) Ib(Q1) I(X1.Rcx) I(X1.Rbx)
.Probe
.End
VB110 - nv231a01 Nominal Early Voltage
* Current-driven Base
* Ic vs. Vce , Beta vs. f
*
Vsub 4 0 -20v
Vce 5 0 5v
Q1 5 1 0 4 nv231a01
X1 5 x 0 4 nv231a01
Ibb 0 b DC 100uA
Vbb b 1 DC 0v
Fbx 0 x Vbb 1.0
.Lib NPNNOM.LIB
.DC Vce -15 15 .2 Ibb 20uA 100uA 20uA
.Print DC Ic(Q1) I(X1.Rcx)
.Probe
.End

```

```

VB110 - nv231,431,362,663a01 Nominal VCEsat Curves
* Voltage-driven Base
* Ic vs. Vbe , gm vs. f
*
*.TEMP -25 0 25 75 100
Vce 5 0 5v
Q1 5 1 0 0 nv231a01
X1 5 1 0 0 nv231a01
Q2 5 1 0 0 nv431a01
X2 5 1 0 0 nv431a01
Q3 5 1 0 0 nv362a01
X3 5 1 0 0 nv362a01
Q6 5 1 0 0 nv663a01
X6 5 1 0 0 nv663a01
Vbe 1 0 DC 0.75v
.Lib NPNNOM.LIB
.OP
.DC Vce 0 5 .05 Vbe 0.8 0.9 .05
.Print DC Ic(Q1) I(X1.Rcx)
.Probe
.End
VB110 - nv231a01 Nominal ft vs. Ic
* Current-driven Emitter
* Beta vs. Ic , Beta vs. f
*
*.TEMP -25 0 25 75 100
Vsub 4 0 -5.2v
Vcb 5 0 2.2v
Q1 5 0 1 4 nv231a01
X1 5 0 x 4 nv231a01
Iee e 0 DC 1mA AC 1
Vee 1 e DC 0v
Fex x 0 Vee 1.0
.Lib NPNNOM.LIB
.OP
.AC DEC 20 10MEG 15G
.STEP DEC Iee 100uA 25mA 10
.Print AC Ic(Q1) Ib(Q1) I(X1.Rcx) I(X1.Rbx)
.Probe Ic(Q1) Ib(Q1) I(X1.Rcx) I(X1.Rbx)
.Options acct noecho nomod nopage
.End

```

## PNP Test Circuits

```

VB110 - pv231,432,392,693a01 Nominal Vbe Case
* Voltage-driven Base
* Ic vs. Vbe , gm vs. f
*
Vec 5 0 5v
Q1 0 1 5 5 pv231a01
X1 0 1 5 5 pv231a01
Q2 0 1 5 5 pv432a01
X2 0 1 5 5 pv432a01
Q4 0 1 5 5 pv392a01
X4 0 1 5 5 pv392a01
Q9 0 1 5 5 pv693a01
X9 0 1 5 5 pv693a01
Veb 5 1 DC 0.75v
.Lib PNPNO.M.LIB
.DC Veb 0.3 1.0 0.02 Vec 2 9 3
.Print DC Ic(Q1) I(X1.Rcx)
.Probe
.End
VB110 - pv231a01 Nominal Beta Case
* Current-driven Emitter
* Beta vs. Ic , Beta vs. f
*
Vbc 5 0 5v
Q1 0 5 1 1 pv231a01
X1 0 5 x x pv231a01
Iee 0 e DC 1mA
Vee 1 e DC 0v
Fex x 0 Vee 1.0
.Lib PNPNO.M.LIB
.DC DEC Iee 10nA 20mA 10 Vbc 2 9 3
.Print DC Ic(Q1) Ib(Q1) I(X1.Rcx) I(X1.Rbx)
.Probe
.End
VB110 - pv231a01 Nominal Early Voltage
* Current-driven Base
* Ic vs. Vce , Beta vs. f
*
Vepi 3 0 20v
Vec 5 0 5v
Q1 0 1 5 3 pv231a01
X1 0 x 5 3 pv231a01
Ibb 0 b DC -100uA
Vbb b 1 DC 0v
Fbx 0 x Vbb 1.0
.Lib PNPNO.M.LIB
.DC Vec -15 15 .2 Ibb -50uA -250uA -50uA
.Print DC Ic(Q1) I(X1.Rcx)
.Probe
.End

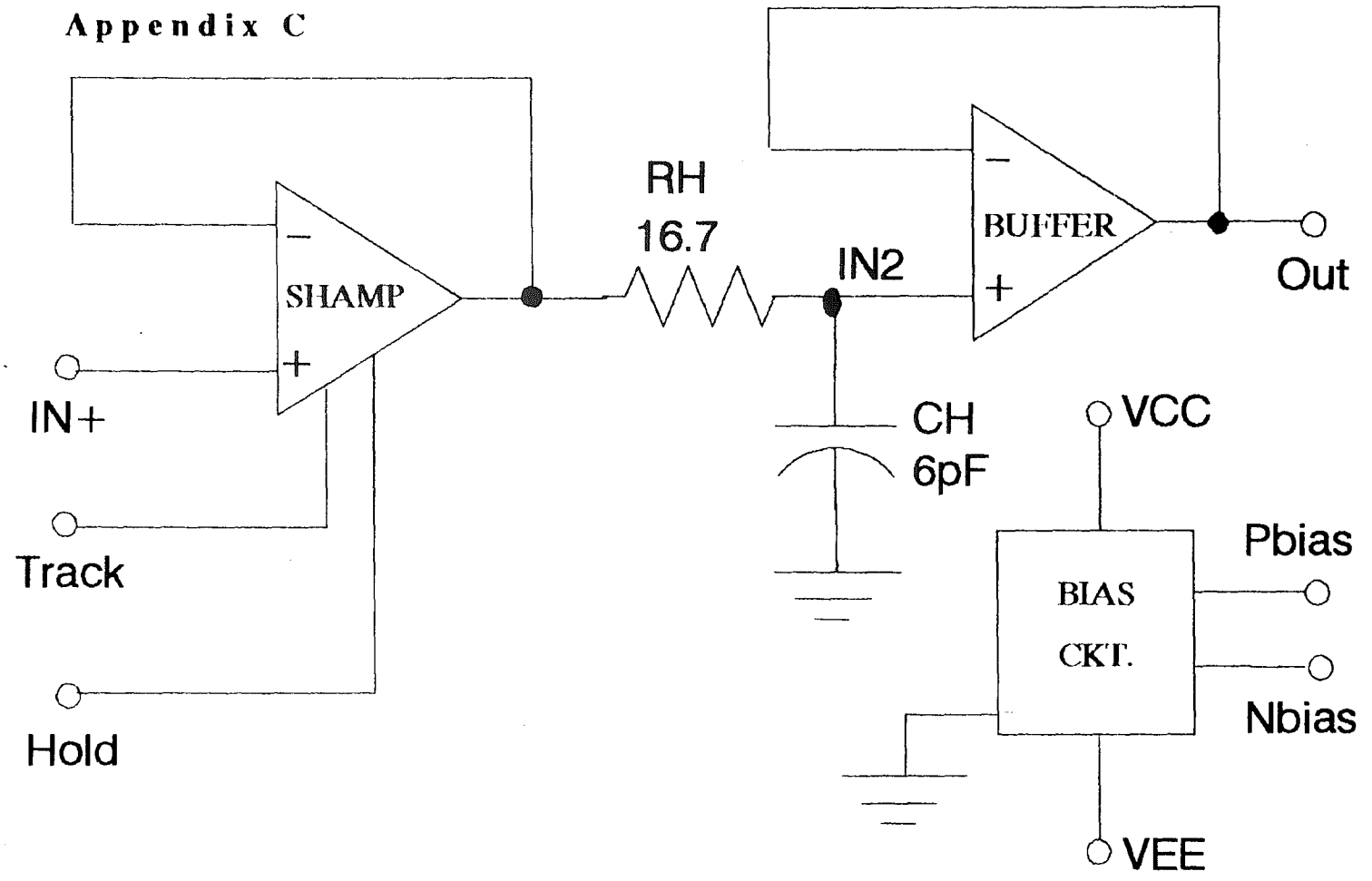
```

```

VB110 - pv231,432,392,693a01 Nominal VCEsat Curves
* Voltage-driven Base
* Ic vs. Vbe , gm vs. f
*
*.TEMP -25 0 25 75 100
Vec 5 0 5v
Q1 0 1 5 5 pv231a01
X1 0 1 5 5 pv231a01
Q2 0 1 5 5 pv432a01
X2 0 1 5 5 pv432a01
Q4 0 1 5 5 pv392a01
X4 0 1 5 5 pv392a01
Q9 0 1 5 5 pv693a01
X9 0 1 5 5 pv693a01
Veb 5 1 DC 0.75v
.Lib PNPNO.M.LIB
.OP
.DC Vec 0 5 .05 Veb 0.8 0.9 .05
.Print DC Ic(Q1) I(X1.Rcx)
.Probe
.End
VB110 - pv231a01 Nominal ft vs. Ic
* Current-driven Emitter
* Beta vs. Ic , Beta vs. f
*
*.TEMP -25 0 25 75 100
Vepi 5 0 5.0v
Vbc 3 0 2.2v
Q1 0 3 1 5 pv231a01
X1 0 3 x 5 pv231a01
Iee 0 e DC 1mA AC 1
Vee 1 e DC 0v
Fex x 0 Vee 1.0
.Lib PNPNO.M.LIB
.OP
.AC DEC 20 10MEG 10G
.STEP DEC Iee 100uA 25mA 10
.Print AC Ic(Q1) Ib(Q1) I(X1.Rcx) I(X1.Rbx)
.Probe Ic(Q1) Ib(Q1) I(X1.Rcx) I(X1.Rbx)
.Options acct noecho nomod nopage
.End

```

Appendix C



103

Figure A1. CBIC-V Sample/Hold Block Diagram



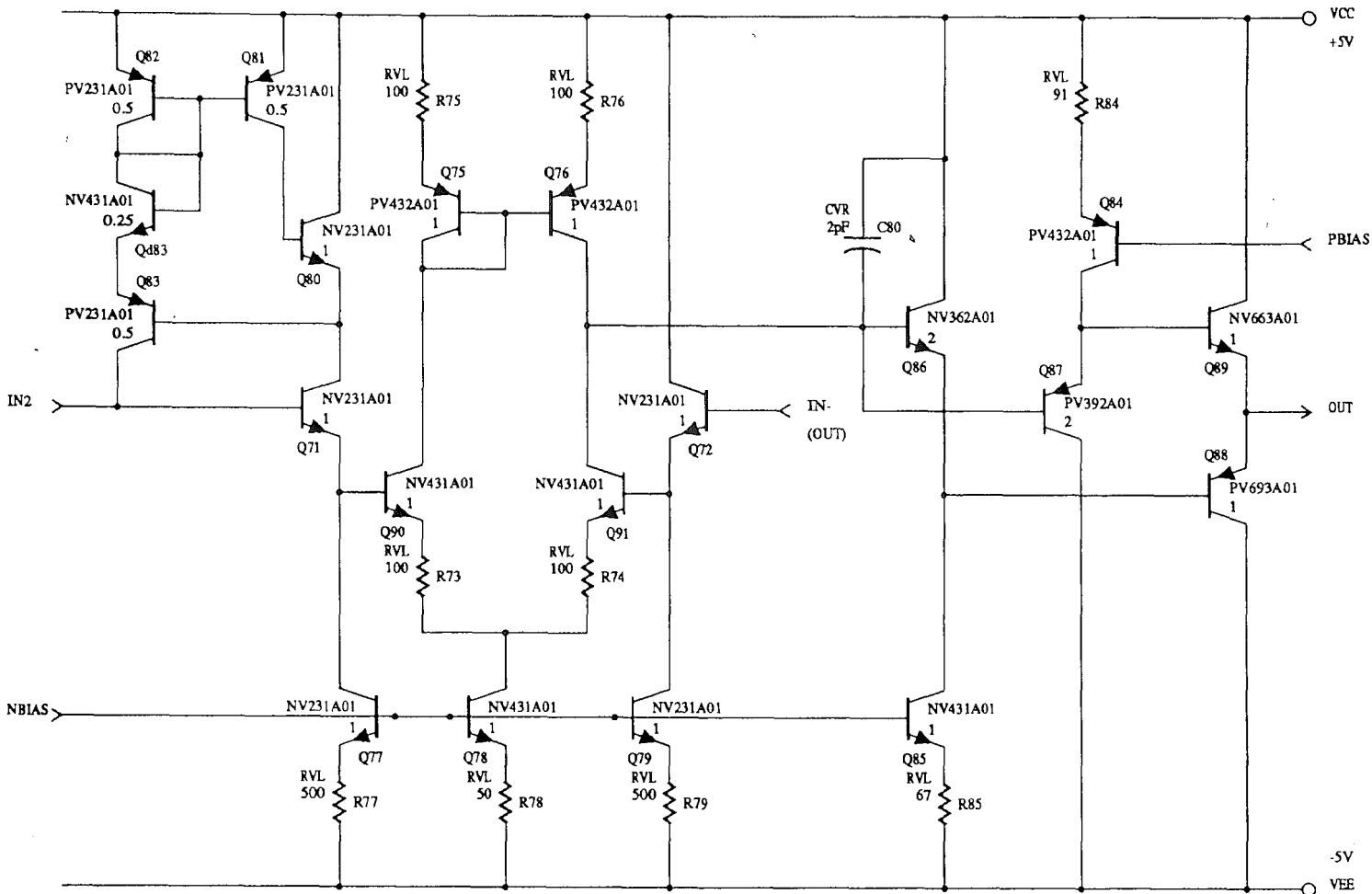


Figure A2. Schematic for Sample/Hold Output Buffer in Figure A1

## References

## REFERENCES

- <sup>1</sup>Ebers, J.J., and Moll, J.L., "Large Signal Behavior of Junction Transistors" Proc. IRE, Vol. 42 (Dec. 1954), pp. 1761-1772.
- <sup>2</sup>Nagel, L.W., and Pederson, D.O., "Simulation Program with Integrated Circuit Emphasis" Proc. Sixteenth Midwest Symposium on Circuit Theory, Waterloo, Canada, 1973; available as Memorandum No. ERL-M382, Electronics Research Laboratory, University of California, Berkeley.
- <sup>3</sup>Nagel, L.W., "SPICE2: A Computer Program to Simulate Semiconductor Circuits" Electronics Research Laboratory Memorandum No. ERL-M520, University of California, Berkeley, May 1975.
- <sup>4</sup>Early, J.M., "Effects of Space-Charge Layer Widening in Junction Transistors" Proc. IRE, Vol. 46 (Nov. 1952), pp. 1401-1406.
- <sup>5</sup>Gummel, H.K., "A Charge Control Relation for Bipolar Transistors" Bell Syst. Tech., Vol. 49 (Jan. 1970), pp. 115-120.
- <sup>6</sup>Gummel, H.K., and Poon, H.C., "An Integral Charge Control Model of Bipolar Transistors" Bell Syst. Tech., Vol. 49 (May-June 1970), pp. 827-852.
- <sup>7</sup>Poon, H.C., and Meckwood, J.C., "Modeling of Avalanche Effect in Integral Charge Control Model" IEEE Trans. Electron Devices, Vol. ED-19, No. 1 (Jan. 1972), pp. 90-97.
- <sup>8</sup>Dutton, R.W., "Bipolar Transistor Modeling of Avalanche Generation for Computer Circuit Simulation" IEEE Trans. Electron Devices, Vol. ED-22, No. 6 (June 1975), pp. 334-338.
- <sup>9</sup>Nagel, L.W., "ADVICE for Circuit Simulation" Proc. ISCAS, Houston, Texas, 1980.
- <sup>10</sup>Webster, W.M., "On the Variation of Junction-Transistor Current-Amplification Factor with Emitter Current" Proc. IRE, Vol. 42 (June 1954), pp. 914-920.
- <sup>11</sup>Kirk, Jr., C.T., "A Theory of Transistor Cutoff Frequency ( $f_T$ ) Falloff at High Current Densities" IRE Trans. Electron Devices, Vol. ED-9 (Mar. 1962), pp. 164-174.

- 
- 12 Messenger, G.C., "An Analysis of Switching Effects in High Power Diffused Base Silicon Transistors" presented at the Electron Devices Meeting, Washington, D.C., 1959.
- 13 Hahn, Larry A., "The Saturation Characteristics of High-Voltage Transistors" Proc. IEEE, Vol. 55, No. 8 (August 1967), pp. 1384-1388.
- 14 Hahn, Larry A., "The Effect of Collector Resistance Upon the High Current Capability of n-p-v-n Transistors" IEEE Trans. Electron Devices, Vol. ED-16, No. 7 (July 1969), pp. 654-656.
- 15 Rein, H.-M., Stübing, H., and Schröter, M., "Verification of the Integral Charge-Control Relation for High-Speed Bipolar Transistors at High Current Densities" IEEE Trans. Electron Devices, Vol. ED-32 (June 1985), pp. 1070-1076.
- 16 Tang, D.D., and Solomon, P.M., "Bipolar Transistor design for Optimized Power-Delay Logic Circuits" IEEE J. Solid State Circuits, Vol. SC-14 (1979), pp. 679-684.
- 17 Ranfft, R., and Rein, H.-M., "High-Speed Bipolar Logic Circuits with Low Power Consumption for LSI - A Comparison" IEEE J. Solid State Circuits, Vol. SC-17 (1982), pp. 703-712.
- 18 Poon, H.C., "Implications of Transistor Frequency Dependence on Intermodulation Distortion" IEEE Trans. Electron Devices, Vol. ED-21 (Jan. 1974), pp. 110-112.
- 19 Getreu, I.E., *Modeling the Bipolar Transistor*. Beaverton, Ore.: Tektronix, Inc., 1976.
- 20 Beaufoy, R., and Sparkes, J.J., "The Junction Transistor as a Charge-Controlled Device" ATE J. (London), 13, No. 4 (October 1957), pp. 310-324.
- 21 Muller, Richard S., and Kamins, Theodore I. *Device Electronics for Integrated Circuits*. New York: John Wiley & Sons, Inc., 1977.
- 22 Szeto, Simon, and Reif, Rafael, "Reduction of  $f_T$  by Nonuniform Base Bandgap Narrowing" IEEE Electron Dev. Letters, Vol. 10, No. 8 (August 1989), pp. 341-343.
- 23 Clark, Lowell E., "Characteristics of Two-Region Saturation Phenomena" IEEE Trans. Electron Devices, Vol. ED-16, No. 1 (Jan. 1969), pp. 113-116.

- 
- <sup>24</sup>Antognetti, Paolo, and Massobrio, Giuseppe, *Semiconductor Device Modeling with SPICE*. New York: McGraw-Hill, Inc., 1988.
- <sup>25</sup>Antognetti, Paolo (ed.), *Power Integrated Circuits*. New York: McGraw-Hill, Inc., 1986.
- <sup>26</sup>Gummel, Hermann K., "A Self-Consistent Iterative Scheme for One-Dimensional Steady State Transistor Calculations" *IEEE Trans. Electron Devices*, Vol. ED-11 (Oct. 1964), pp. 455-465.
- <sup>27</sup>Poon, H.C., Gummel, H.K., and Scharfetter, Donald L., "High Injection in Epitaxial Transistors" *IEEE Trans. Electron Devices*, Vol. ED-16, (May 1969), pp. 455-457.
- <sup>28</sup>Bowler, David L., and Lindholm, Fredrik A., "High Current Regimes in Transistor Collector Regions" *IEEE Trans. Electron Devices*, Vol. ED-20, (Mar 1973), pp. 257-263.
- <sup>29</sup>van der Ziel, A., and Agouridis, D., "The Cutoff Frequency Falloff in UHF Transistors at High Currents" *Proc. IEEE*, Vol. 54, No. 3 (Mar. 1966), pp. 411-412.
- <sup>30</sup>Beale, J.R.A., and Slatter, J.A.G., "The Equivalent Circuit of a Transistor with a Lightly Doped Collector Operating in Saturation" *Solid-State Electronics*, Vol. 11 (1968), pp. 241-252.
- <sup>31</sup>Whittier, R.J., and Tremere, D.A., "Current Gain and Cutoff Frequency Falloff at High Currents" *IEEE Trans. Electron Devices*, Vol. ED-16, No. 1 (1969), pp. 39-57.
- <sup>32</sup>de Graaff, H.C., "Collector Models for Bipolar Transistors" *Solid-State Electronics*, Vol. 16 (1973), pp. 587-600.
- <sup>33</sup>Rey, G., Dupuy, F., and Bailbe, J.P., "A Unified Approach to the Base Widening Mechanism in Bipolar Transistors" *Solid-State Electronics*, Vol. 18 (1975), pp. 863-866.
- <sup>34</sup>Kumar, Rakesh, and Hunter, Lloyd P., "Collector Capacitance and High-Level Injection Effects in Bipolar Transistors" *IEEE Trans. Electron Devices*, Vol. ED-22, No. 2 (Feb. 1975), pp. 51-60.
- <sup>35</sup>Kull, George M., Nagel, L.W., Lee, Shiuh-Wu, Lloyd, Peter, Prendergast, E. James, and Dirks, Heinz K., "A Unified Circuit Model for Bipolar Transistors Including Quasi-Saturation Effects" *IEEE Trans. Electron Devices*, Vol. ED-32, No. 6 (June 1985), pp. 1103-1113.

- 
- <sup>36</sup>Turgeon, L.J., and Mathews, J.R., "A Bipolar Transistor Model of Quasi-saturation For Use in Computer Aided Design (CAD)" Paper presented at IEDM Tech. Conf., Washington, D.C., December 1980.
- <sup>37</sup>Sze, S.M., *Physics of Semiconductor Devices*, 2nd Edition. New York: John Wiley & Sons, Inc., 1981.
- <sup>38</sup>Sze, S.M., *Semiconductor Devices, Physics and Technology*. New York: John Wiley & Sons, Inc., 1985.
- <sup>39</sup>Feyngenson, A., Buchanan, Jr., W.L., Langer, P.H., and Paulnack, C.L., "Application Of Selective Epitaxy In Advanced Bipolar Technology" internal AT&T Technical Memorandum 52256-880122-02TM, January 22, 1988.
- <sup>40</sup>Feyngenson, A., Buchanan, Jr., W.L., and Bastek, J.J., "High Performance Complementary Silicon Bipolar Process: Part 1. An Overview" internal AT&T Technical Memorandum 52256-880331-04TM, March 31, 1988.
- <sup>41</sup>Reilly, T.A., "Gain - Bandwidth Problems with the SPICE BJT Model" Unpublished memo to MicroSim Corporation, Lafayette College, Easton, Penna., June 28, 1989.
- <sup>42</sup>Fang, T.F., D.F. Guise, G.M. Kull, S. Liu, B.R. Penumalli, and T.A. Pfannkoch, "ADVICE 1L User's Guide" internal Technical Memorandum 52233-841001-01, October 1, 1984.
- <sup>43</sup>*PSpice Program User's Guide*, MicroSim Corporation, Irvine, California, January 1990.
- <sup>44</sup>Fossum, Jerry G., "A Bipolar Device Modeling Technique Applicable to Computer-Aided Circuit Analysis and Design" IEEE Trans. Electron Devices, Vol. ED-20, No. 6 (June 1973), pp. 582-593.
- <sup>45</sup>Baek, J., "BJT Cutoff Frequency Modeling Using ADVICE" Internal Memorandum 52253-890306-04IM, March 6, 1989.

## "VITA"

Kenneth E. Gross received the B.S. and M.S. degrees in electrical engineering from Lehigh University in 1984 and 1992, respectively. He was born May 22, 1961 in the city of Philadelphia, PA to Mr. Richard C. and Jean K. (Eble) Gross.

Since 1984, he has been working for AT&T-ME, in Reading, PA, where he became involved in the modeling of bipolar transistors. From 1987 to 1989 he worked with OEM customers on the design/development of custom ASIC's for applications outside of AT&T. He is currently a Design/Test Group Leader in the Linear Bipolar ASICs organization. His interests include integrated circuit design and modeling.

Mr. Gross is a member of The Institute of Electrical and Electronics Engineers.

**END**

**OF**

**TITLE**